AFRL-MN-EG-TR-2003-7013

POLARIZATION SIGNATURE RESEARCH

Dennis H. Goldstein

AFRL/MNGI
101 W Eglin Blvd Suite 280
EGLIN AFB FL 32542

FEBRUARY 2003

FINAL REPORT FOR PERIOD OCTOBER 1997 - OCTOBER 2002

AIR FORCE RESEARCH LABORATORY, MUNITIONS DIRECTORATE

Air Force Materiel Command ■ United States Air Force ■ Eglin Air Force Base

NOTICE

When Government drawings, specifications, or other data are used for any purpose other than in connection with a definitely Government-related procurement, the United States Government incurs no responsibility or any obligation whatsoever. The fact that the Government may have formulated or in any way supplied the said drawings, specifications, or other data, is not to be regarded by implication, or otherwise in any manner construed, as licensing the holder, or any other person or corporation; or as conveying any rights or permission to manufacture, use, or sell any patented invention that may in any way be related thereto.

This technical report is releasable to the National Technical Information Services (NTIS). At NTIS it will be available to the general public, including foreign nations.

This technical report has been reviewed and is approved for publication.

FOR THE COMMANDER

Maria L Schreffler

MARIA L. SCHREFFLER, LtCol, USAF
Deputy Chief, Advanced Guidance Division

Anyone having need for a copy of this report should first contact the Defense Technical Information Center (DTIC) at the address shown below. If you are a registered DTIC User, DTIC can provide you with a copy. Please do not request copies from the Air Force Research Laboratory, Munitions Directorate. Requests for additional copies should be directed to:

Defense Technical Information Center (DTIC)
8725 John J. Kingman Road, Ste 0944
Ft Belvoir, VA 22060-6218

This report is published in the interest of the scientific and technical information exchange. Publication of this report does not constitute approval or disapproval of the ideas or findings

If your address has changed, if you wish to be removed from our mailing list, or if your organization no longer employs the addressee, please notify AFRL/MNGI, Eglin AFB FL 32542-6810, to help us maintain a current mailing list. Do not return copies of this report unless contractual obligations or notice on a specific document requires that it be returned.

REPORT DOCUMENTATION PAGE

Form Approved
OMB No. 0704-0188

1. AGENCY USE ONLY *(Leave blank)*	2. REPORT DATE	3. REPORT TYPE AND DATES COVERED
	FEBRUARY 2003	Final Technical Report 10/97 – 10/02

4. TITLE AND SUBTITLE
POLARIZATION SIGNATURE RESEARCH

5. FUNDING NUMBERS
JON: 20683037 PE: 62602F
PR: 2068
TA: 30
WU: 37

6. AUTHOR(S)
Dennis H. Goldstein

7. PERFORMING ORGANIZATION NAME(S) AND ADDRESS(ES)
AFRL/MNGI
101 W Eglin Blvd Suite 280
EGLIN AFB FL 32542

8. PERFORMING ORGANIZATION REPORT NUMBER
AFRL-MN-EG-TR-2003-7013

9. SPONSORING/MONITORING AGENCY NAME(S) AND ADDRESS(ES)
(Program Mgr Name & Ph #)

10. SPONSORING/MONITORING AGENCY REPORT NUMBER

11. SUPPLEMENTARY NOTES
Availability of this report is specified on the front cover and its reverse.

12a. DISTRIBUTION/AVAILABILITY STATEMENT
DISTRIBUTION A: Approved for public release; distribution unlimited

12b. DISTRIBUTION CODE
(Leave this block blank)

13. ABSTRACT:

Documentation of work in Mueller matrix spectropolarimetry, Mueller matrix laser polarimetry, and near infrared imaging polarimetry is presented. Spectropolarimetric reflectometer instrumentation is described, and measurements made with this instrumentation on Spectralon and Federal Standard paint samples are given. Laser polarimeter measurements on sapphire and quartz plates with small birefringence are discussed. Results from an imaging near infrared rotating retarder Stokes polarimeter are presented.

14. SUBJECT TERM
Polarimetry, spectropolarimeter, Mueller matrix, birefringence, diattenuation, polarizance, Spectralon, near infrared polarimetry, polarization imaging, Stokes polarimetry, reflectometer

15. NUMBER OF PAGES
86

16. PRICE CODE

17. SECURITY CLASSIFICATION OF REPORT	18. SECURITY CLASSIFICATION OF THIS PAGE	19. SECURITY CLASSIFICATION OF ABSTRACT	20. LIMITATION OF ABSTRACT
UNCLASSIFIED	UNCLASSIFIED	UNCLASSIFIED	UL

PREFACE

Dennis H. Goldstein, Air Force Research Laboratory (AFRL) Munitions Directorate, Advanced Guidance Division, Eglin AFB FL 32542-6810, conducted the research described herein and prepared this final report. The research was conducted during the period October 1997 to October 2002.

TO BE LEFT BLANK

TABLE OF CONTENTS

1.0 Introduction

The purpose of this project was the investigation of polarization phenomenology and signatures. Whenever light interacts with matter, there is likely to be a polarization change. The papers in this volume document phenomenological measurements with Mueller matrix polarimeters and imaging measurements with Stokes polarimeters.

2.0 Discussion

The six papers in the Appendices cover approximately five years of work. Four of the papers (in Appendices A, B, C, and F) deal with Mueller matrix spectropolarimetry. Appendix F is a detailed description of the spectropolarimeter instrumentation and an explanation of its Mueller matrix capability. Appendix B and C describe measurements of the reflectance standard Spectralon and various Federal Standard paint samples, and are primarily concerned with the polarizance of these materials. Appendix A is a description of the use of the spectropolarimeter for transmission measurements, and includes some results on various optical elements. Appendix E describes laser polarimeter measurements made on some sapphire and quartz plates in transmission. Finally, Appendix D describes near infrared imaging polarimetry results collected with a rotating retarder polarimeter.

3.0 Summary

This report documents work in polarimetry over a five-year period and includes six conference proceedings and journal papers.

APPENDIX A

Fourier Transform Spectropolarimetry for Optical Diagnostics of Transmissive Materials

David B. Chenault, Dennis H. Goldstein, and Diana M. Hayes

Proceedings of SPIE Volume 3425, July 1998

Fourier Transform Spectropolarimetry for Optical Diagnostics of Transmissive Materials

David B. Chenault
SY Technology, Inc.
654 Discovery Drive,
Huntsville, AL 35806,

Dennis H. Goldstein
Air Force Research Laboratory
Munitions Directorate
101 West Eglin Blvd
Eglin AFB, FL 32542

Diana M. Hayes
Department of Mathematics
University of North Texas

ABSTRACT

Accurate measurement of polarization properties of materials in transmission is becoming increasingly important as polarization devices and effects are utilized in remote sensing, displays, and other applications. Polarization components in these systems require careful calibration and specification as a function of wavelength. This paper describes a Fourier transform spectropolarimeter, an instrument designed for measurement of polarization properties in transmission. Complete Mueller matrix spectra are acquired using a dual rotating retarder polarimeter placed in the sample compartment of a Fourier transform spectrometer. Several sets of detectors and sources for the spectrometer provide spectral Mueller matrix data from the ultraviolet to the infrared. We have extended data reduction algorithms and calibration techniques developed for an FTIR instrument to the new spectral regimes, including routines to analyze the Mueller matrix data in terms of diattenuation and retardance. This paper describes the instrument, the data reduction and analysis algorithms, and examples of data from several transmissive samples.

KEYWORDS: Polarimetry, spectropolarimeter, Mueller matrix, birefringence, diattenuation

1. INTRODUCTION

The development of many optical systems for optical computing, optical signal processing, optical data storage, displays, target detection, and scene simulation applications is dependent on the spectral polarization properties of polarization elements and modulator materials. The impetus for the work described here was the lack of information on materials for spatial light modulators; this prompted the previous development of a Fourier transform (FT) infrared spectropolarimeter to address this need for the infrared[1,2,3]

A more recent requirement to characterize polarization elements for polarimetry and other applications has resulted in the need for new and better spectropolarimeter instrumentation capable in many regions of the optical regime. One reason for this is because commercially available polarization elements frequently do not meet specifications provided by the vendor, and Mueller matrices for the elements are not provided. The lack of information may be annoying, actually harmful, or may unnecessarily restrict the use of a polarization element. For example, there are spectral regions where the diattenuation of polarizers drops below 90% (an extinction ratio of less than 10). Retardances in birefringent waveplates may vary from nominal retardance by more than 10%[4]. Another reason for development of new instrumentation is that spectropolarimetry of modulator materials is still required for determination of fundamental electrooptical properties.

The development of a new generation of FT spectropolarimeter is described in this paper. More than a decade ago, a spectropolarimeter based on a Nicolet FT infrared spectrometer was designed. This instrument operates only in the infrared (from 3 – 14 μm) but has high spectral resolution (better than 4 cm^{-1})[1]. More recently, a spectropolarimeter for the visible has been developed that utilizes a broadband source and a filter wheel with suitable filters[5]. Here the spectral resolution and the number of number of spectral elements are limited by the filter bandpass and the practical size of the filter wheel. We believe that FT spectrometer-based spectropolarimeters are the most convenient and productive method of gathering large quantities of polarimetric data.

Current FT spectrometers from a number of manufacturers operate from the ultra-violet (uv) to the infrared, covering a wavelength range from less than 0.4 to more than 25 μm. In this work, we describe the development of a spectropolarimeter exploiting the broad spectral capability of these FT spectrometers.

2. FT SPECTROPOLARIMETRY

2.1 Instrumentation

The spectropolarimeter we have developed is a FT spectrometer modified by the insertion of a polarimeter in the sample compartment. The external appearance of the spectrometer is shown in the photo in Figure 1. A diagram of the spectrometer with polarimeter in the sample compartment is shown in Figure 2. Figure 3 shows a photo of the sample compartment with polarization rotation stages (note that there are five stages).

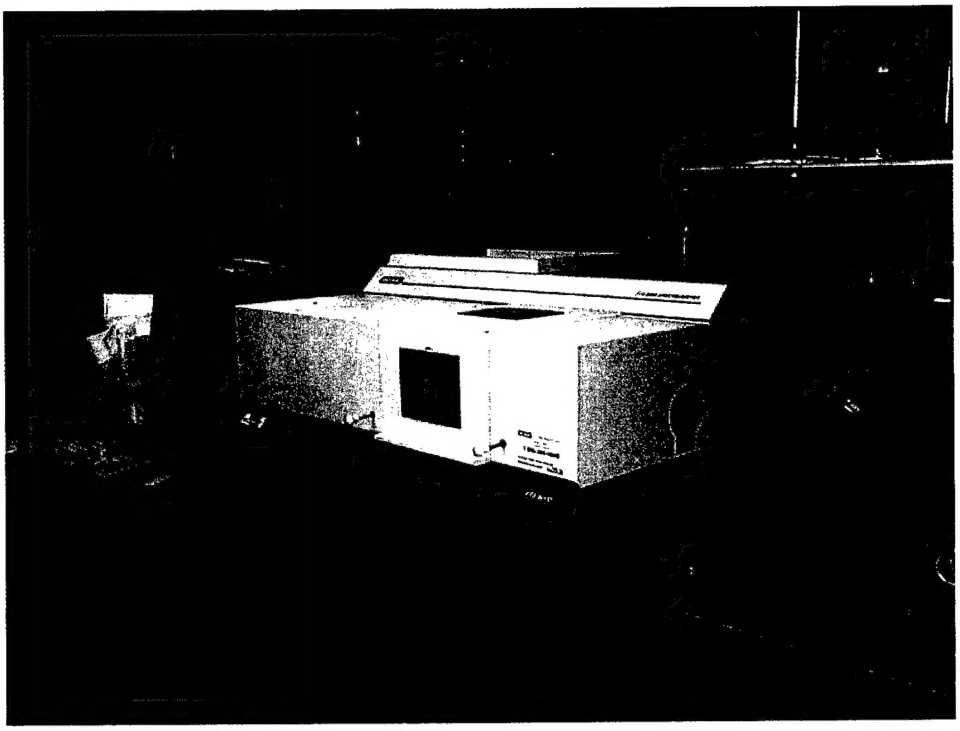

Figure 1. Photograph of FT spectrometer

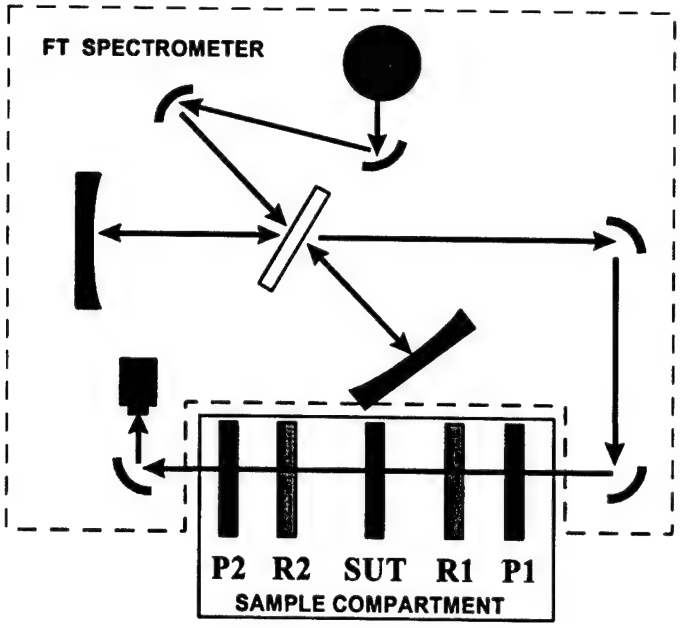

Figure 2. Diagram of FT spectropolarimeter

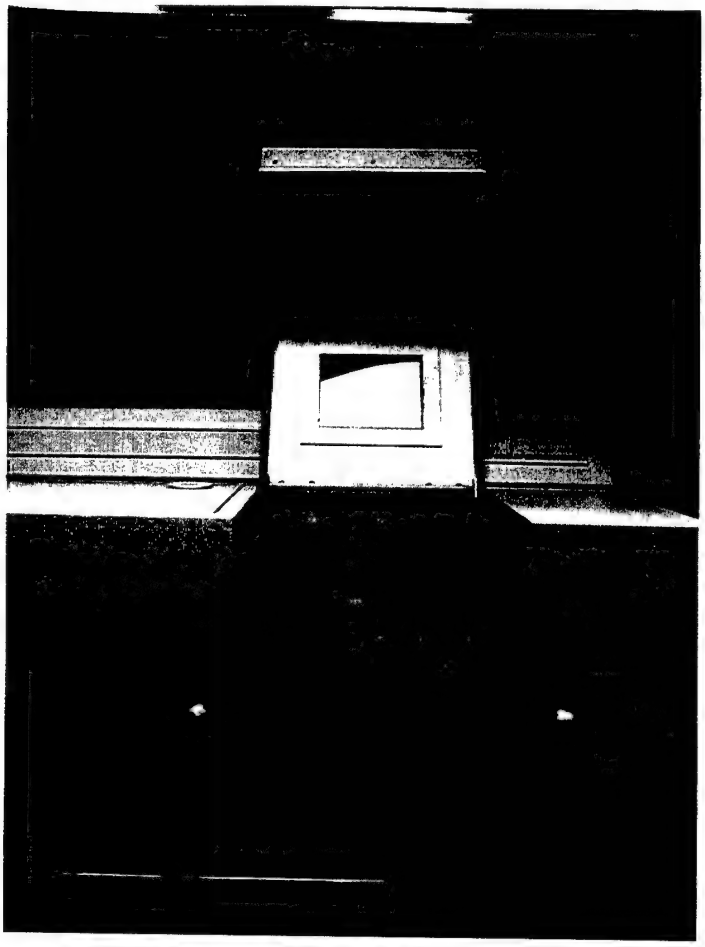

Figure 3. Sample compartment of spectropolarimeter

The spectrometer is operated in the normal fashion for one orientation of the polarization elements in the polarimeter. A series of spectra are taken with the polarization elements in a set of predetermined orientations. The spectra at all of the polarimeter settings (element orientations) are reduced as a single data set. Data reduction is performed on this data set one wavelength at a time resulting in Mueller matrix spectra. Further data reduction can produce diattenuation, retardance and depolarization spectra.

The spectrometer has a spectral range of 0.45 μm to 25μm. Three sources, three beamsplitters, and four detectors are used to cover this spectral range (with overlap). This broad spectral range also requires multiple polarization elements. Ideal polarization elements would have perfectly achromatic response; in practice, polarization elements are far from ideal, and measurement of the actual polarization element response is part of the calibration process. Polarizers are more likely to have achromatic-like response, and in many cases we assume achromaticity. Achromatic behavior of the quarter wave retarders is not a natural consequence of retarder design. In addition, the need to rotate the retarders places further restrictions on the retarder design; angular or lateral beam deviations are to be minimized. Conventional multiple-order waveplates, consisting of a single plate of birefringent material, are extremely wavelength dependent. Achromatic response can be achieved by using two multiple-order waveplates whose fast axes are perpendicular to each other[6]. The material can be the same or different for the two plates. Fresnel rhombs exhibit good achromatic behavior but also have a beam displacement. A modified Fresnel rhomb has been designed with two internal reflections that does not displace the beam and is thus suitable for rotation[7]. Polarization element types that are in current use with the spectropolarimeter are shown in Table 1.

Table 1 – Polarization element types used for various spectral ranges

	Visible	NIR (to 1.6 μm)	IR
Polarizers	Dichroic sheet	Dichroic sheet	Wire grid on BaF_2, Ge
Retarders	Two plate MgF_2	Two plate MgF_2	CdS + CdSe

2.2 Calibration and Data Reduction

The Mueller matrix provides the most complete polarization information about a sample and requires the most sophisticated polarimeter configuration and data reduction techniques. We have followed the dual rotating retarder method described by Azzam[8]. Figure 4 shows the configuration of a dual rotating retarder polarimeter in the sample compartment of the spectropolarimeter. It consists of a sample between a polarization state generator and polarization state analyzer each comprised of a stationary linear polarizer and rotating quarter-wave linear retarder. When the retarders are rotated in a five to one ratio, all sixteen elements of the sample Mueller matrix are encoded onto twelve harmonics of the detected intensity signal, which can then be Fourier analyzed to recover the Mueller matrix elements. Diattenuation, retardance, and depolarization (scattering) can be obtained from the Mueller matrix.

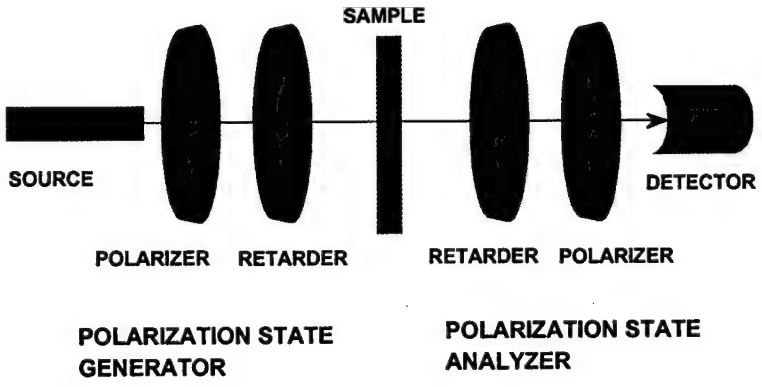

Figure 4. Dual rotating retarder configuration

The data reduction algorithm for this polarimeter as originally presented by Azzam assumes ideal polarization elements and no orientation errors. The data reduction algorithms may be generalized to compensate for systematic errors which result

when orientation misalignment and non-ideal retarders are used. If the polarization elements are rotationally misaligned, or the retarders do not have exactly one-quarter wave of retardance, the changes in Fourier amplitudes and phases result in errors in the sample Mueller matrix. Even small orientation and retardance errors (<1°) can lead to large errors in the measured Mueller matrix (> 10% in some matrix elements). These errors become especially important when the retardance and alignment vary significantly from their nominal values such as in multi-wavelength or spectral instruments. We have incorporated correction terms for large orientation and retardance errors into the dual rotating retarder data reduction algorithm. The data reduction equations we have developed correct for orientation errors up to 22.5° and retardance errors up to $\lambda/8$. These equations are quite lengthy and the reader is referred to prior presentations[9].

The dual rotating retarder configuration has a number of advantages. First, the effect of any instrumental polarization preceding the polarizing optics or following the polarimeter is negated by the fixed position of the polarizers. Second, the Fourier transform on the data automatically performs a least squares fit to the overdetermined data set. Third, this configuration is largely immune to beam wander if measurements are made over a 2π cycle. In this case, modulation from beam wander produced by wedges in the rotating retarders is encoded principally on the first and fifth Fourier amplitudes. Since the polarimeter does not modulate these frequencies, the beam wander signal does not affect the accuracy of the measured Mueller matrix.

The Mueller matrix provides the most complete description of the polarizing nature of an optical element including any depolarization. The effect of the optical element on an arbitrary incident Stokes vector can also be determined through the Mueller matrix. However, many samples of interest are non-depolarizing and display only one or a few polarization properties. Polarizers generally only display diattenuation and retarders display only retardance and small amounts of diattenuation. In order to facilitate understanding and interpretation of our Mueller matrix data, we generally apply the Mueller matrix decomposition originally developed by Lu[10] and elucidated by Hayes[11].

We briefly describe this analysis here for the non-depolarizing case. Non-depolarizing Mueller matrices have the decomposition $M = M_R M_D$, and the original Mueller matrix is normalized and denoted by

$$M = \begin{bmatrix} 1 & m_{01} & m_{02} & m_{03} \\ m_{10} & m_{11} & m_{12} & m_{13} \\ m_{20} & m_{21} & m_{22} & m_{23} \\ m_{30} & m_{31} & m_{32} & m_{33} \end{bmatrix}.$$

The diattenuator component has the form

$$M_D = \begin{bmatrix} 1 & m_{01} & m_{02} & m_{03} \\ m_{01} & a + b(m_{01})^2 & b(m_{01}m_{02}) & b(m_{01}m_{03}) \\ m_{02} & b(m_{02}m_{01}) & a + b(m_{02})^2 & b(m_{02}m_{03}) \\ m_{03} & b(m_{03}m_{01}) & b(m_{03}m_{02}) & a + b(m_{03})^2 \end{bmatrix},$$

where $a = \sqrt{1 - (m_{01}{}^2 + m_{02}{}^2 + m_{03}{}^2)}$ and $b = \dfrac{1 - \sqrt{1 - (m_{01}{}^2 + m_{02}{}^2 + m_{03}{}^2)}}{(m_{01}{}^2 + m_{02}{}^2 + m_{03}{}^2)}$.

Furthermore, the diattenuation vector is given simply by the first row of M,

$$\overline{D} = \begin{bmatrix} D_H \\ D_{45} \\ D_C \end{bmatrix} = \begin{bmatrix} m_{01} \\ m_{02} \\ m_{03} \end{bmatrix}, \text{ and total diattenuation } D = \sqrt{m_{01}{}^2 + m_{02}{}^2 + m_{03}{}^2}.$$

Hence, the magnitude of the diattenuation is solely determined by the first row of M. The retarder matrix in the non-depolarizing case is expressed as

$$M_R = \frac{1}{a}\begin{bmatrix} a & 0 & 0 & 0 \\ 0 & m_{11} - b(m_{10}m_{01}) & m_{12} - b(m_{10}m_{02}) & m_{13} - b(m_{10}m_{03}) \\ 0 & m_{21} - b(m_{20}m_{01}) & m_{22} - b(m_{20}m_{02}) & m_{23} - b(m_{20}m_{03}) \\ 0 & m_{31} - b(m_{30}m_{01}) & m_{32} - b(m_{30}m_{02}) & m_{33} - b(m_{30}m_{03}) \end{bmatrix}.$$

The overall retardance can be expressed as

$$R = \left|\overline{R}\right| = \cos^{-1}\left(\frac{tr(m_R) - 1}{2}\right)$$

and for the non-depolarizing case is given by

$$R = \cos^{-1}\left(\frac{1}{2a}\left[m_{11} + m_{22} + m_{33} - b\left(m_{10}m_{01} + m_{20}m_{02} + m_{30}m_{03}\right) - a\right]\right),$$

and the retardance vector has the form

$$\overline{R} = \begin{bmatrix} m_{23} - m_{32} - b\left(m_{20}m_{03} - m_{30}m_{02}\right) \\ m_{31} - m_{13} - b\left(m_{30}m_{01} - m_{10}m_{03}\right) \\ m_{12} - m_{21} - b\left(m_{10}m_{02} - m_{20}m_{01}\right) \end{bmatrix} \frac{\cos^{-1}\left(\frac{1}{2a}\left[m_{11} + m_{22} + m_{33} - b\left(m_{10}m_{01} + m_{20}m_{02} + m_{30}m_{03}\right) - a\right]\right)}{\sqrt{4a^2 - \left[m_{11} + m_{22} + m_{33} - b\left(m_{10}m_{01} + m_{20}m_{02} + m_{30}m_{03}\right) - a\right]^2}}$$

The elements of the diattenuation and retardance vectors represent the horizontal/vertical, ±45°, and circular components of each vector.

3. EXPERIMENTAL RESULTS

3.1 Spectrometer Configuration

The spectrometer configuration used in these first measurements covered the wavelength range from approximately 0.68μm to 1.15μm and consisted of a near-IR source, a silicon detector, and a quartz beamsplitter. There were two polarimeter configurations used. The first configuration, for the visible, consisted of polarizers made from a dichroic polymer material placed on a glass substrate. The retarders are made of MgF_2 and are designed to have a nominal λ/4 wave of retardance from 400 - 700 nm. They are anti-reflection coated. The second polarimeter configuration for the near-IR consists of polarizers made of dichroic polymers on an IR transmitting plastic substrate that are polarizing from 0.68μm to 2.2μm. The retarders are made of MgF_2, are anti-reflection coated, and are designed to have a nominal λ/4 wave retardance from 0.7 - 1.1μm. The combination of polarimeter and spectrometer spectral responses results in two spectral bands that were utilized in these measurements: one band from 0.68 to 0.83μm, hereafter referred to as the "visible" band, and the second from 0.68 to 1.17μm, hereafter referred to as the near IR band.

3.2 Calibration

Calibration runs with no sample are made. The calibration produces orientation error spectra for each of the final three elements of the polarimeter. The orientation variation with wavelength apparent in Figure 5 is most likely due to imperfections of the polarizers in the polarimeter. As will be discussed below, the near IR polarizers have less than ideal performance in the region just where the largest variation in orientation is located, in the band 0.83μm to 1.03μm. For initial calibrations that show large orientation errors (>2°), the elements are realigned. For orientation error less than about 2°, the elements are not realigned but the errors are retained for correction in the Mueller matrix data reduction. The retardances obtained in the calibration step are retained for use in the Mueller matrix data reduction. Figure 6 shows sample calibration results for the visible polarimeter. Note that in both Figures 5 and 6, the retardance curves fall almost on top of each other.

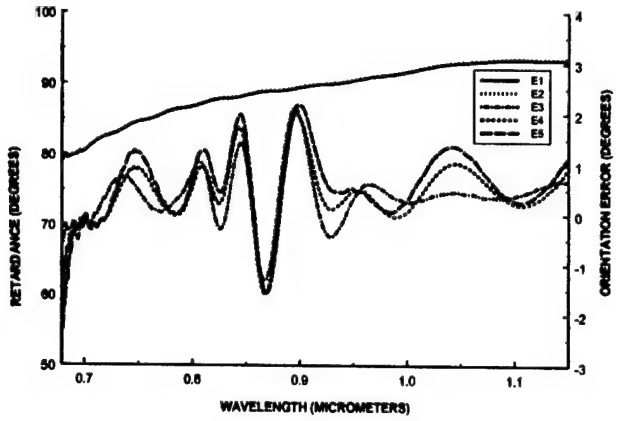

Figure 5. Orientation errors and retardances of near IR spectropolarimeter

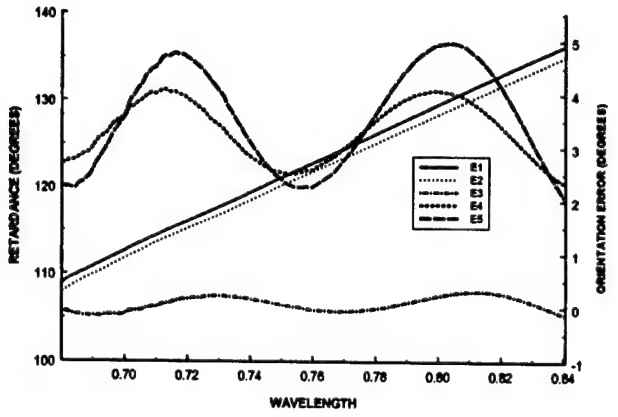

Figure 6. Orientation errors and retardances of visible spectropolarimeter

3.3 Visible polarizers and retarders

Figure 7 shows the transmission curves for parallel and crossed polarizers for the visible dichroic polarizers. These curves are qualitatively consistent with what the manufacturer reports although the bump that peaks at 0.8μm in the crossed polarizer curve does not appear in the manufacturer's data. The crossed polarizer curve shows slightly larger transmission than the parallel polarizer curve. This is most likely due to the instrumental polarization that occurs in this transmissive region of the polarizers. The long wavelength limit of the effective region of the polarizer at about 0.83μm is the long wavelength limit for the visible polarimeter.

Figure 8 shows the retardance and diattenuation computed from the Mueller matrix spectrum of the visible retarder measured with the near IR polarimeter in the region from approximately 0.68 μm to 1.15 μm. The retardance increases approximately linearly with wavelength as expected over the waveband and is consistent with the retardance data measured in calibration of the visible polarimeter shown in Figure 6. The diattenuation is relatively low in the middle of the band but increases slightly near the ends of the measured band.

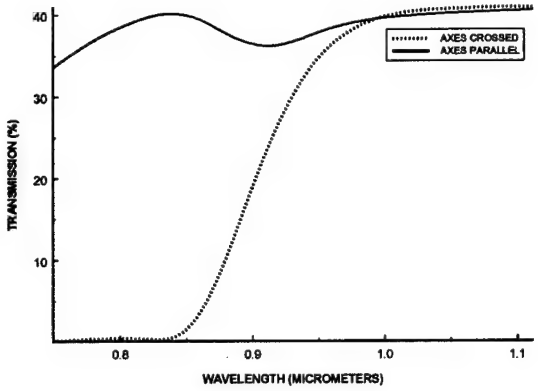

Figure 7. Visible polarizer transmission curves

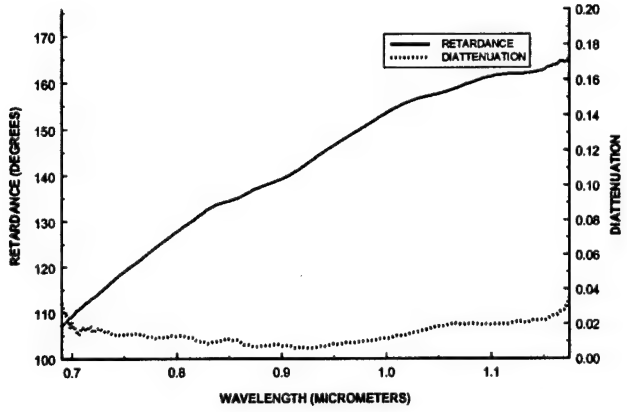

Figure 8. Characterization of visible retarder with near IR polarimeter

3.4 Near IR polarizers and retarders

The transmission curves for parallel and perpendicular near-IR polarizers are shown in Figure 9. The polarizer does not transmit significantly below about 0.7μm. The qualitative transmission performance of the parallel polarizers agrees well with the manufacturer's specification although the peak transmission measured here (32%) is slightly higher than that reported by the manufacturer (27%). The wavelength of the peak measured is in good agreement. The performance for crossed polarizers is, however, not as good as that reported by the manufacturer. The bump in transmission at approximately 0.89μm is nearly 2.5 times that reported by the manufacturer. The peak reported by the manufacturer is at 0.92μm. Mueller matrix measurements are less accurate in the region from 0.83μm to 1.03μm where the transmission for the crossed polarizers is above approximately 0.5%. The modulation produced by the rotating elements is reduced due to the lower diattenuation in this region.

Figure 10 shows the retardance and diattenuation of the achromatic retarders calculated from the Mueller matrix measurement in the region from approximately 0.68μm to 0.82μm. The retardance is increasing with wavelength over the range as expected. Each of the three retarders measured show similar response with one retarder within about 1° and the other within about 3° of the one shown. The manufacturer does not report the retardance in the specification. The diattenuation shows modulation with wavelength that is most likely due to interference effects in the AR coating on the retarder. The diattenuation is increasing toward shorter wavelengths and becomes significant (>2%) below 0.7μm.

Characterization of a second near-IR retarder is shown in Figure 11. Note that the region of lower fidelity lies between 0.83μm and 1.03μm where the polarizers in the near-IR polarimeter have significantly lower diattenuation. However, the diattenuation is large in the long wavelength region above 1.03μm (approximately 7%). This could be significant for some applications where the diattenuation affects signal modulation or ellipticity of the polarization state produced.

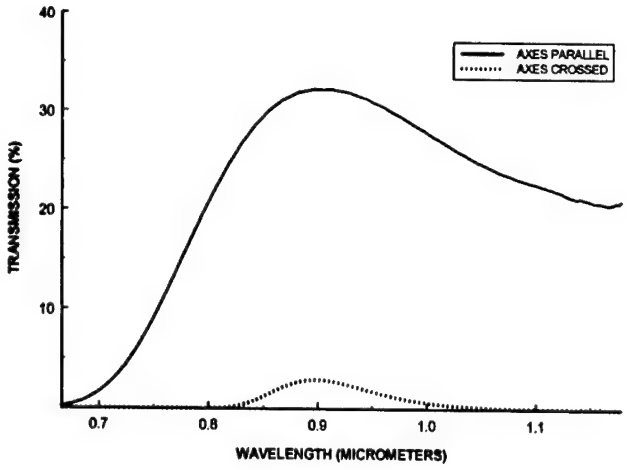

Figure 9. Near IR polarizer transmission curves

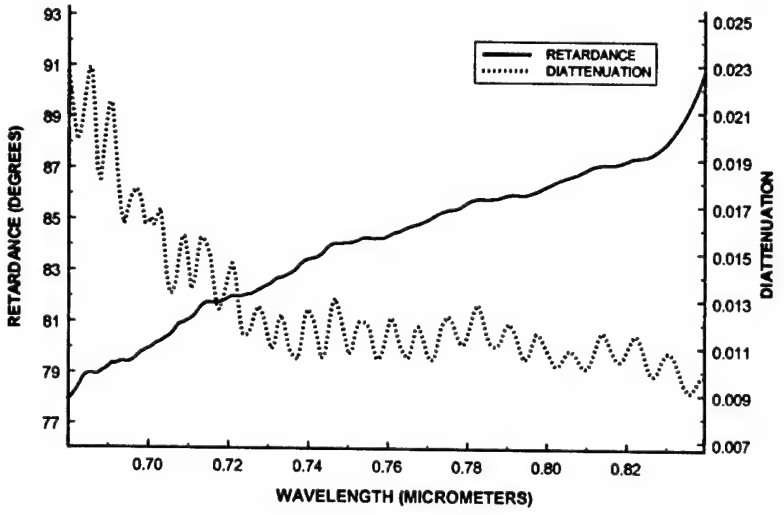

Figure 10. Characterization of near IR retarders with visible polarimeter

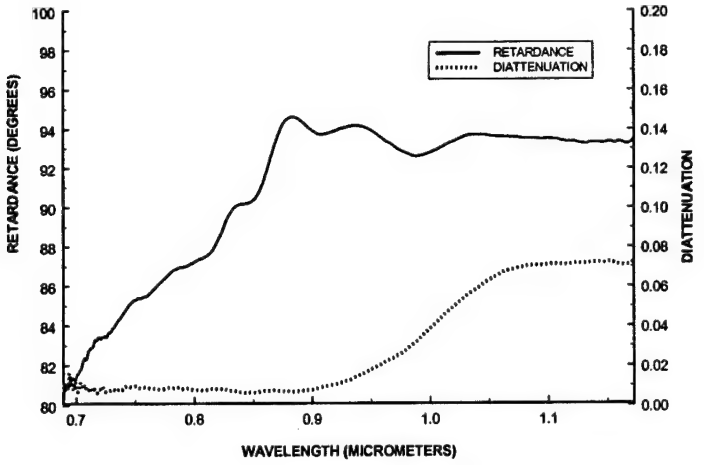

Figure 11. Characterization of near IR retarder with near IR polarimeter

3.5. Infrared Modulator Measurements

The electro-optic coefficient spectrum of cadmium telluride (CdTe) was measured using an FTIR spectropolarimeter[3,12] and will serve to demonstrate the Mueller matrix measurements that can be made with a spectropolarimeter. CdTe modulators exploit the linear electro-optical effect for modulating the retardance with an applied voltage. Used by itself, a CdTe modulator can modulate the phase by more than a half of a wave at 10.6μm. When used in conjunction with a pair of polarizers, the device serves as an intensity modulator. CdTe is typically used in laser systems at 10.6μm. To determine its suitability for use in broadband systems, however, it was necessary to characterize the device's response at other wavelengths in the infrared.

The linear electrooptic effect is the change in the ordinary and extraordinary refractive indices that is caused by and is proportional to an electric field applied across the crystal. The relationship between the refractive index change and the electric field is given by the electrooptic tensor. For a CdTe modulator operated in transverse mode, the electrooptic relationship is reduced to a single element of the electrooptic tensor, the r_{41} element and the retardance is given by

$$\delta(\lambda) = \frac{2\pi n^3 r_{41} V L}{\lambda d}$$

where n is the refractive index, V is the applied voltage, L is the length of the crystal, and d is the electrode separation. For the device measured here, the half-wave voltage is about 2400 volts. Here, we report the electro-optic response of the device in terms of the $n^3 r_{41}$ product.

A series of Mueller matrix measurements were made as the voltage applied to the modulator was ramped from 0 to 2700 volts in 300 volt increments. Figure 12 shows the Mueller matrix spectra for the 900 V measurement. The Mueller matrix has been normalized to the (1,1) element, which has been replaced by the transmission spectrum. Note that for this case (applied voltage = 900 V), the device acts as a quarter-wave retarder at 4μm. The retardance spectrum of the device was extracted from the Mueller matrix data at each voltage and the $n^3 r_{41}$ product computed by performing a linear regression on the resulting set of retardance spectra. Figure 13 shows the computed $n^3 r_{41}$ spectrum. Note that the values are relatively constant across the 3-14μm band except for the ~5% deviation that occurs in the region of low transmission. The value at 10.6μm agrees with other published data to within 6%.

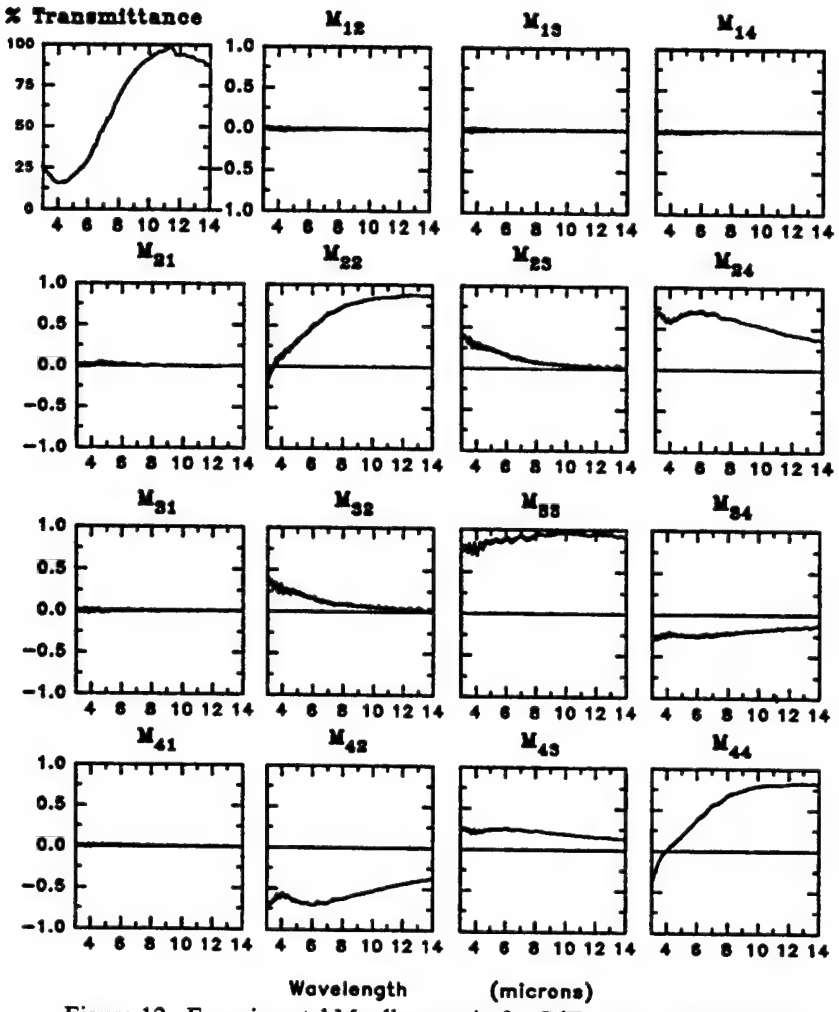

Figure 12. Experimental Mueller matrix for CdTe over an IR spectrum

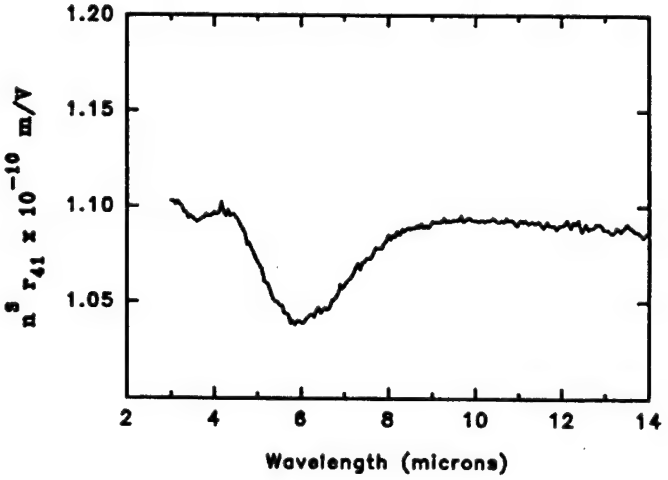

Figure 13. Spectrum of the quantity $n^3 r_{41}$

4. SUMMARY AND FUTURE WORK

We have described the development of a spectropolarimeter based on the most current generation of FT spectrometers. The spectropolarimeter is easy to use and is capable of gathering and reducing large quantities of polarimetric data in a short

period of time. The spectropolarimeter operates over a large wavelength range with changes in polarization and spectrometer elements, from less than .4 μm to greater than 25 μm. Systematic errors due to polarization element orientation misalignment and non-ideal retarders are compensated through calibration procedures and error compensation equations developed for this instrument.

Work to be completed in the immediate future includes addition of diattenuation compensation to the error correction procedures and a spectropolarimetric reflectance measurement capability. As seen in results presented here, non-ideal diattenuation can be a significant problem with some polarization elements. Compensation for measured diattenuation of polarimeter elements can be accomplished, and one of us (Hayes) has developed the necessary equations. Reflectance measurement capability, while not discussed here, is of great interest for remote sensing applications. Using the external port of the spectrometer, we are developing a spectropolarimetric reflectance capability to satisfy the need for material reflectance measurements.

5. REFERENCES

1. Goldstein, D.H. and R.A. Chipman, "Spectropolarimetry of Electro-Optical Materials," Workshop on Electronics and Electro-Optical Materials, Redstone Arsenal, May 13, 1987 (published in GACIAC proceedings).

2. D. H. Goldstein, R. A. Chipman, and D. B. Chenault Infrared, "Spectropolarimetry," *Opt. Eng.* **28** (2), pp. 120-125, 1989.

3. D. B. Chenault, "Infrared Spectropolarimetry," Ph.D. dissertation, University of Alabama in Huntsville, 1992.

4. D. H. Goldstein and D. B. Chenault, "Evaluation of a selection of commercial polarizers and retarders at visible and near-infrared wavelengths," Proc. SPIE 3121, Polarization: Analysis, Measurement, and Remote Sensing, July 1997.

5. E. A. Sornsin and R. A. Chipman, "Visible Mueller matrix spectropolarimetry," Proc. SPIE 3121, Polarization: Measurement, Analysis, and Remote Sensing, July 1997.

6. D. B. Chenault and R. A. Chipman, "Infrared achromatic retarder", U.S. Patent No. 4,961,634, October 1990.

7. D. H. Goldstein, "Infrared achromatic retarder," U.S. Patent No. 4,917,461, April 1990.

8. R. M. A. Azzam, "Photopolarimetric measurement of the Mueller matrix by Fourier analysis of a single detected signal," *Opt. Lett.* **2**, 6 pp. 148-150, 1978.

9. D. B. Chenault, J. L. Pezzaniti, and R. A. Chipman, "Mueller Matrix Polarimeter Algorithms," *SPIE* 1746, 231-246 (1992).

10. Shih-Yau Lu, "An interpretation of polarization matrices," Ph.D. dissertation, University of Alabama in Huntsville, 1995.

11. D. M. Hayes, "Error propagation in decomposition of Mueller matrices," Proc. SPIE 3121, Polarization: Measurement, Analysis, and Remote Sensing, July 1997.

12. D. B. Chenault and R. A. Chipman"Electro-optic Coefficient Spectrum of Cadmium Telluride," *Applied Optics* 33, (31), 7382-7389 (1994).

APPENDIX B

Polarimetric characterization of Spectralon

Dennis H. Goldstein, David B. Chenault, and J. Larry Pezzaniti

Proceedings of SPIE Volume 3754, July 1999

Polarimetric characterization of Spectralon

Dennis H. Goldstein
Air Force Research Laboratory
101 West Eglin Blvd
Eglin AFB, FL 32542

David B. Chenault and Larry Pezzaniti
SY Technology, Inc.
654 Discovery Drive,
Huntsville, AL 35806,

ABSTRACT

A polarimetric characterization of the reflective standard material Spectralon is presented. Samples of Spectralon with reflectances of 2%, 50%, 75% and 99% were examined. The characterization was accomplished using the Air Force Research Laboratory's spectropolarimeter in reflection mode. Data are presented for the spectral region .65 to 1.0 micrometers. Polarizance was measured for the four Spectralon samples at eight input beam incidence angles. All observations were made from normal to the Spectralon. It was found that as the incidence beam angle increases, the polarizance increases; and as the reflectance of the sample decreases, the polarizance increases.

Keywords: Polarimetry, spectropolarimeter, Mueller matrix, Spectralon, polarizance.

1. INTRODUCTION AND BACKGROUND

Spectralon is a standard reflectance material sold by Labsphere, Inc since 1986[1]. It is composed of polytetrafluoroethylene (PTFE) powder compressed by a proprietary process into a solid[2,3]. The undoped material has a hemispherical reflectance of approximately 0.99 from 400 to 1900 nm as shown in Figure 1[4]. Spectralon also approximates a lambertian reflector, a property thought to result from a porous structure and multiple internal reflections resulting in a random distribution of reflected light. Measurement results presented by Bruegge et al[3] show a slight preference for forward scattering when illuminated by a laser off normal incidence, but no specular component was observed as shown in Figure 2. Gray and colored Spectralon is produced by introducing dopants.

The motivation for this polarimetric characterization of Spectralon originated from experiments conducted on a large reflective-optic projection system. We desired to test the hypothesis that the reflective optics would induce a polarization in the radiation from an unpolarized source. A source, consisting of a 2 in diameter sample of Spectralon illuminated by an incandescent light source through an aperture, was placed at the focus of the optical system. The projection system produces a collimated beam at its exit aperture. An imaging polarimeter was placed at this aperture and focused on the source. Results from this experiment indicated that the optical system induced a uniform polarization of approximately 3% over the face of the Spectralon. However, consideration of the method of illumination of the Spectralon sample led to a requirement for additional tests. Figure 3 shows the reflective optics test configuration. The Spectralon had to be illuminated from the side because of limited space at the sample location. Subsequent qualitative tests in the absence of intervening optics confirmed that a polarization is induced in the reflected light observed at normal incidence when the illumination is from large angles off normal.

Data presented in the Labsphere catalog and shown in Figure 4[1] indicate that, at least under polarized illumination, the bidirectional reflectance distribution function of Spectralon is polarization dependent.

The data that is presented in this paper was taken with a spectropolarimeter developed at the Air Force Research Laboratory and described briefly below.

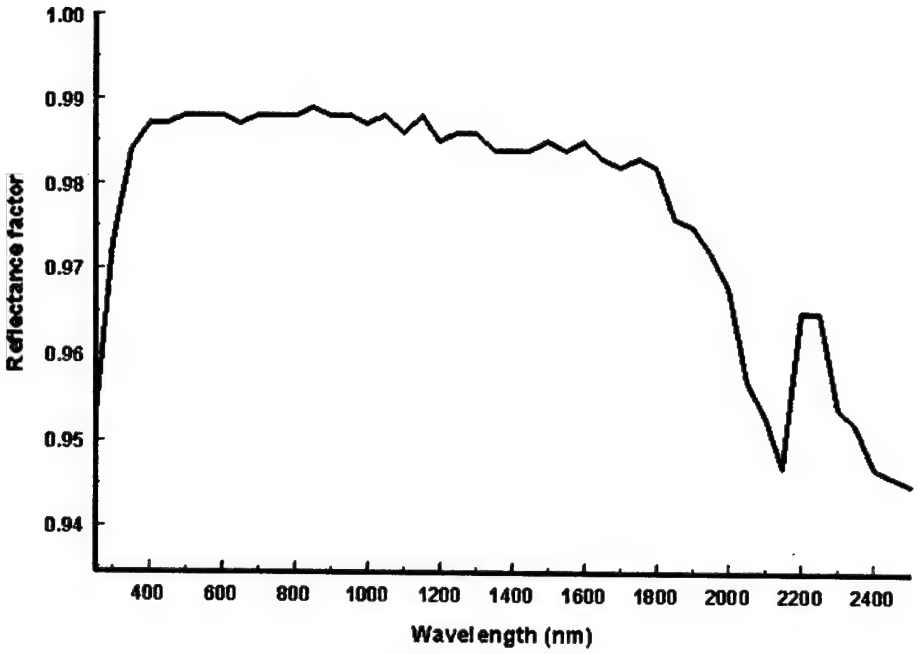

Figure 1. 8° /Hemispherical Spectral Reflectance Factor for SRS-99-020.

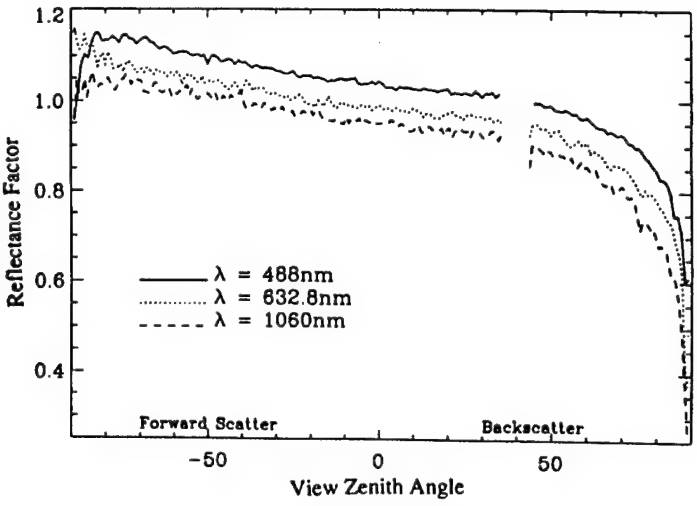

Figure 2. Reflectance factor for Spectralon illuminated with lasers at 40° (Brugge et al).

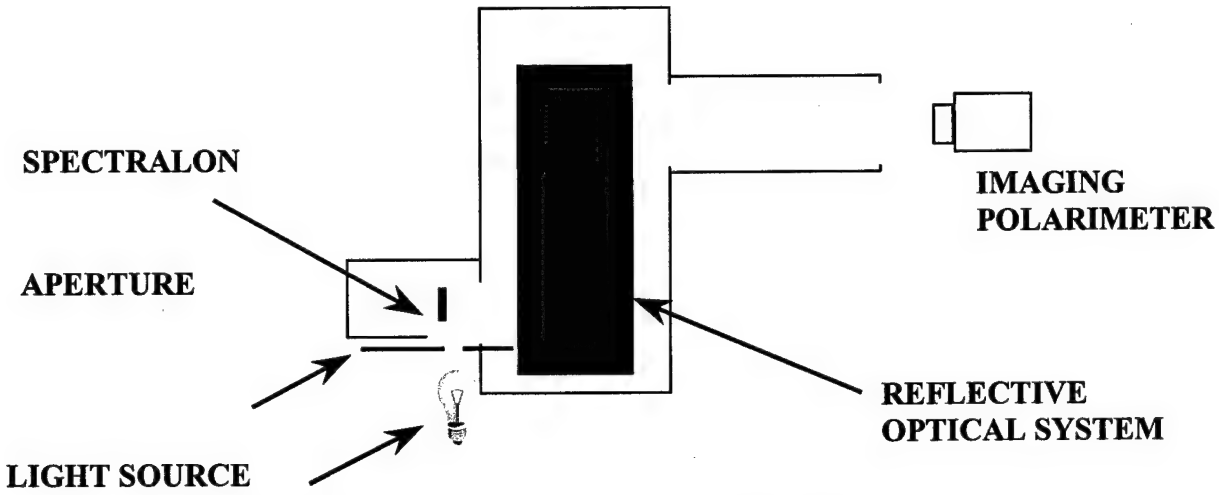

Figure 3. Reflective optical system measurement configuration.

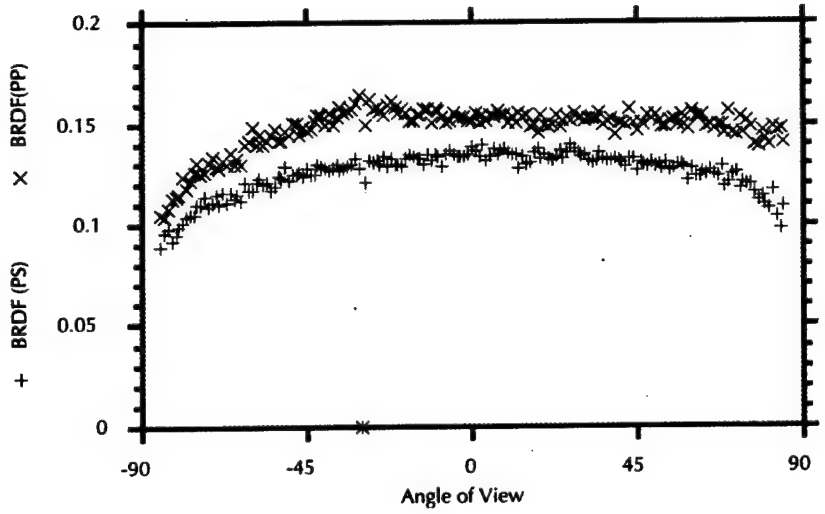

Figure 4a. In-plane BRDF for Spectralon, linearly polarized laser source (633 nm) at –30° (Labsphere).

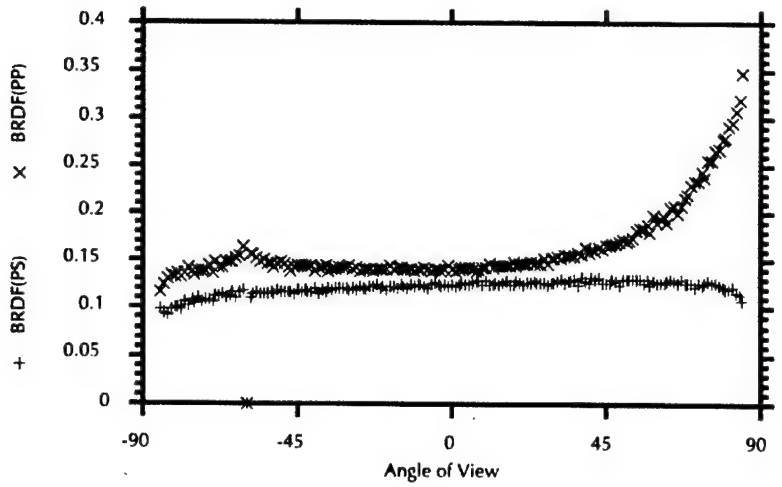

Figure 4b. In-plane BRDF for Spectralon, linearly polarized laser source (633 nm) at –60°(Labsphere).

2. FOURIER TRANSFORM SPECTROPOLARIMETRY

More than a decade ago, a spectropolarimeter based on a Nicolet Fourier transform (FT) infrared spectrometer was designed.[7,8] This instrument operates in the infrared (from 3 – 14 μm) but has high spectral resolution (better than 4 cm^{-1}). More recently, a spectropolarimeter for the visible has been developed that utilizes a broadband source and a filter wheel with suitable filters[9]. Here the spectral resolution and the number of number of spectral elements are limited by the filter bandpass and the practical size of the filter wheel.

Current FT spectrometers from a number of manufacturers operate from the ultra-violet to the infrared, covering a wavelength range from less than 0.4 to more than 25 μm. We have developed a spectropolarimeter based on one of these modern FT spectrometers. We believe that FT spectrometer-based spectropolarimeters are the most convenient and productive method of gathering large quantities of polarimetric data.

2.1 Instrumentation

The external appearance of the spectropolarimeter is shown in the photo in Figure 5. Figure 6 shows the measurement configuration. The spectrometer is operated in the normal fashion for one orientation of the polarization elements in the polarimeter. A series of spectra is taken with the polarization elements in a set of predetermined orientations. The spectra at all of the polarimeter settings (element orientations) are reduced as a single data set. Data reduction is performed on this data set one wavelength at a time resulting in Mueller matrix spectra. Further data reduction can produce diattenuation, retardance, depolarization, and other spectra.

Measurements for the present study were made from 0.4 μm to 1.0 μm. The polarization elements used in the spectropolarimetric measurements were Glan-Thompson polarizers and Karl Lambrecht achromatic retarders.

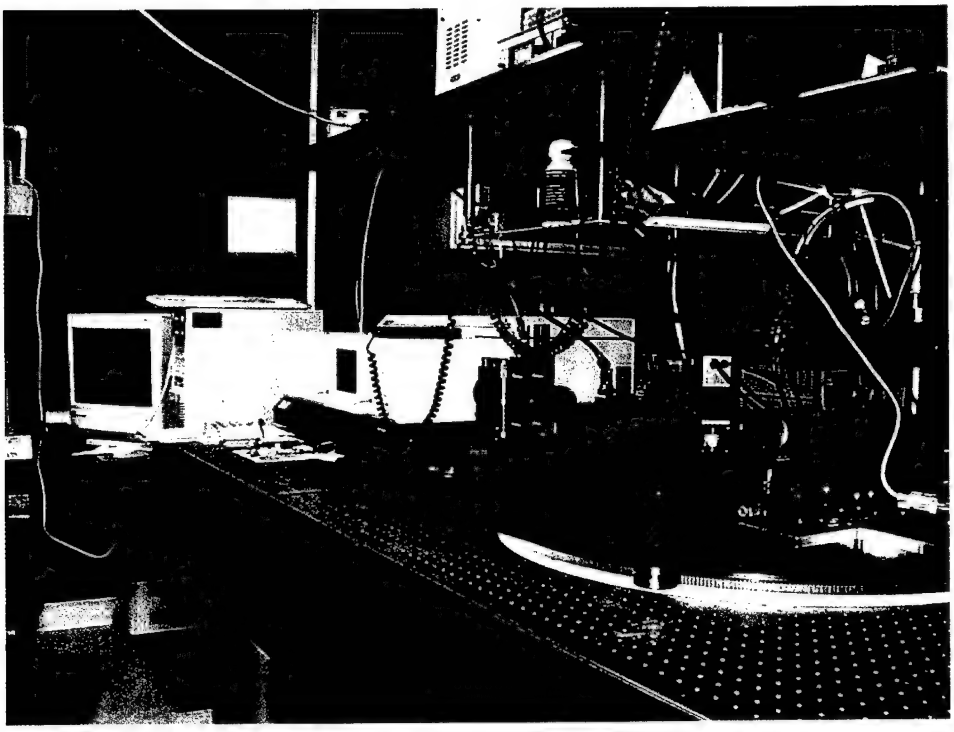

Figure 5. Photograph of FT spectropolarimeter

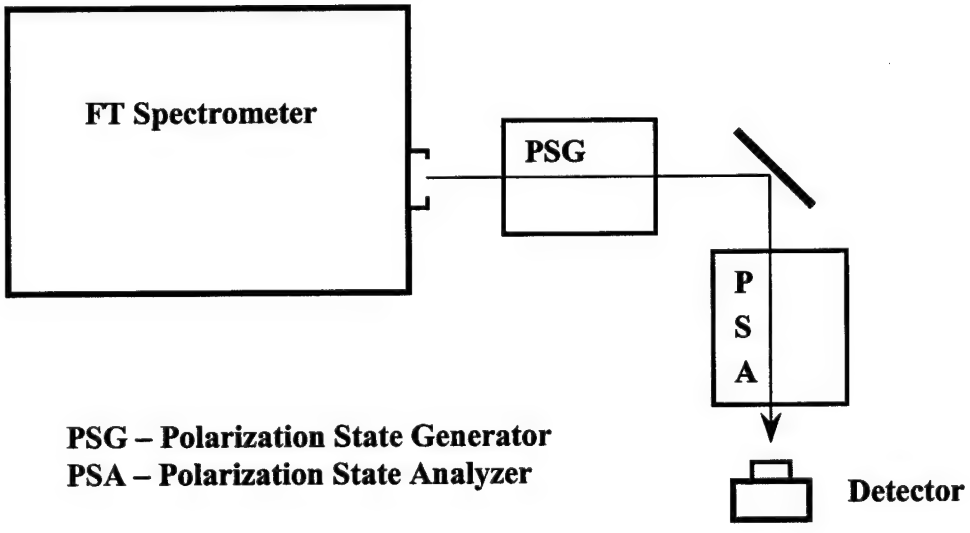

Figure 6. Diagram of FT spectropolarimeter

2.2 Data Reduction

The Mueller matrix provides the most complete polarization information about a sample and requires the most sophisticated polarimeter configuration and data reduction techniques. We have followed the dual rotating retarder method described by Azzam[11]. Figure 7 shows the configuration of a dual rotating retarder polarimeter. It consists of a sample between a polarization state generator and polarization state analyzer each comprised of a stationary linear polarizer and rotating quarter-wave linear retarder. When the retarders are rotated in a five to one ratio, all sixteen elements of the sample Mueller

matrix are encoded onto twelve harmonics of the detected intensity signal, which can then be Fourier analyzed to recover the Mueller matrix elements. Quantities such as diattenuation, retardance, and depolarization (scattering) can be obtained from the Mueller matrix.

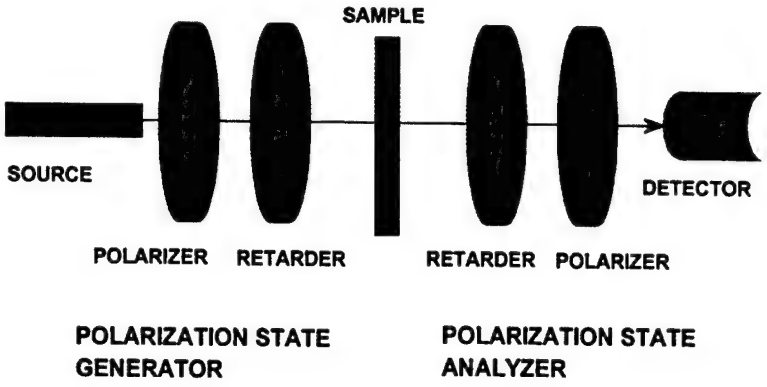

Figure 7. Dual rotating retarder configuration

The data reduction algorithm for this polarimeter as originally presented by Azzam assumes ideal polarization elements and no orientation errors. The data reduction algorithms may be generalized to compensate for systematic errors which result when orientation misalignment and non-ideal retarders are used. If the polarization elements are rotationally misaligned, or the retarders do not have exactly one-quarter wave of retardance, the changes in Fourier amplitudes and phases result in errors in the sample Mueller matrix. Even small orientation and retardance errors (<1°) can lead to large errors in the measured Mueller matrix (> 10% in some matrix elements). These errors become especially important when the retardance and alignment vary significantly from their nominal values such as in multi-wavelength or spectral instruments. We have incorporated correction terms for large orientation and retardance errors into the dual rotating retarder data reduction algorithm. The data reduction equations we have developed correct for orientation errors up to 22.5° and retardance errors up to $\lambda/8$. These equations are quite lengthy and the reader is referred to prior presentations[12].

3. EXPERIMENTAL TECHNIQUE AND RESULTS

Four samples of Spectralon having nominal reflectances of 2%, 50%, 75%, and 99% were used in the measurements. These are shown in Figure 8. The samples were placed in the spectropolarimeter and rotated to nine angles. Data were collected at these nine angles such that the detector was always aligned to the normal of the surface of the Spectralon sample. The coordinate system is shown in Figure 9, and a table of the angles used is given below. Angles measured in the clockwise direction are positive and angles measured in the counterclockwise direction are negative.

Sample	Detector
-45	135
-60	120
-75	105
-80	100
-83	97
-85	95
-87	93
-88	92
-89	91

Table 1. Sample and detector angles used in data collection.

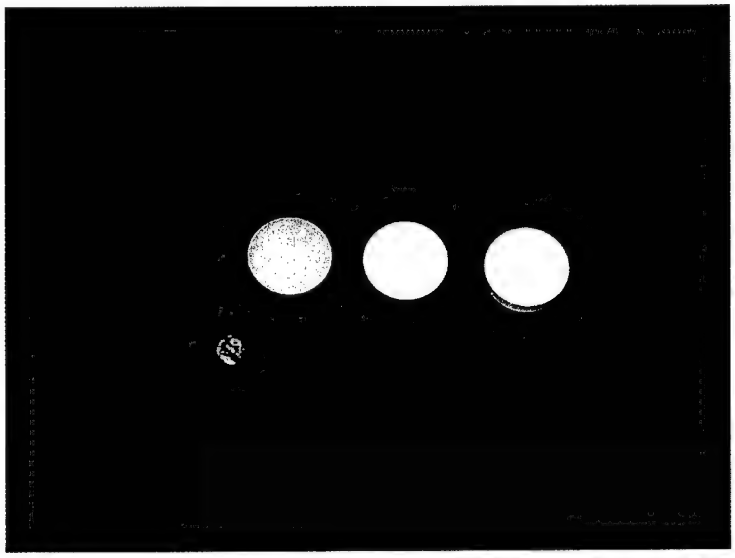

Figure 8. Spectralon samples of 2%, 50%, 75%, and 99% reflectance, left to right (a dime appears in the photo for scale).

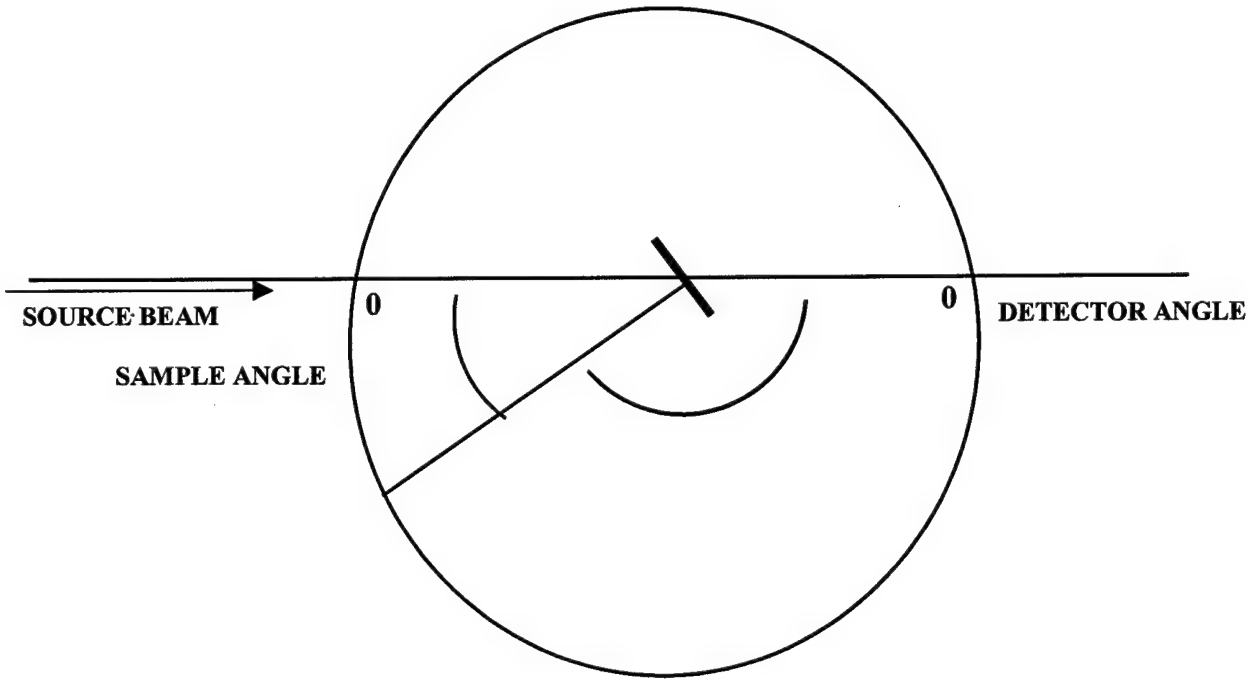

Figure 9. Spectropolarimeter coordinate system.

Data from the measurements were reduced to normalized Mueller matrices. Polarizance, the degree of polarization of the transmitted light when unpolarized light is incident[13], was computed from the Mueller matrices as

$$P = \frac{\sqrt{m_{10}^2 + m_{20}^2 + m_{30}^2}}{m_{00}}.$$

A plot of polarizance versus wavelength for the four Spectralon samples oriented at –80° is shown in Figure 10. The data that are used in all subsequent calculations and plots are for .65 to 1.0 μm. Because of the spectral content of the light source

used, the signal to noise ratio of the spectrometer is poor in the .4 to .65 μm when the entire .4 to 1.0 μm spectrum is collected. Filtering of .65 to 1.0 μm light would solve this problem.

It is evident from the results plotted in Figure 10 that the polarizance of these samples is roughly constant across this spectral range and that the lower the reflectance, the higher the polarizance. The polarizance of the 2% reflectance Spectralon is noisy because of the low signal from the sample.

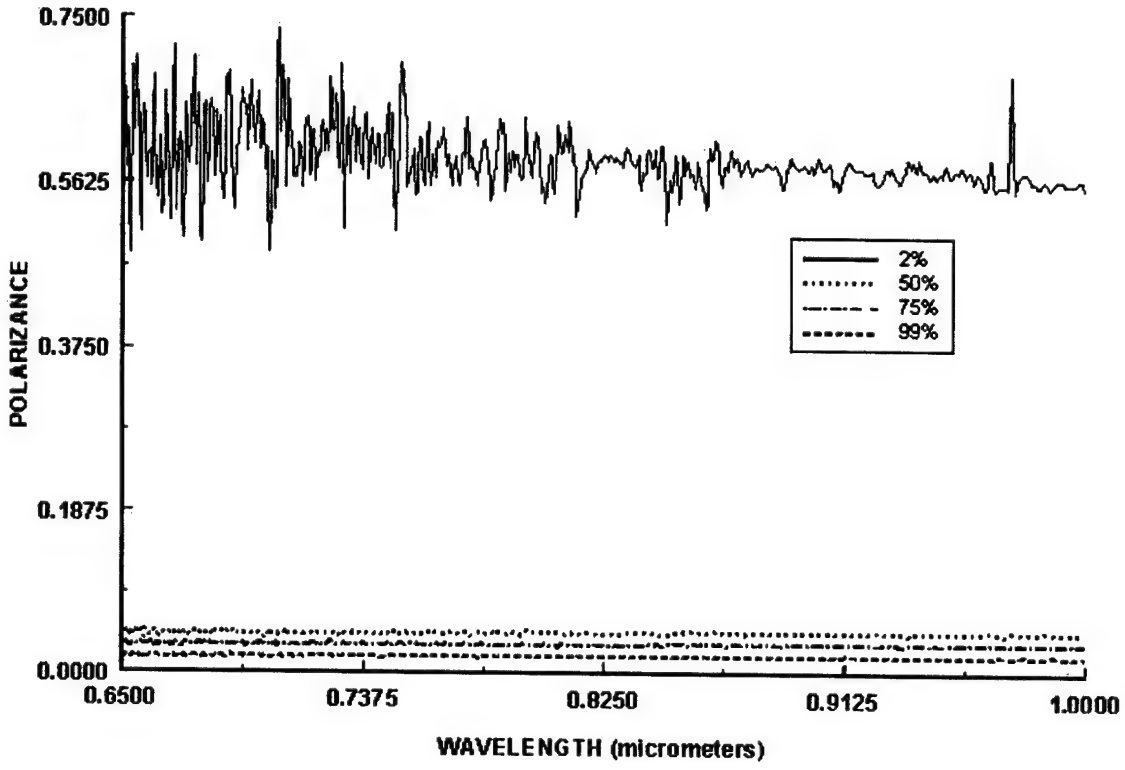

Figure 10. Spectral polarizance for four Spectralon samples, -80° source incidence angle.

The polarizance across the .65 to 1.0 μm spectral band was averaged for all subsequent analysis since it was observed to be roughly constant. Polarizance versus source beam incidence angle is plotted in Figure 11 (data from the sample angle -89° are not used, the low signal make these data very noisy). The polarizance is observed to increase as the incidence angle increases and to increase as the reflectance of the Spectralon decreases.

The polarizance versus Spectralon reflectance for each of the eight incidence angles is plotted in Figure 12. Polarizance is seen to uniformly increase with increasing incidence angle.

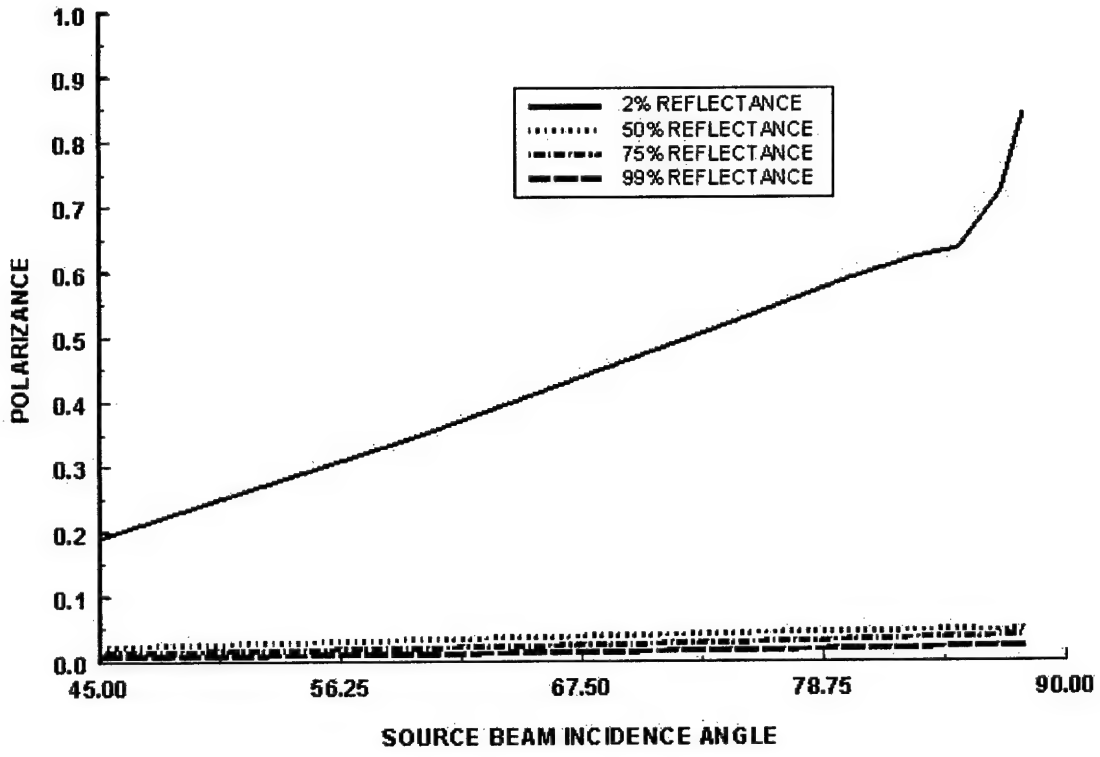

Figure 11. Averaged polarizance vs. source beam incidence angle for four values of Spectralon reflectance.

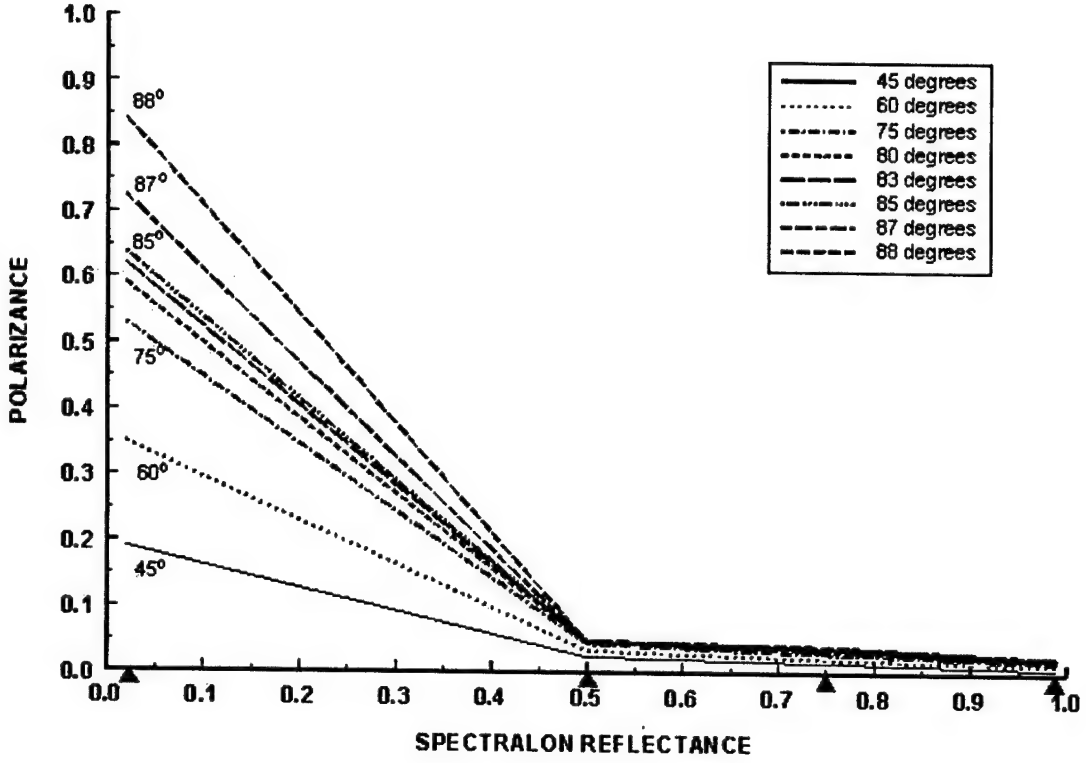

Figure 12. Averaged polarizance vs. Spectralon reflectance for eight incidence angles.

4. SUMMARY AND CONCLUSIONS

Samples of Spectralon with four nominal reflectances have been examined for polarizance over the spectral region .65 to 1.0 μm. Polarizance over this spectral region was found to be roughly constant and polarizance was averaged for all subsequent analysis. Spectralon, while a highly lambertian and predictable reflectance standard, exhibits polarizance that increases with increasing incidence angle. Polarizance also increases with decreasing reflectance.

These results tell us that the test of the reflective optical system described earlier in this paper must be done with a diffuse non-directional light source. Some of the polarization found in that test was undoubtedly due to the method of illumination of the Spectralon.

In addition to the results reported here, a large number of measurements of Spectralon were done at additional incidence angles and detector positions. These data will be used in future to perform more complete polarimetric analyses of Spectralon as a function of scatter angle.

5. REFERENCES

1. Labsphere, Diffuse Reflectance Coatings and Materials, 1997 Catalog I

2. A. E. Stiegman, C. J. Bruegge, and A. W. Springsteen, "Ultraviolet stability and contamination analysis of Spectralon diffuse reflectance material," *Opt. Eng.* **32**, (4) pp. 799-804, 1993.

3. C. J. Bruegge, A. E. Stiegman, R. A. Rainen, and A. W. Springsteen, "Use of Spectralon as a diffuse reflectance standard for in-flight calibration of earth-orbiting sensors," *Opt. Eng.* **32** (4), pp. 805-814, 1993.

4. Calibration certificate for 8° Hemispherical Reflectance Factor for SRS-99-020, Labsphere, 1998.

5. B. T. McGuckin, D. A. Haner, and R. T. Menzies, "Multiangle Imaging Spectroradiometer: optical characterization of the calibration panels," *Appl. Opt.* **36** (27), pp. 7016-7022, 1997.

6. D. A. Haner, B. T. McGuckin, R. T. Menzies, C. J. Bruegge, and V. Duval, "Directional-hemispherical reflectance for Spectralon by integration of its bidirectional reflectance," *Appl. Opt.*, **37** (18), pp. 3996-3999, 1998.

7. D. H. Goldstein. and R.A. Chipman, "Spectropolarimetry of Electro-Optical Materials," Workshop on Electronics and Electro-Optical Materials, Redstone Arsenal, May 13, 1987 (published in GACIAC proceedings).

8. D. H. Goldstein, R. A. Chipman, and D. B. Chenault, "Infrared Spectropolarimetry," *Opt. Eng.* **28** (2), pp. 120-125, 1989.

9. E. A. Sornsin and R. A. Chipman, "Visible Mueller matrix spectropolarimetry," Proc. SPIE 3121, *Polarization: Measurement, Analysis, and Remote Sensing*, pp. 156-160, July 1997.

10. D. H. Goldstein and D. B. Chenault, "Evaluation of a selection of commercial polarizers and retarders at visible and near-infrared wavelengths," Proc. SPIE 3121, *Polarization: Analysis, Measurement, and Remote Sensing*, pp. 203-212, July 1997.

11. R. M. A. Azzam, "Photopolarimetric measurement of the Mueller matrix by Fourier analysis of a single detected signal," *Opt. Lett.* **2**, (6), pp. 148-150, 1978.

12. D. B. Chenault, J. L. Pezzaniti, and R. A. Chipman, "Mueller Matrix Polarimeter Algorithms," Proc. SPIE 1746, *Polarization Analysis and Measurement*, pp. 231-246, 1992.

13. R. A. Chipman, "Polarimetry," Chapter 22 in *Handbook of Optics*, McGraw-Hill, Inc., 1995.

APPENDIX C

Polarimetric characterization of Federal Standard paints

Dennis H. Goldstein

Proceedings of SPIE Volume 4133, pp. 112-123, August 2000

Polarimetric characterization of Federal Standard paints

Dennis H. Goldstein
Air Force Research Laboratory
101 West Eglin Blvd
Eglin AFB, FL 32542

ABSTRACT

A limited polarimetric characterization of paint samples on aluminum substrates is presented. Twelve painted aluminum panels, representing various colors, reflectances, and surface finishes, were examined in a spectropolarimetric reflectometer. Data were analyzed in detail for the 0.9 to 1.0 micrometer wavelength region, although data were taken over a wider spectral range. Polarizance was measured for the twelve samples at eight input beam incidence angles. All observations were made from normal to the sample. Characterization of the surface roughness of the samples was done using profilometers. It was found that as the incidence beam angle increases, the polarizance increases; and as the reflectance of the sample decreases, the polarizance increases.

Keywords: Polarimetry, spectropolarimeter, Mueller matrix, paint, polarizance.

1. INTRODUCTION AND BACKGROUND

In a previous study[1], samples of Spectralon with four nominal reflectances were examined for polarizance over the spectral region .65 to 1.0 μm. Polarizance over this spectral region was found to be roughly constant. Spectralon, while a highly lambertian and predictable reflectance standard, exhibits polarizance that increases with increasing incidence angle. Polarizance also increases with decreasing reflectance.

Spectralon has special characteristics because of its scattering properties. Do painted surfaces exhibit the same properties? This is the question to be answered in the present work.

In order that the painted samples be referenced to some standard, paints which match Federal Standard colors (according to the manufacturer) were used. Aluminum panels painted with paints referenced to Federal Standard colors were placed in a spectropolarimetric reflectometer. Mueller matrices were collected on the painted samples and polarizance calculated.

2. FEDERAL STANDARD PAINTS AND SAMPLE PREPARATION

Federal Standard paints and colors are described in Federal Standard No. 595B, *Colors Used in Government Procurement.* Standard colors are identified by a five digit code. The first digit of the code represents finish, i.e. gloss, semi-gloss, or flat. The second digit represents a color grouping. The first two digits are then assigned as shown in Table 1.

First Digit	Finish	Second Digit	Color Grouping
1	Gloss	0	Brown
2	Semi-Gloss	1	Red
3	Flat	2	Orange
		3	Yellow
		4	Green
		5	Blue
		6	Gray
		7	Miscellaneous
		8	Fluorescent

Table 1. First two digits of Federal Standard Paint Code

The last three digits are assigned as the reflectance, from 000 to 999, where a higher reflectance has a larger number. Color chips, produced as part of the Federal Standard, are to be matched to meet the Standard. A list of suggested pigments and pigment combinations for each Federal Standard color are given. Other documents, such as the American Society for Testing and Materials Standard D 1729 and D 2244 are referenced for color matching criteria.

A source for paints referenced to Federal Standard colors is the Model Master line of paints made by the Testor Corporation. A selection of a dozen Model Master colors was chosen for this study. The colors, grouped by finish and in order of reflectance, is given in Table 2.

Gloss Color	Color Number	Semi-Gloss Color	Color Number	Flat Color	Color Number
Gloss White	17925	Tan	20400	Flat White	37875
Gloss Black	17038	Dark Drab (B52)	24091	Light Gray	36495
				Air Mobility Command Gray	36173
				Dark Green (B52)	34096
				Olive Drab	34087
				Marine Corps Green	34052
				Flat Black	37038
				US Army Helo Drab	34031

Table 2. Federal Standard paint colors used in study

These paints were sprayed with an airbrush onto 4"x4" aluminum panels. The aluminum panels were cut by water jet to retain flatness from 16-gage sheet stock. Panels were selected that had uniform finish and were free of significant marring.

3. FOURIER TRANSFORM SPECTROPOLARIMETRY

More than a decade ago, a spectropolarimeter based on a Nicolet Fourier transform (FT) infrared spectrometer was designed.[2,3] This instrument operates in the infrared (from 3 – 14 μm) but has high spectral resolution (better than 4 cm^{-1}). More recently, a spectropolarimeter for the visible has been developed that utilizes a broadband source and a filter wheel with suitable filters[4]. Here the spectral resolution and the number of spectral elements are limited by the filter bandpass and the practical size of the filter wheel.

Current FT spectrometers from a number of manufacturers operate from the ultra-violet to the infrared, covering a wavelength range from less than 0.4 to more than 25 μm. A spectropolarimeter based on one of these modern FT spectrometers has been developed. FT spectrometer-based spectropolarimeters are the most convenient and productive method of gathering large quantities of polarimetric data.

3.1 Instrumentation

The external appearance of the spectropolarimeter is shown in the photo in Figure 1. Figure 2 shows a diagram of the measurement configuration. The spectrometer is operated in the normal fashion for one orientation of the polarization elements in the polarimeter. A series of spectra is taken with the polarization elements in a set of predetermined orientations. The spectra at all of the polarimeter settings (element orientations) are reduced as a single data set. Data reduction is performed on this data set one wavelength at a time resulting in Mueller matrix spectra. Further data reduction can produce diattenuation, retardance, depolarization, and other spectra.

Measurements for the present study were made from 0..65 μm to 1.0 μm. The polarization elements used in the spectropolarimetric measurements were Glan-Thompson polarizers and Karl Lambrecht achromatic retarders.

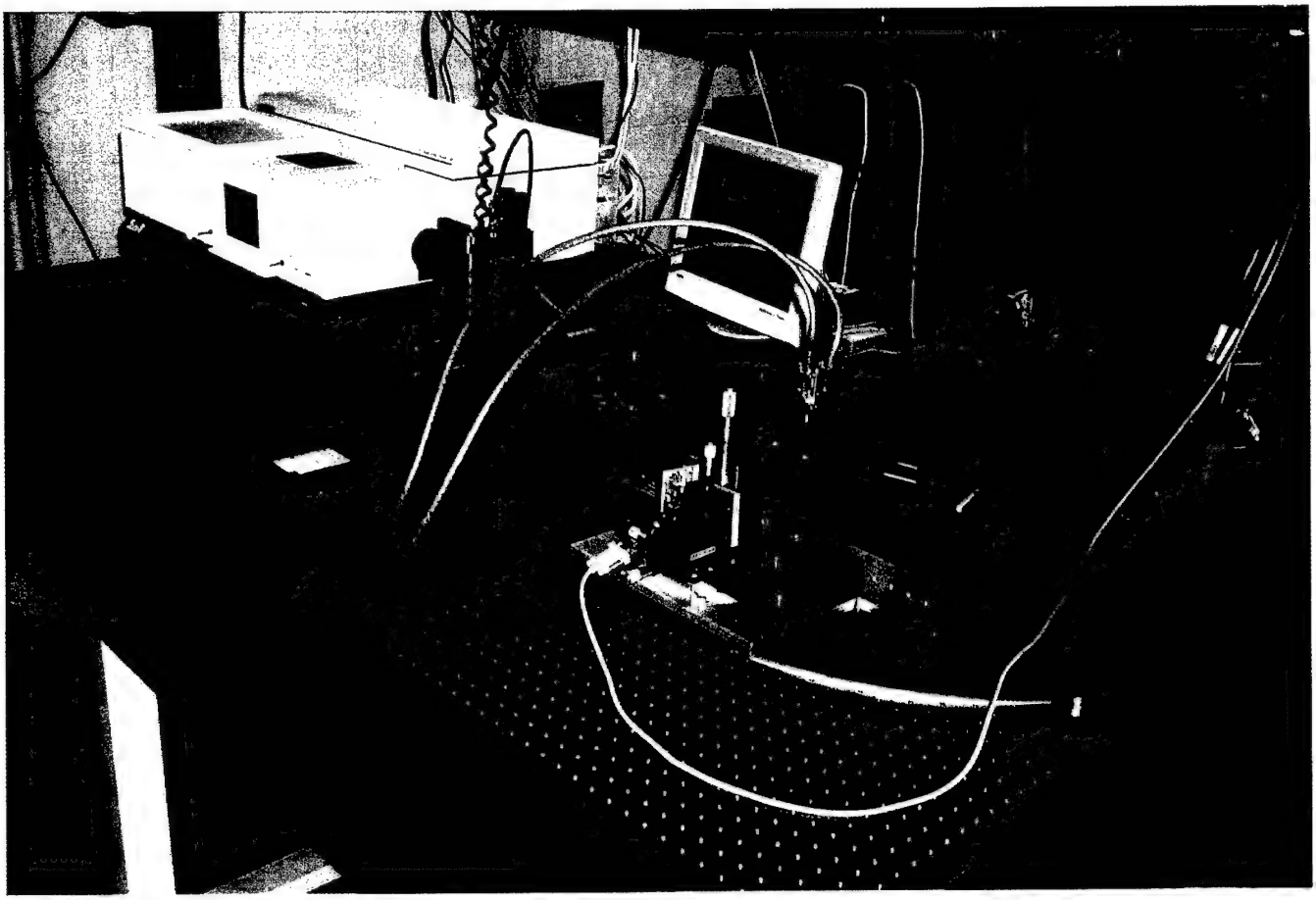

Figure 1. Photograph of FT spectropolarimetric reflectometer

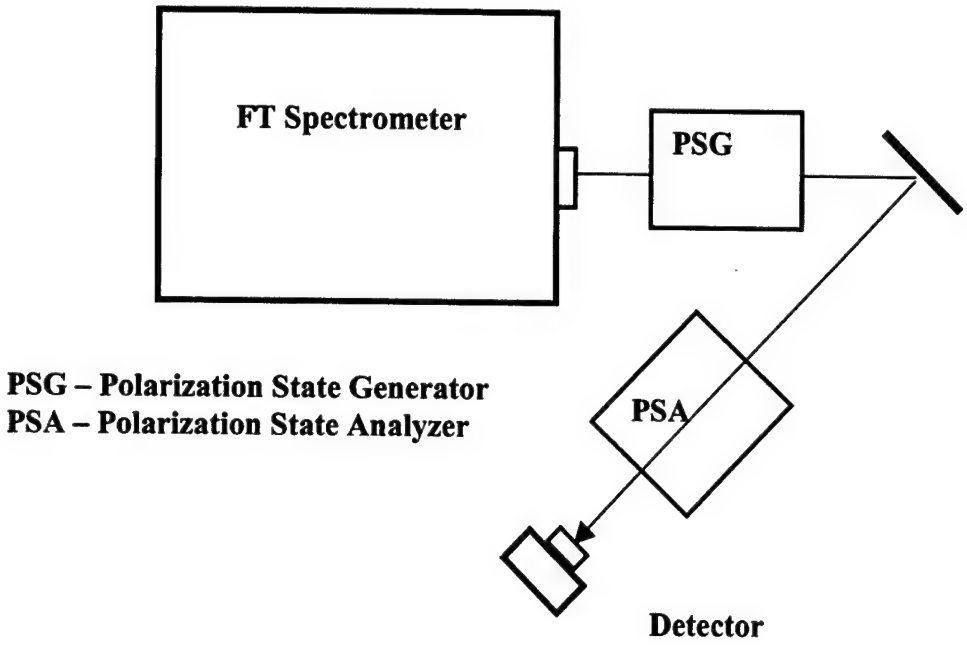

Figure 2. Diagram of FT spectropolarimeter

3.2 Data Reduction

The Mueller matrix provides the most complete polarization information about a sample and requires the most sophisticated polarimeter configuration and data reduction techniques. We have followed the dual rotating retarder method described by Azzam[5]. Figure 3 shows the configuration of a dual rotating retarder polarimeter. It consists of a sample between a polarization state generator and polarization state analyzer each comprised of a stationary linear polarizer and rotating quarter-wave linear retarder. When the retarders are rotated in a five to one ratio, all sixteen elements of the sample Mueller matrix are encoded onto twelve harmonics of the detected intensity signal, which can then be Fourier analyzed to recover the Mueller matrix elements. Quantities such as diattenuation, retardance, and depolarization (scattering) can be obtained from the Mueller matrix.

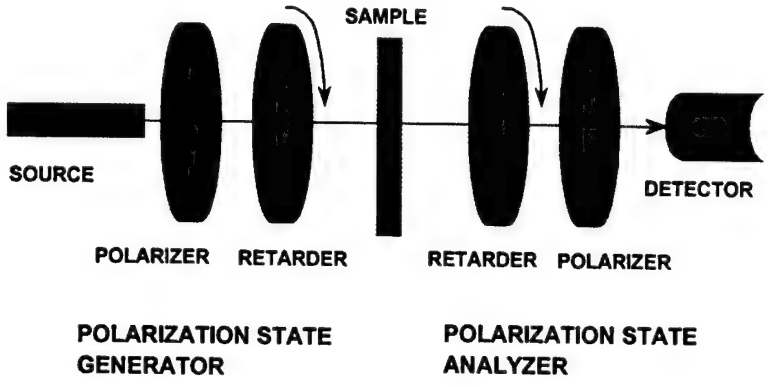

Figure 3. Dual rotating retarder configuration

The data reduction algorithm for this polarimeter as originally presented by Azzam assumes ideal polarization elements and no orientation errors. The data reduction algorithms may be generalized to compensate for systematic errors which result

when orientation misalignment and non-ideal retarders are used. If the polarization elements are rotationally misaligned, or the retarders do not have exactly one-quarter wave of retardance, the changes in Fourier amplitudes and phases result in errors in the sample Mueller matrix. Even small orientation and retardance errors (<1°) can lead to large errors in the measured Mueller matrix (> 10% in some matrix elements). These errors become especially important when the retardance and alignment vary significantly from their nominal values such as in multi-wavelength or spectral instruments. We have incorporated correction terms for large orientation and retardance errors into the dual rotating retarder data reduction algorithm. The data reduction equations we have developed correct for orientation errors up to 22.5° and retardance errors up to $\lambda/8$. These equations are quite lengthy and the reader is referred to prior presentations[6].

4. EXPERIMENTAL TECHNIQUE AND RESULTS

The painted aluminum panels are shown in Figure 4. The samples were placed in the spectropolarimeter and rotated to nine angles. Data were collected at these nine angles such that the detector was always aligned to the normal of the surface of the sample. The coordinate system is shown in Figure 5, and a table of the angles used is given in Table 3. Angles measured in the clockwise direction are positive and angles measured in the counterclockwise direction are negative.

Sample	Detector
-45	135
-60	120
-75	105
-80	100
-83	97
-85	95
-87	93
-88	92
-89	91

Table 3. Sample and detector angles used in data collection.

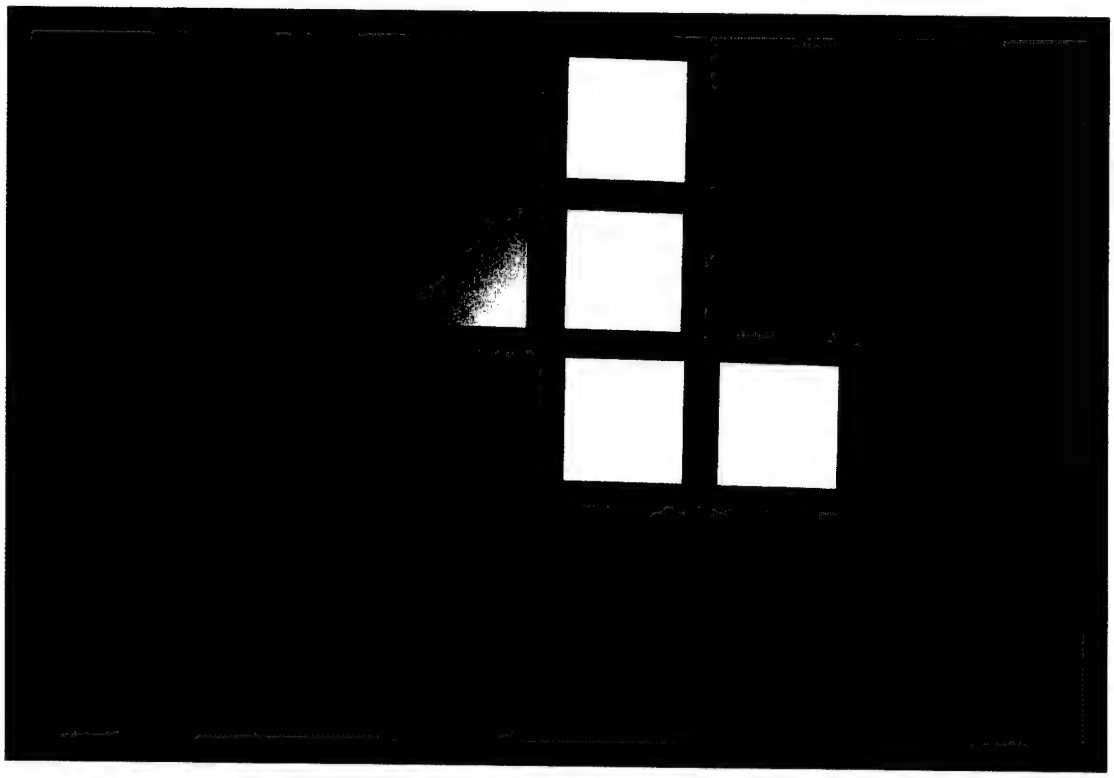

Figure 4. Painted aluminum panels.

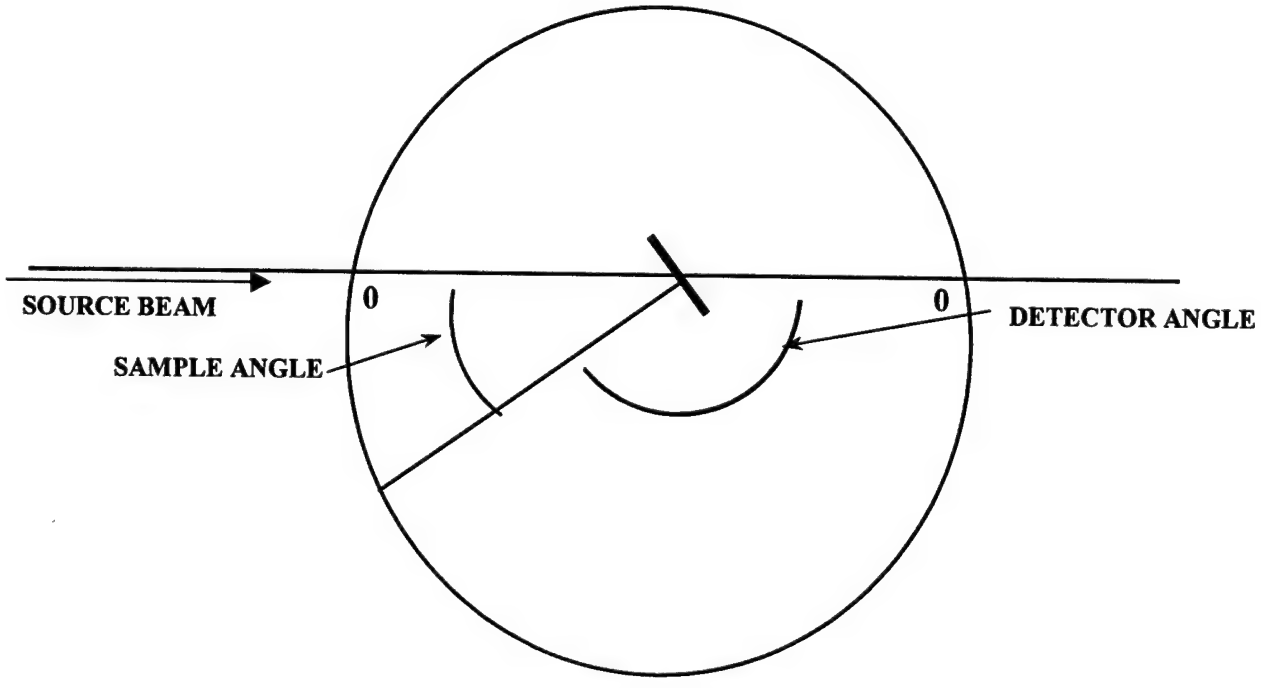

Figure 5. Spectropolarimeter coordinate system.

Data from the measurements were reduced to normalized Mueller matrices. Polarizance, the degree of polarization of the transmitted light when unpolarized light is incident[7], was computed from the Mueller matrices as

$$P = \frac{\sqrt{m_{10}^2 + m_{20}^2 + m_{30}^2}}{m_{00}}.$$

A plot of polarizance versus wavelength from .65 to 1.0 μm for five samples oriented at –45° is shown in Figure 6. The polarizance for Spectralon was constant across this spectral range, but the painted samples have structure, particularly in the 0.65 to 0.85 μm region. Polarizance is approximately constant over the 0.9 to 1.0 μm spectral region and all subsequent calculations and plots are for this region.

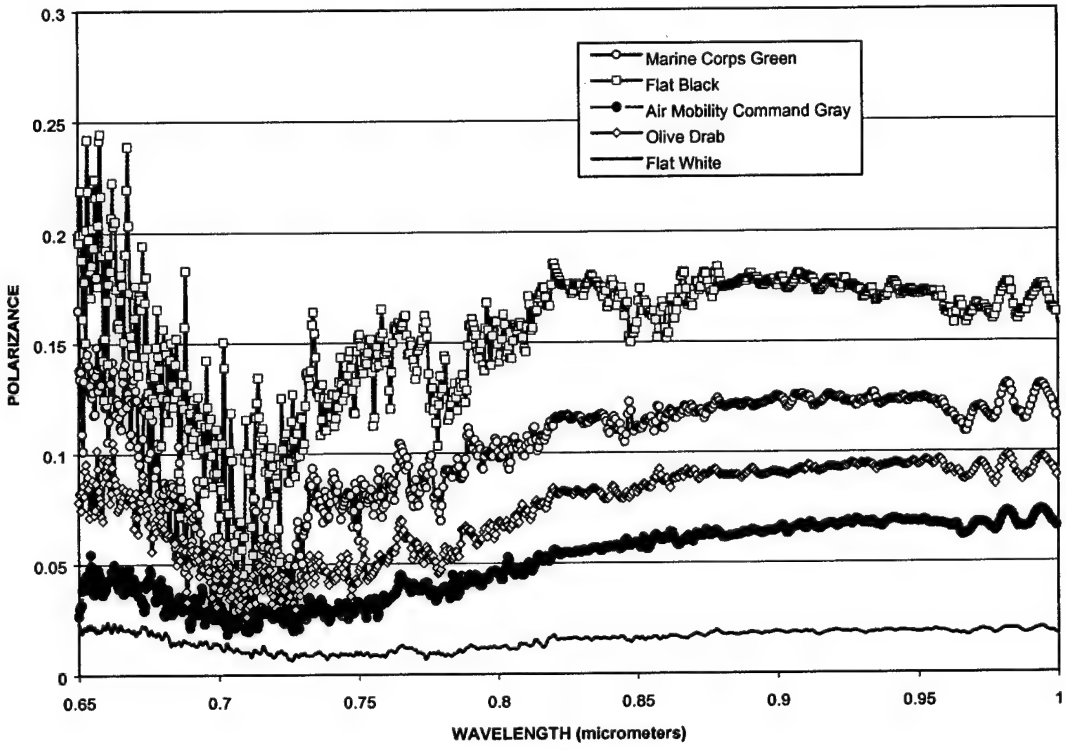

Figure 6. Spectral polarizance for five samples, -45° source incidence angle.

An average reflectance at a -15° source incidence angle (as close to normal reflectance as can be measured with this instrument) was measured for all the samples. These results are shown in Table 4.

Gloss Color	Reflectance	Semi-Gloss Color	Reflectance	Flat Color	Reflectance
Gloss White	.556	Tan	.598	Flat White	.630
Gloss Black	.006	Dark Drab (B52)	.128	Light Gray	.391
				Air Mobility Command Gray	.173
				Dark Green (B52)	.175
				Olive Drab	.088
				Marine Corps Green	.131
				Flat Black	.035
				US Army Helo Drab	.101

Table 4. Average reflectance of Federal Standard paints at -15° source incidence angle.

Surface roughness of the samples was measured with two types of profilometers. Results from the measurements made with a Zygo profilometer are given in Table 5, and these results are consistent with those obtained with a Tencor profilometer (not

given here). The surfaces painted with the flat paints have a roughness in the 1-3 μm range, the semi-gloss paints have a roughness of approximately 0.5 μm, and the gloss paints are an order of magnitude smaller in roughness at 0.05 μm. A bare aluminum sample was also measured and found to have a roughness of .38 μm or less, although microscopic examination of the bare metal shows stria not found in the painted samples.

Gloss Color	RMS Roughness	Semi-Gloss Color	RMS Roughness	Flat Color	RMS Roughness
Gloss White	60 nm	Tan	430 nm	Flat White	3260 nm
Gloss Black	50 nm	Dark Drab (B52)	460 nm	Light Gray	2530 nm
				Air Mobility Command Gray	1380 nm
				Dark Green (B52)	1070 nm
		Bare Aluminum	380 nm	Olive Drab	2290 nm
				Marine Corps Green	1150 nm
				Flat Black	2400 nm
				US Army Helo Drab	1210 nm

Table 5. RMS roughness of painted panels.

Polarizance versus source beam incidence angle is plotted in Figure 7, 8 and 9. The polarizance is observed to increase as the incidence angle increases and to increase as the reflectance of the paint decreases.

The polarizance versus paint reflectance for five incidence angles and six paint samples is plotted in Figure 10. Polarizance is seen to uniformly increase with increasing incidence angle.

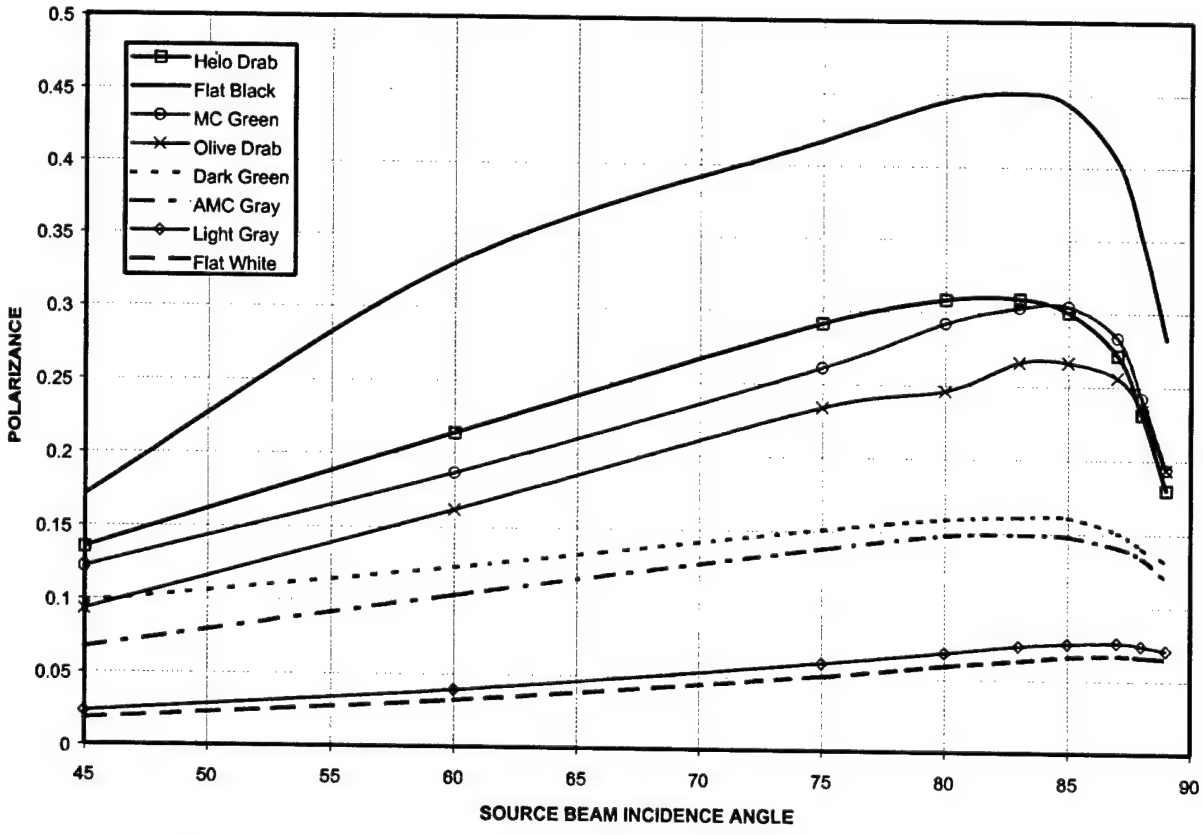

Figure 7. Averaged polarizance vs. source beam incidence angle for eight flat paints

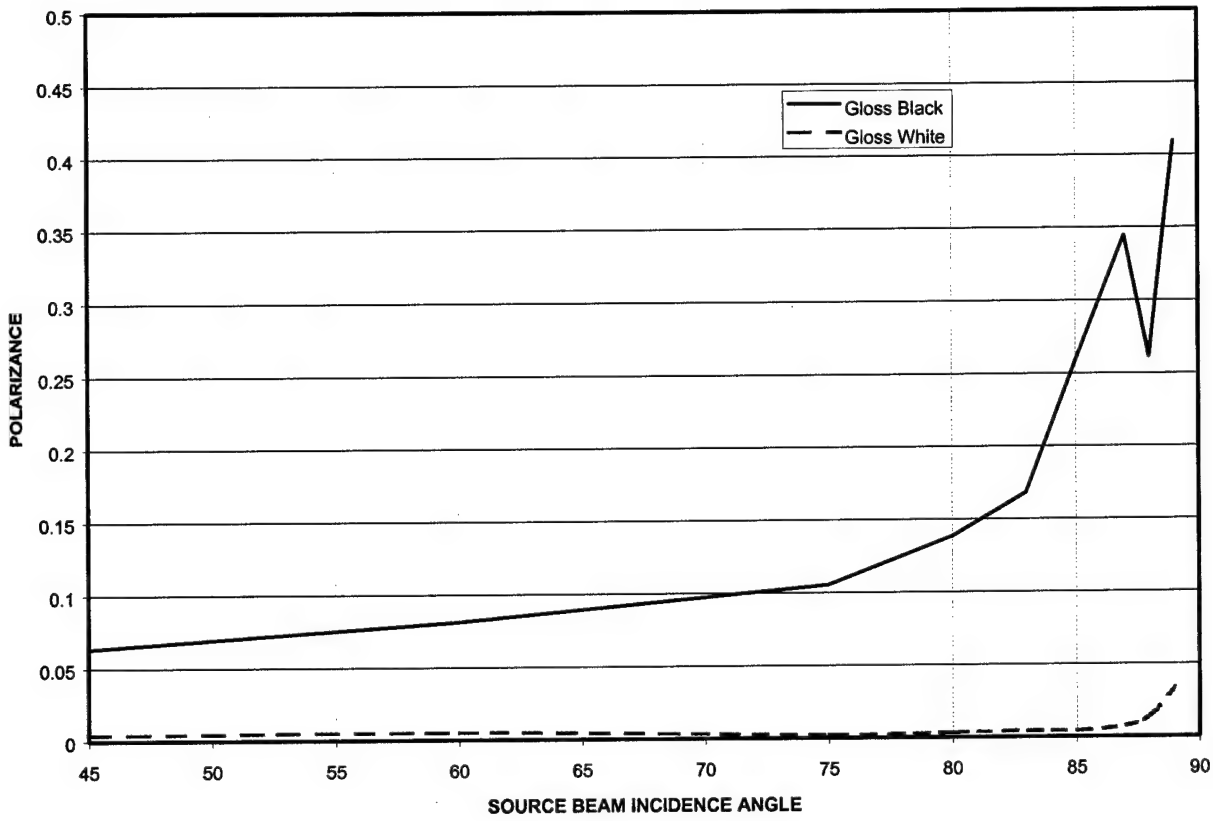

Figure 8. Averaged polarizance vs. source beam incidence angle for two gloss paints

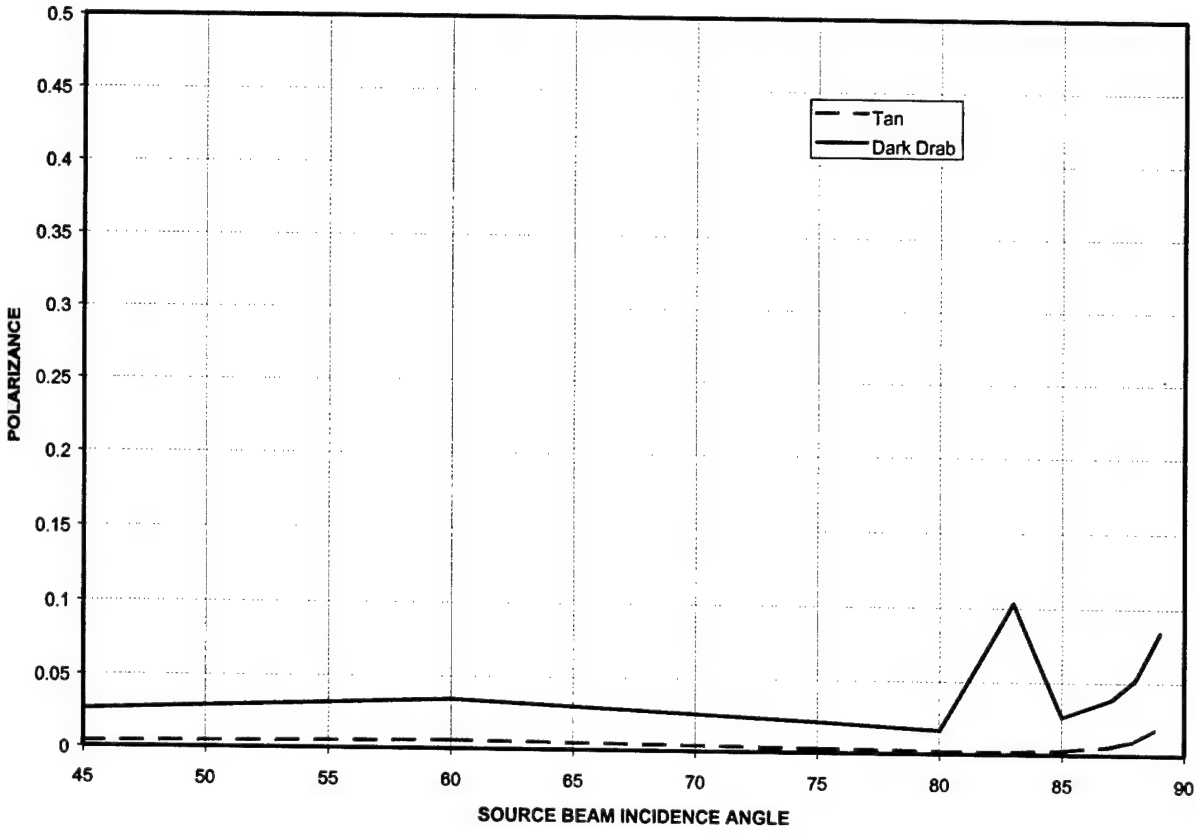

Figure 9. Averaged polarizance vs. source beam incidence angle for two semi-gloss paints.

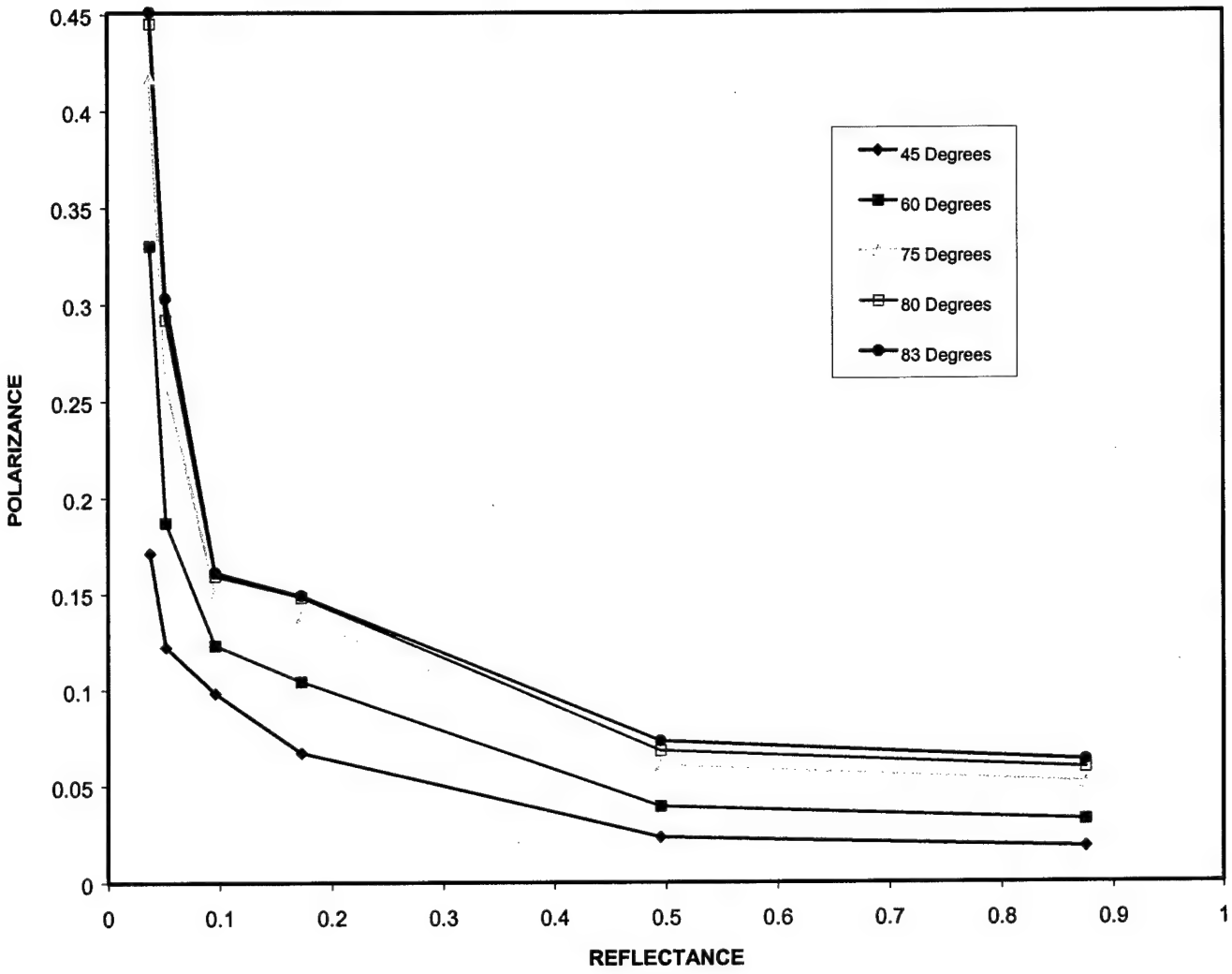

Figure 10. Averaged polarizance vs. reflectance for six paint samples and five incidence angles.

5. SUMMARY AND CONCLUSIONS

Twelve samples of aluminum painted with Federal Standard paints were examined with a spectropolarimetric reflectometer over the 0.9 to 1.0 μm spectral region. Polarizance was computed from measured Mueller matrices. The polarizance values given in this paper were averaged values over this spectral region since the polarizance was nearly constant.

The purpose of this work was to relate the polarizance to reflectance of the paint and the incidence angle. As was found for Spectralon in an earlier work[1], polarizance was found to increase with decreasing reflectance and to increase with increasing incidence angle. This generalization holds true for all surface roughnesses if they are compared to like surfaces.

ACKNOWLEDGEMENTS

The author wishes to acknowledge the profilometer measurements of the samples done by David Chenault, Larry Pezzaniti, and Michelle Banish of SY Technology, Inc., Huntsville AL under USAF Cooperative Research and Development Agreement Number 00-MN-02.

REFERENCES

1. D.H. Goldstein, D.B. Chenault, and L. Pezzaniti, "Polarimetric characterization of Spectralon," Proc. SPIE 3754, *Polarization: Measurement, Analysis, and Remote Sensing II*, pp. 126-136, July 1999.

2. D. H. Goldstein. and R.A. Chipman, "Spectropolarimetry of Electro-Optical Materials," Workshop on Electronics and Electro-Optical Materials, Redstone Arsenal, May 13, 1987 (published in GACIAC proceedings).

3. D. H. Goldstein, R. A. Chipman, and D. B. Chenault, "Infrared Spectropolarimetry," *Opt. Eng.* **28** (2), pp. 120-125, 1989.

4. E. A. Sornsin and R. A. Chipman, "Visible Mueller matrix spectropolarimetry," Proc. SPIE 3121, *Polarization: Measurement, Analysis, and Remote Sensing*, pp. 156-160, July 1997.

5. R. M. A. Azzam, "Photopolarimetric measurement of the Mueller matrix by Fourier analysis of a single detected signal," *Opt. Lett.* **2**, (6), pp. 148-150, 1978.

6. D. B. Chenault, J. L. Pezzaniti, and R. A. Chipman, "Mueller Matrix Polarimeter Algorithms," Proc. SPIE 1746, *Polarization Analysis and Measurement*, pp. 231-246, 1992.

7. R. A. Chipman, "Polarimetry," Chapter 22 in *Handbook of Optics*, McGraw-Hill, Inc., 1995.

APPENDIX D

Near infrared imaging polarimetry

Dennis H. Goldstein, David B. Chenault, Michael Gulley, and Kevin Spradley

Proceedings of SPIE Volume 4481, pp. 100-108, July 2001

Near infrared imaging polarimetry

Dennis H. Goldstein
Air Force Research Laboratory
101 West Eglin Blvd
Eglin AFB, FL 32542

David B. Chenault
Michael Gulley
Kevin Spradley

SY Technology, Inc.
654 Discovery Drive
Huntsville AL 35806

ABSTRACT

A near infrared Stokes imaging polarimeter is described. Basic principles of operation are presented, system specifications are given, and polarization elements are characterized. System control software and data reduction techniques are briefly explained. Examples of scenes collected as visible photos, visible and near infrared intensity images, and visible and near infrared polarization images are presented.

Keywords: Polarization, near infrared polarimetry, polarization imaging, Stokes polarimetry.

1. INTRODUCTION AND BACKGROUND

This paper describes a near infrared Stokes imaging polarimeter. There are a number of different techniques to acquire full Stokes vector information on an extended scene[1-6]. We have used rotating retarder polarimetry in this work. An illustration of this technique is shown in Figure 1. A focal plane detector array images light from the image source. A polarizer and retarder are placed in front of the focusing optics. The polarizer is closest to the optics and its polarization axis is fixed in some convenient orientation. A quarter wave retarder is then placed in front of the polarizer. During image collection, the retarder is rotated to many different positions. An image is collected and stored for each of the retarder positions and a Stokes vector is computed for each pixel of the imaging array during a later data reduction computation. This rotating retarder method has the advantage that implementation is relatively easy and straightforward. Components that make up the system may be purchased; most of the development required is for software. The polarimeter system is rugged and portable. We have previously built and operated a Stokes imaging polarimeter for the visible based on a silicon focal plane array and using the same principles[6]; the work described here concerns a near-infrared polarimeter.

2. SYSTEM DESCRIPTION

2.1 Instrumentation

A system block diagram is shown in Figure 2. A computer, which may be a laptop in a docking station, controls the operation of the system. Image acquisition and stage controller boards are inserted into the computer. In this case the image acquisition card is a National Instruments PCI 1424 digital acquisition card and is connected to the camera electronics. The stage controller is a Newport product and is connected via an interface box to Newport 495B rotary stages. These stages have high resolution (0.001°) but are not very fast (8° per second). Both the polarizer and retarder are placed in rotating stages for alignment purposes; the retarder is the only element which rotates during data collection. The polarizer is a Melles Griot near-infrared polarizer and the retarder is a Lambrecht SiO2/MgF2 achromatic near-infrared retarder. Parallel and perpendicular transmission of the polarizer referenced to Glan-Thompson prisms is shown in Figure 3. Retardance vs. wavelength is plotted in Figure 4. A filter may be placed in front of the rotating retarder in order to restrict the wavelength

range of the system. A silicon window makes a good filter for this system. Silicon transmission is shown in Figure 5. The camera is a Sensors Unlimited InGaAs model SU320-1.7RT-D. The format is 320x240 with 40μm pixel pitch. It is sensitive to .9 to 1.7 μm radiation. Typical responsivity for InGaAs is shown in Figure 6. Digitization is 12 bit uncorrected. Our camera has many dead pixels and requires a nonuniformity correction for best results. We have taken data in order to accomplish the nonuniformity correction, but have not implemented this correction. Data obtained for this paper is raw camera data with a background subtraction. The background subtraction and nonuniformity correction procedures are described in the section on calibration. LabView was used to operate the system and control data collection. A photograph of the system is shown in Figure 7.

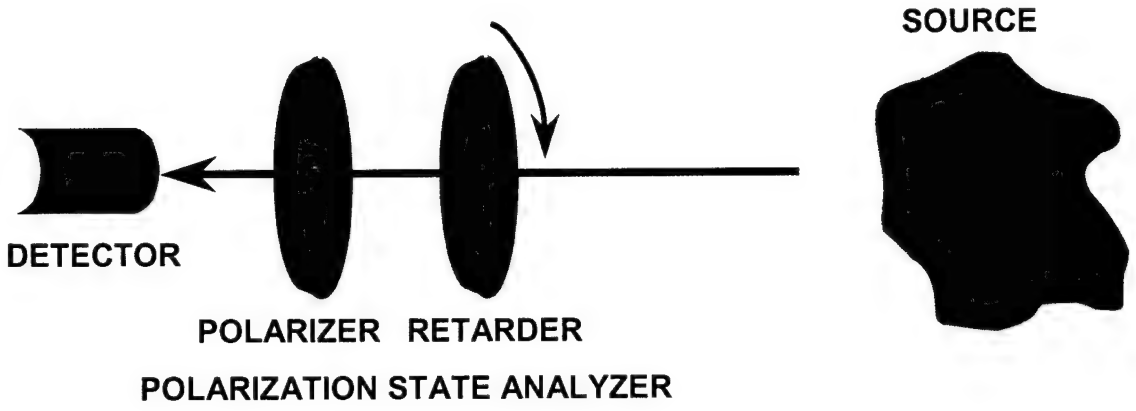

Figure 1. Diagram of rotating retarder Stokes polarimetry

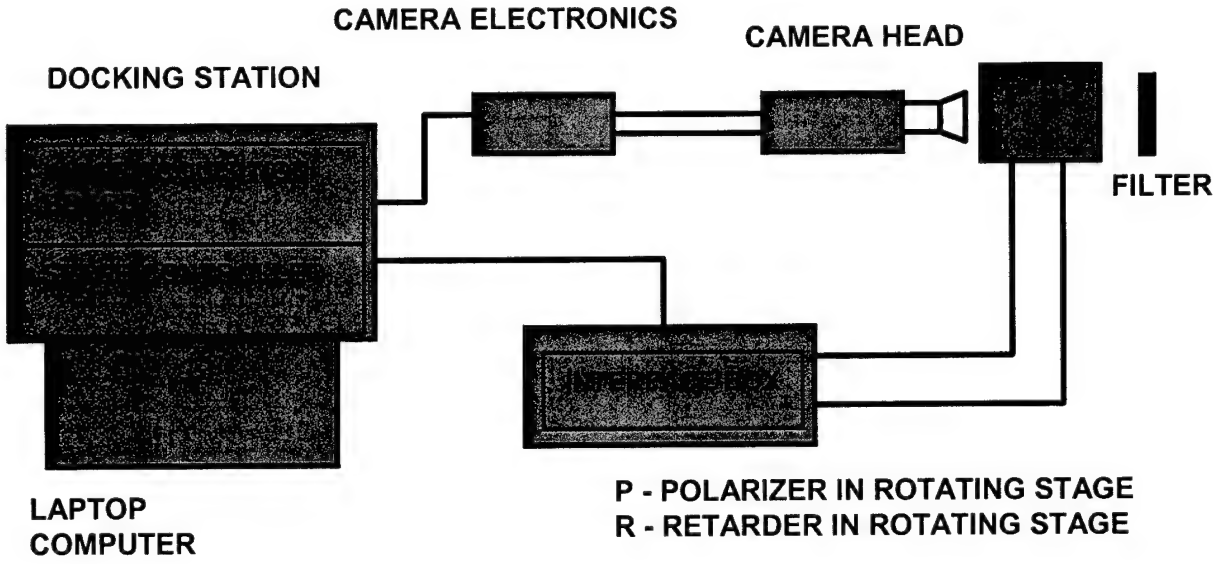

Figure 2. System block diagram

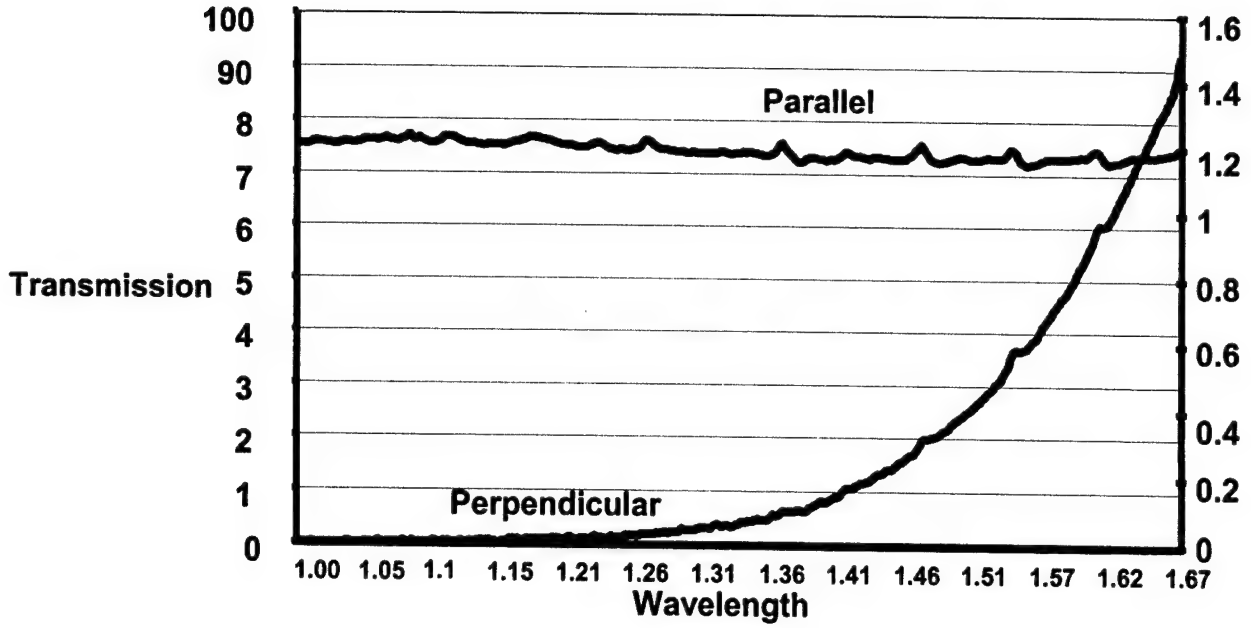

Figure 3. Measured transmission vs. wavelength of near infrared polarizer

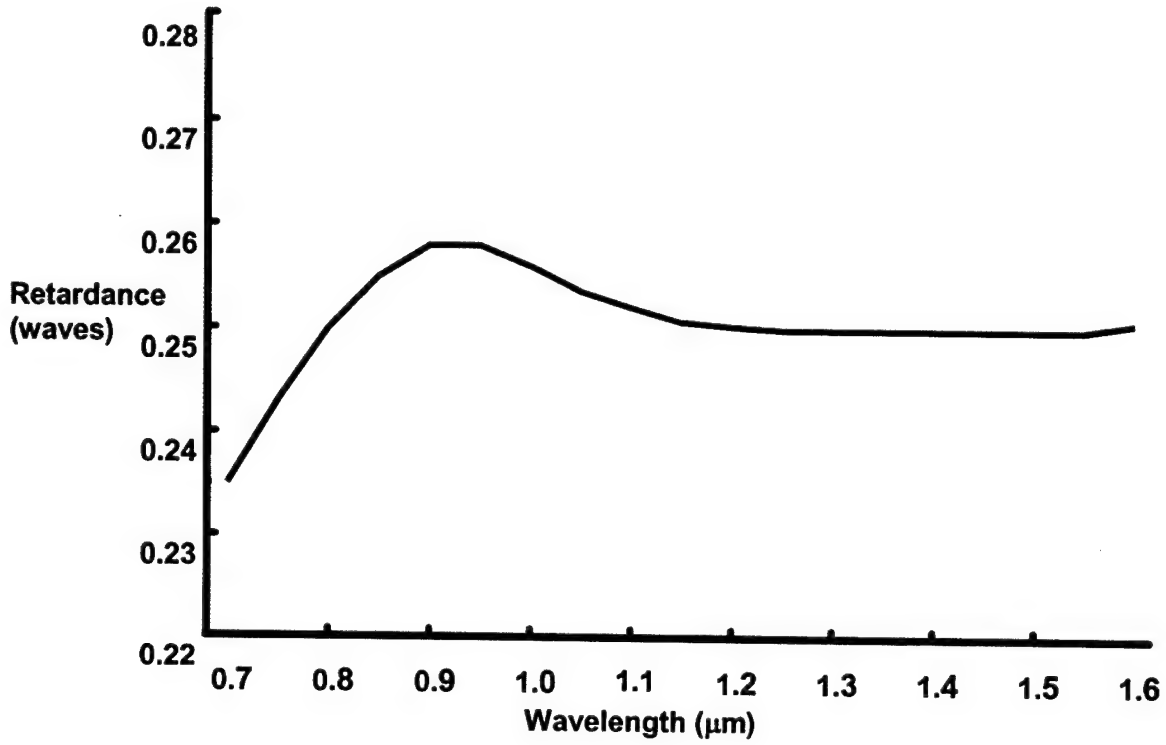

Figure 4. Retardance vs. wavelength (theoretical), Lambrecht retarder

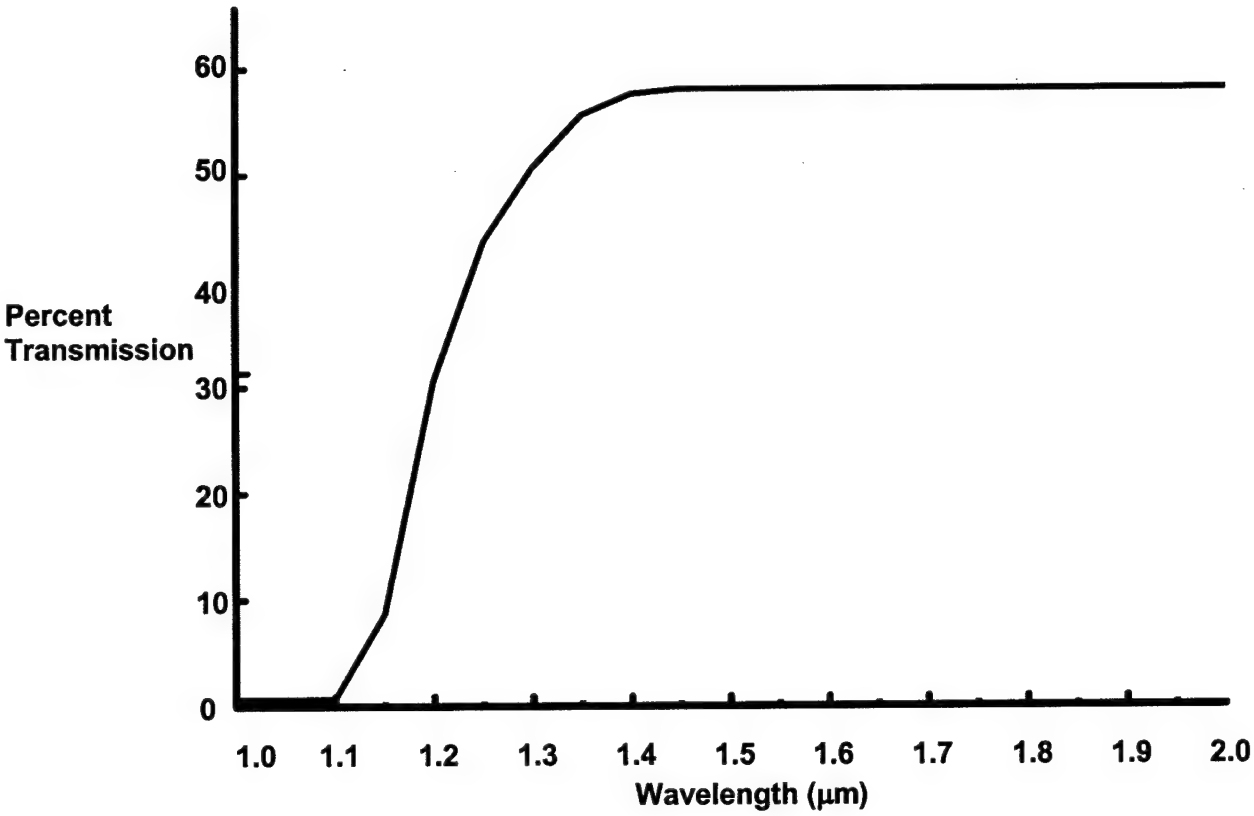

Figure 5. Transmission of Silicon in the near-infrared

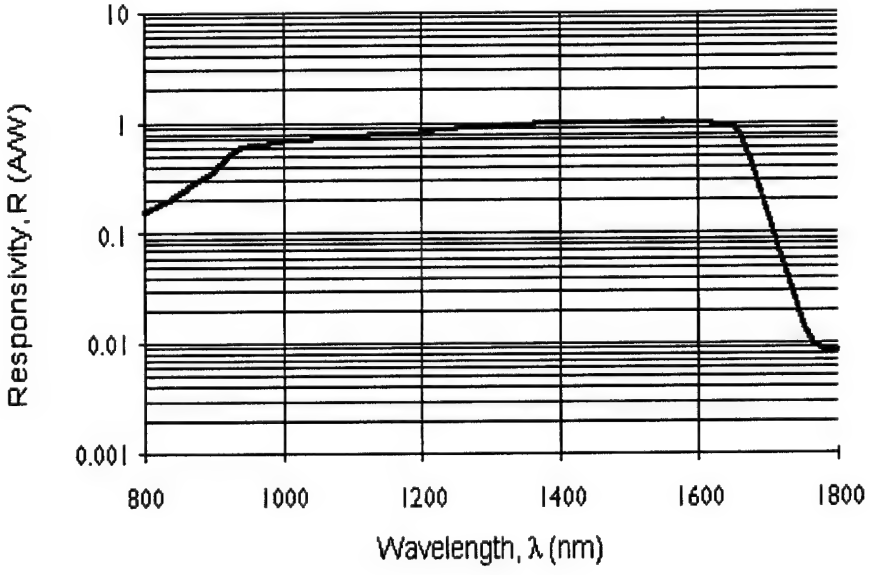

Figure 6. Typical responsivity of InGaAs

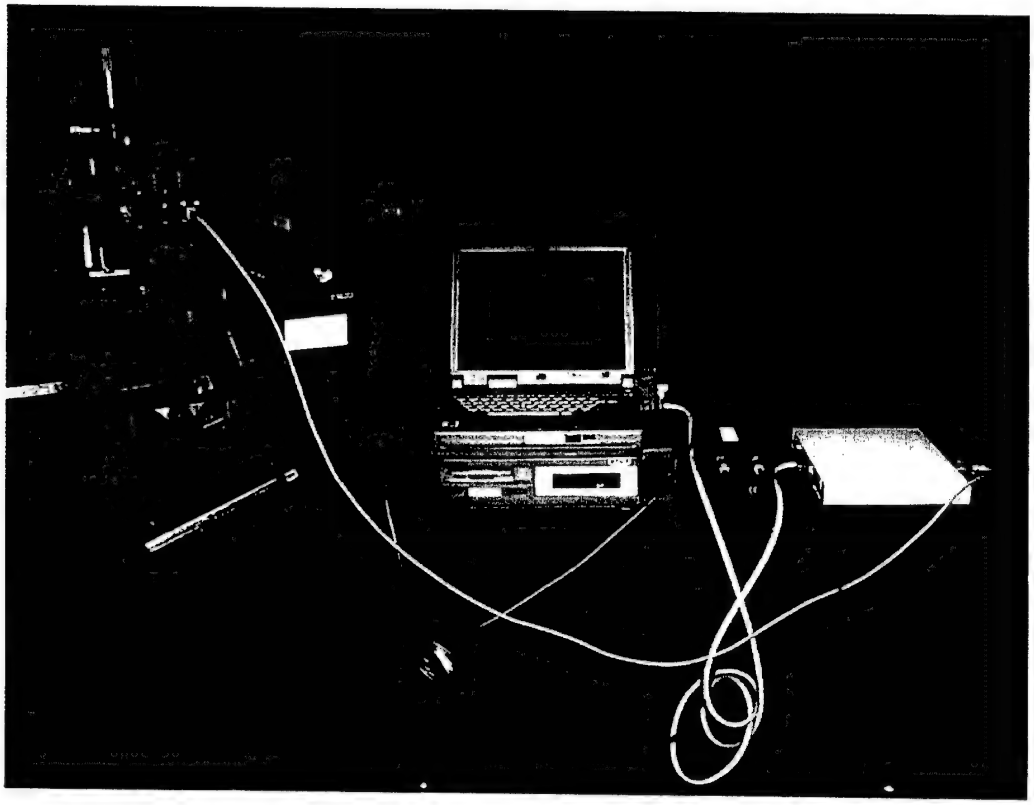

Figure 7. Photograph of the imaging system hardware

2.2 Data acquisition and reduction

Images are acquired at 8 or 16 positions of the retarder, i.e. over a 180° or 360° total rotation, and this is selected by the user at the start of the data collection. Subsequent calculations are performed on a per pixel basis to eventually obtain a Stokes vector for each pixel for each image. Derived quantities such as degree of linear polarization, degree of circular polarization, degree of polarization, ellipticity, and orientation also can be calculated and provided in an image format.

The data reduction is accomplished using the measurement matrix method[7]. A row vector is formed from the top row of the polarization optics Mueller matrix:

$$\vec{A} = \begin{pmatrix} m_{00} & m_{01} & m_{02} & m_{03} \end{pmatrix} \tag{1}$$

The detected intensity for a single position of the polarization optics with an incident Stokes vector is

$$i = \vec{A}\vec{S}_{inc} \tag{2}$$

We then form the measurement matrix from N positions of the polarization elements:

$$W = \begin{pmatrix} a_{0,0} & a_{0,1} & a_{0,2} & a_{0,3} \\ a_{1,0} & a_{1,1} & a_{1,2} & a_{1,3} \\ \vdots & & \ddots & \\ a_{N-1,0} & a_{N-1,1} & a_{N-1,2} & a_{N-1,3} \end{pmatrix} \tag{3}$$

The detected intensity I for a sequence of polarization optics positions is

$$\vec{i} = \begin{pmatrix} i_0 \\ i_1 \\ \vdots \\ i_{N-1} \end{pmatrix} = W\vec{S}_{inc} \tag{4}$$

The inverse of the measurement matrix is then multiplied times the detected intensity vector to obtain the incident Stokes vector, i.e.

$$S_{inc} = W^{-1}\vec{i} \tag{5}$$

The advantages of this approach are that the data reduction matrix is computed from ideal polarization element response, the data is derived from measured individual polarization elements, and the polarimetric data reduction matrix is measured during calibration of the polarization optics as a system. The computation is over-determined, and the pseudo-inverse performs a least squares fit to the data, equivalent to a Fourier data reduction. The computation is efficient; it is implemented in software as a matrix multiplication.

2.3 Calibration and nonuniformity correction

It is our intent to calibrate the reponse of the camera in order to compensate for nonuniformities and to remove the effect of dead pixels. Data has been taken using an integrating sphere system; however this data has not been reduced yet. We intend to use the following procedure: We take the difference between a bright uniform scene and a dark field uniform scene. Any pixel with a difference outside of "N" standard deviations (user-defined) from the mean is considered bad. This procedure is used to locate all the bad pixels and to provide gain and offset corrections for the good pixels. In the final image, bad pixels are replaced by an average of the 8 neighbors and each good pixel's response is corrected using the gain and offset values.

For the work described here, a background count image was collected and stored. During data reduction, background values are subtracted from the raw image. This procedure significantly improves the imagery, but does not remove dead pixels.

3. RESULTS

We show a few examples of scenes taken with the Stokes near infrared imaging polarimeter as well as photographs and visible Stokes polarimeter images for comparison.

Figure 8 is a photo of a scene of a car on a muddy field. Figure 9 is the same scene taken with the near infrared camera, and is the intensity image, or the image that is the S_0 component of the Stokes vector. Figure 10 is the degree of linear polarization (DOLP) image. Although this was an overcast day, the rear window of the car has a significant polarization signature, a DOLP above 0.2. The muddy areas in this image have a DOLP of around 0.02, whereas the grass DOLP is around 0.015 or less. Figure 11 is the near infrared orientation. Most of the scene is at a –45° or greater orientation whereas the side window of the car is at approximately +45°. The visible camera intensity image is shown in Figure 12. Figure 13 is the image that corresponds to the S_2 component of the Stokes vector. Most of the scene has a value of S_2 near 0, but the car windows have significant and orthogonal values. The orientation image in Figure 14 emphasizes this, as the car windows have orientations on either side of 0°. Figure 15 is a photo of a crane. Figure 16 is the near infrared intensity image and Figure 17 is the near infrared DOLP. It is difficult to distinguish the crane from the background, the movement of the vegetation causes a false polarization signature. The water in a puddle in front of the crane has a DOLP higher than anything else in the scene. The pictures shown here, as well as many more that we have collected, are much more meaningful in color.

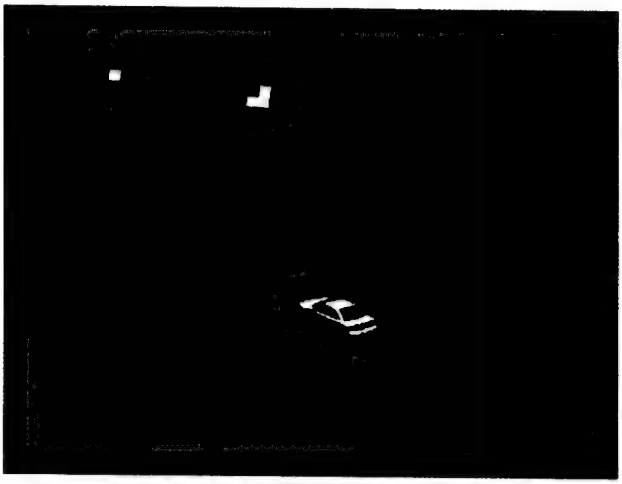

Figure 8. Photo of car in muddy field.

Figure 9. Near infrared intensity image of car

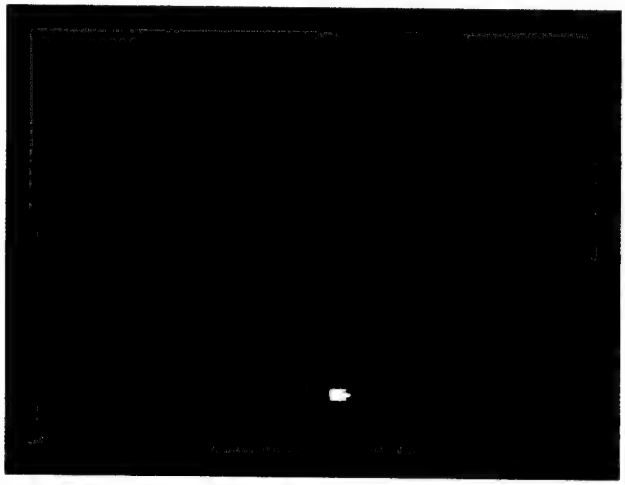

Figure 10. Near infrared DOLP

Figure 11. Near infrared orientation

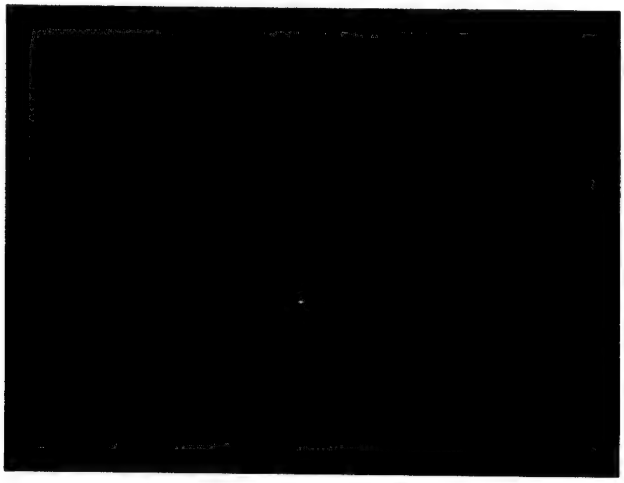

Figure 12. Visible intensity image

Figure 13. Visible S_2 image

Figure 14. Visible orientation image

Figure 15. Crane

Figure 16. Near infrared intensity image of crane

Figure 17. Near infrared DOLP

4. SUMMARY AND CONCLUSIONS

We have built and operated a near infrared imaging Stokes polarimeter. Imagery from the polarimeter has shown that there are interesting polarization effects in this spectral region. Further work in calibration, nonuniformity correction, and spectral filtering is needed to better obtain quantitative near infrared measurement results.

ACKNOWLEDGEMENTS

The authors wish to acknowledge the image data collection efforts of Anne-Marie Dorsett of SY Technology, Inc., Huntsville AL under USAF Contract Number F08630-00-C-0072, and the assistance with polarizer measurements by Dr. Lynn Deibler of the Air Force Research Lanoratory.

REFERENCES

1. L.J. November and L.M. Wilkins, "The Liquid Crystal Polarimeter for solid-state imaging of solar vector magnetic fields," Proc. SPIE 2265, *Polarization Analysis and Measurement II*, pp. 210-221, July 1994.

2. C.U. Keller, H.P Hovel, and J.O. Stenflo, "Zurich Imaging Stokes Polarimeters I and II," Proc. SPIE 2265, *Polarization Analysis and Measurement II*, pp. 222-230, July 1994.

3. C.S.L. Chun, D.L. Fleming, W.A. Harvey, and E.J. Torok, "Polarization-Sensitive Infrared Sensor for Target Discrimination," Proc. SPIE 3121, *Polarization: Measurement, Analysis, and Remote Sensing*, pp. 55-62, July 1997.

4. V.L. Gamiz, and J.F. Belsher, "Performance Limitations of a Four Channel Polarimeter In the Presence of Detection Noise, Proc. SPIE 3754, *Polarization: Measurement, Analysis, and Remote Sensing II*, pp. 204-216, July 1999.

5. A. Hofmann, "Liquid crystal-based Stokes polarimeter," Proc. SPIE 4133, Polarization Analysis, Measurement, and Remote Sensing III, pp. 44-54, August 2000.

6. D.B. Chenault and J.L. Pezzaniti, "Polarization Imaging Through Scattering Media," Proc. SPIE 4133, *Polarization Analysis, Measurement, and Remote Sensing III*, pp. 124-133, August 2000.

7. R.A. Chipman, "Polarimetric Impulse Response," Proc. SPIE 1317, *Polarimetry: Radar, Infrared, Visible, Ultraviolet, and X-Ray*, pp.223-241, May 1990.

APPENDIX E

Measurement of small birefringence in sapphire
and quartz plates

Dennis H. Goldstein, Lynn L. Deibler, and Baoliang Bob Wang

Proceedings of SPIE Volume 4819 July 2002

Measurement of small birefringence in sapphire and quartz plates

Dennis H. Goldstein
Lynn L. Deibler

Air Force Research Laboratory
101 West Eglin Blvd
Eglin AFB, FL 32542

Baoliang Bob Wang

Hinds Instruments, Inc.
3175 N. W. Aloclek Drive
Hillsboro, OR 97124-7135

ABSTRACT

Birefringence in quartz and sapphire plates was measured at 632.8 nm. The observed birefringence is presumed to be caused by a tilt in the optic axis with respect to the plate geometry. Two instrumental methods were used to make the measurements. A Mueller matrix laser polarimeter was used at the Air Force Research Laboratory, and the Exicor system was used at Hinds. The measurement techniques are described and results are presented.

Keywords: Birefringence, sapphire, quartz, polarimetry.

1. INTRODUCTION AND BACKGROUND

Quartz and sapphire are uniaxial crystals, and the birefringence of these materials can be easily observed when the crystal is oriented such that a light beam experiences the extraordinary and ordinary indices. If the optic axis of the crystal is aligned with the axis of the optical system, no intrinsic birefringence will be observed. However, if these two axes are not aligned, a birefringence originating in the angle between these two axes will be observable.

Plates of quartz and sapphire were obtained that were cut and polished so that the crystalline optic axis was tilted from the normal to the faces of the plates. The tilt angles, established from x-ray diffraction measurements, are small as is evident from Table 1.

Quartz	Δn	Sapphire	Δn
0.0°	0	0.0°	0
5'	1.92×10^{-8}	5'	-1.71×10^{-8}
15'	1.73×10^{-7}	15'	-1.54×10^{-7}
30'	6.93×10^{-7}	30'	-6.17×10^{-7}
1.5°	6.23×10^{-6}	1.0°	-2.47×10^{-6}
2.0°	1.11×10^{-5}	1.5°	-5.55×10^{-6}
5.0°	6.91×10^{-5}	2.5°	-1.54×10^{-5}
		5.0°	-6.15×10^{-5}

Table 1 Quartz and sapphire sample axis tilts and birefringence

The birefringence experienced by light normally incident on the plates is

$$\Delta n = (n_e - n_o)\sin^2\theta$$

where $(n_e - n_o)$ is the intrinsic birefringence and θ is the tilt angle. Table 1 shows the net birefringence for each tilt angle for both quartz and sapphire. The intrinsic birefringence values at λ = 632.8 nm were taken to be 0.0091 for quartz and –0.0081 for sapphire.

Two of us (Goldstein and Deibler) made measurements of the plates with a Mueller matrix laser polarimeter at AFRL and the one of us (Wang) made measurements with the Hinds Exicor system. The Exicor system is designed to measure extremely small birefringence (to .005 nm). The laser polarimeter is designed to make Mueller matrix measurements. The purposes of the measurement of these tilted axis plates were fourfold: 1) to determine if the nominal tilt angles were found from the measurements, 2) to determine if the samples would be useful low birefringence standards, 3) to compare the laser polarimeter measurements with the Exicor measurements, and 4) to determine the capability of the laser polarimeter for low birefringence measurements. The measurement techniques are described in the following sections.

2. LASER POLARIMETRY

2.1 Instrumentation

The plates were measured with a Mueller matrix laser (stabilized CW HeNe @ 6328 Å) polarimeter[1] using the dual rotating retarder configuration[2]. The detector is connected to a digital multimeter, there is no modulation of the signal, and no lock-in amplification is used. The first retarder is rotated 72 times in 5° increments while the second retarder is rotated in 25° increments. This polarimeter was designed and has been used to measure electrooptic properties of bulk material with or without electric and/or magnetic fields applied. The complete Mueller matrix of the sample is obtained.

One advantage of this method is that the measurement does not depend on the rotational orientation of the sample about the optic axis of the system.

The system is not optimized for measurement of small birefringence. In fact, these measurements were the first use of the system with samples of small birefringence, and elements of the Mueller matrix not used in previous measurements were used in the data reduction for the sapphire plates.

A conservative estimate of the error in orienting the plate normal to the optic axis (the laser beam) is 15' (or .25°) but it is probably considerably smaller than this. When the sapphire plate is placed normal to the (stabilized) laser source, the backreflection destabilizes the laser – when this happens, the beam is very close to normal. In order to counter this, the laser intensity was reduced using neutral density filters (presumably free of birefringence). This has the effect of reducing the signal to noise. In order to be sure that the orientation error is smaller, the distance between the sample and the source would have to be greater. This is currently not practical without moving the laser off the optics table.

A diagram of the optical setup is shown in Figure 1. The dual rotating retarder configuration has two retarders inside two polarizers symmetrically arranged about a sample. In our setup, both laser sources used are highly polarized, and the initial polarizer of the dual rotating retarder configuration is unnecessary. All polarimeter elements as well as the sample were placed in rotary stages. A silicon detector was used. A high quality Glan-Thompson polarizer is used as the final polarizer in the system in each case, and is assumed to have ideal diattenuation. Zero-order waveplates of nominal quarter wave retardance for the laser wavelengths were used as the dual rotating retarders. The detector and associated electronics have a maximum dynamic range of approximately 10^3 so that extinction ratios larger than this can not be measured.

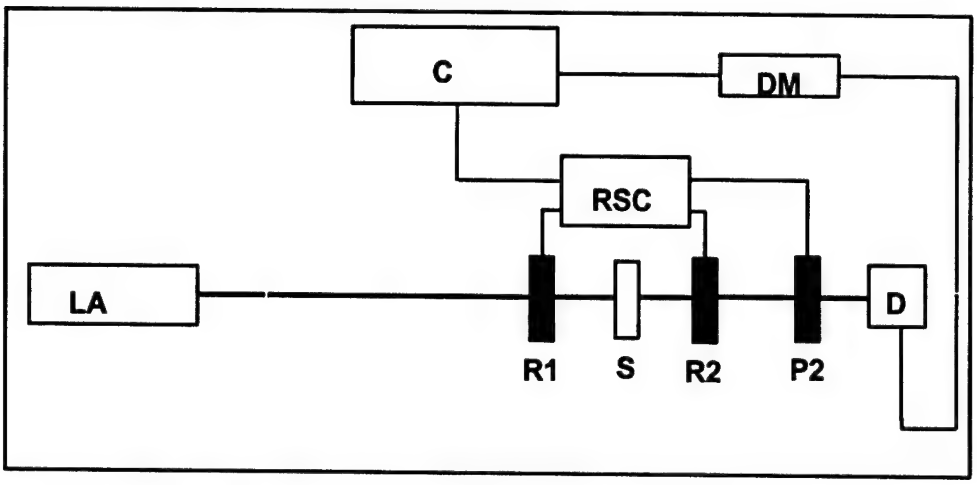

LA	LASER	C	COMPUTER
D	DETECTOR	RSC	ROTARY STAGE CONTROLLER
P2	POLARIZER	DM	DIGITAL MULTIMETER
R1,R2	RETARDERS	S	SAMPLE

Figure 1. Diagram of Mueller matrix laser polarimeter.

2.2 Experimental procedure

The measurements were made by first taking three calibration measurements (measurements without the sample in place) and using this data to determine the rotation misalignment of the retarders and polarizer. Using the equations developed by Goldstein[3] and Chenault[4], these errors are used in the measurements to correct for the misalignment.

We assume that the samples are pure linear retarders so that the data reduction is based on our knowledge of the form of a linear retarder with rotated fast axis. The sample Mueller matrix was measured three times each at 0, 22.5, 45, 67.5 and 90 degrees of rotation about the optic axis. Retardance values for δ for the measured Mueller matrices were calculated using the equations

$$\delta = \sin^{-1}\sqrt{m_{ij}^2(0°) + m_{ij}^2(45°)}$$

$$\delta = \sin^{-1}\sqrt{m_{ij}^2(22.5°) + m_{ij}^2(67.5°)}$$

$$\delta = \sin^{-1}\sqrt{m_{ij}^2(45°) + m_{ij}^2(90°)}$$

where the subscripts ij are the Mueller matrix elements 24, 34, 42, and 43.

The measured tilt angle is then found from

$$\theta = \sin^{-1}\sqrt{\frac{\delta\lambda}{2\pi(.0091)}}\frac{180}{\pi}$$

where t is the thickness, measured to be 0.003581 meters for the quartz samples and 0.003556 meters for the sapphire samples, λ is the wavelength of the HeNe laser 6328 Å, and .0091 is the published birefringence for quartz ($(n_e - n_o)$ = 0.0081 for sapphire) .

3. BIREFRINGENCE MEASUREMENT WITH EXICOR

3.1 Instrumentation

The Exicor system[5,6] consists of three major parts: an optical bench, an electronic compartment, and a computer. A block diagram for the optical bench of this instrument is shown in Figure 2. The optical bench has three modules. The upper module contains a polarized HeNe laser, a Glan-Thompson polarizer, and a photoelastic modulator (PEM). The middle module is a sample holder mounted on a computer-controlled X-Y stage. The Exicor instrument used here has a 6in x 6in X-Y stage that allows the capability of simultaneous mapping of 2-D images for both magnitude and angle of the birefringence in a sample with variable spatial resolutions. The lower module of the optical compartment includes a partial reflection mirror and two detecting assemblies. The partial reflection mirror transmits about half of the light beam after the sample to analyzer 1 and detector 1 (channel 1), and reflects the other half at a small angle (2 - 5°) to analyzer 2 and detector 2 (channel 2). The small reflection angle used in this configuration is crucial to minimizing the polarization artifacts due to reflection. The electronic signals generated at the detector are processed using a single lock-in amplifier (EG&G model 7265) with two inputs for sequential data processing for the two channels. In principle, two lock-in amplifiers can be used for simultaneous measurements to speed performance. In this instrument, the output from the lock-in amplifier is taken into a computer, and the magnitude and angle of the linear birefringence is displayed.

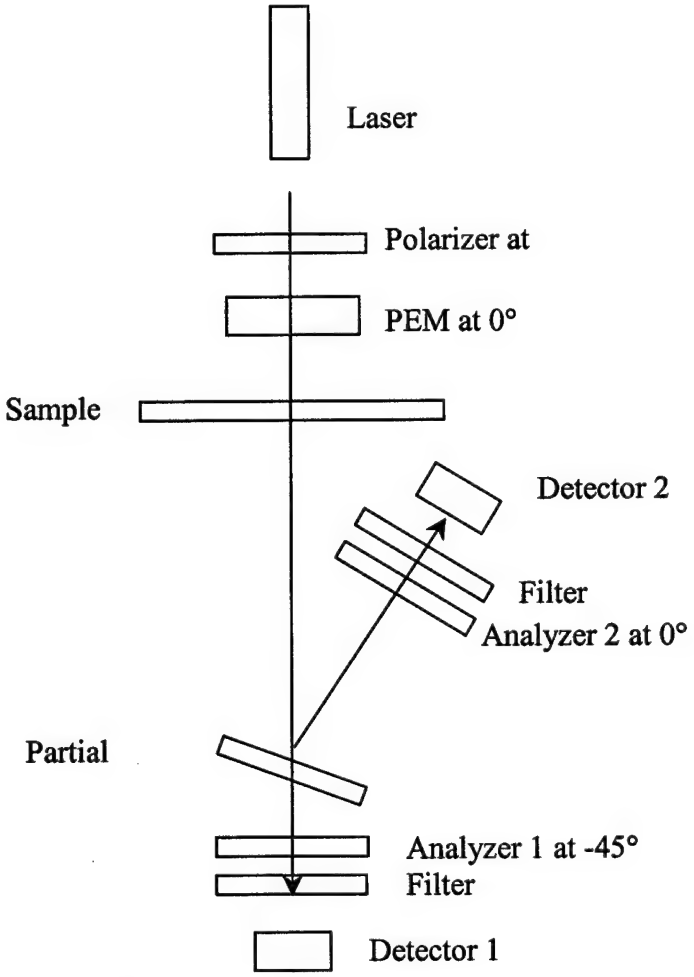

Figure 2. Optical layout of the Exicor birefringence measurement system.

The Exicor birefringence measurement system is specifically designed for measuring very small linear retardation in a sample. The most common application of the Exicor systems is to measure residual linear birefringence in high quality

optical elements used in optical lithography systems.[7,8] A typical optical component used in lithography steppers, such as a photomask blank or a lens blank, is made of either fused silica (amorphous) or calcium fluoride (cubic crystal). Those materials exhibit only residual birefringence in the visible spectral region. When produced by a refined annealing process, a high quality optical component has residual retardation values on the order of only 0.1 nm.[9]

The development of the Exicor birefringence system was primarily motivated by the suppliers of high quality fused silica and calcium fluoride materials to the optical lithography industry. The Exicor birefringence measurement system provides a sensitivity of <0.005 nm (<1/100,000 of a wavelength at 632.8 nm) for linear retardation measurements. This instrument is essentially an incomplete polarimeter applicable to a specific industrial application. The calcium fluoride and fused silica samples for the optical lithography are in the highest optical quality available to the industry. They have high purity, nearly no color centers, and well polished surfaces. Therefore, those samples should have negligible circular birefringence, diattenuation and depolarization. Residual linear birefringence is the primary concern of those samples.

In this paper, we are also primarily concerned with linear retardation. The Exicor birefringence measurement system is applicable to this study. The Exicor system has the capability of measuring more parameters than just linear retardation. For example, the signal for circular birefringence appears at a different harmonic of the PEM's modulation. Since the goal here is to determine low level linear retardance (both magnitude and angle of fast axis) in a sample with high sensitivity, one of the authors (Wang) did not attempt to make this instrument a complete polarimeter for measuring all possible parameters. As reported previously, a dual PEM system is capable of measuring all 16 Mueller matrix elements of a sample.[10-12]

3.2 Experimental procedure

The sapphire and quartz plates are approximately 2.54 cm in diameter. The X-Y stage of the Exicor system changed location by 1 mm intervals, and the beam size used was about 1 mm. Data were collected over the face of the plates within a 2-3 mm margin from the edge of the plates. More than 300 data points were actually recorded for each sample.

4. RESULTS

Measurement results are summarized in Table 2. There are two Exicor results in this table. The first is the average of all data points (>300) measured over the face of the samples. The second is the average over a central region of the plate, either 3×3 or 2×2 data points. The Mueller matrix polarimeter measurements were initially done with the beam passing through the estimated center of the plates, and the central region average from the Exicor data should encompass and represent this estimated center.

There are three comments to be made about the information in this table. First, the laser used for the sapphire measurements, a "stabilized" HeNe, was found to be extremely unstable when we attempted to measure the quartz samples. Another HeNe laser with no stabilization was substituted for the original laser and was found to be much more stable. We were successful in measuring the sample with 0.25° tilt with the second laser, where we could not measure this tilt in the sapphire sample because of the noise, presumably from the original laser. The system noise precludes measurement of tilt smaller than 0.25° with the laser polarimeter.

Second, one can observe that the Exicor results for the average and for the central region are generally different. The reason for this becomes obvious on examination of a plot of the Exicor measurements. Figure 3 shows plots of the Exicor data for the 2° quartz and 2.5° sapphire samples where the retardance is plotted in the z direction. The retardance displays a bullseye pattern with additional diagonal ridges. The values near the center are clearly different from those away from the center. Similar retardation patterns have also been observed for regular waveplates of different materials.[13] The reason for this pattern in retardance and hence birefringence is unknown. The Exicor data shows that the magnitudes of variations increase with the tilt angles of the plates. We suspect that both crystal quality and manufacturing processes may have contributed to the retardation inhomogeneity of those plates.

	Sapphire				Quartz		
Nominal axis tilt	Exicor average	Exicor center	Laser polarimeter	Nominal axis tilt	Exicor average	Exicor center	Laser polarimeter
0.0°	*	*	*	0.0°	0.23°	*	*

0.083°	*	*	*	0.083°	0.29°	*	*
0.25°	0.27°	0.26°	*	0.25°	0.31°	0.25°	0.25°
0.5°	0.34°	0.38°	0.53°	0.5°	0.46°	0.48°	0.49°
1.0°	0.88°	0.98°	1.09°	1.5°	1.32°	1.41°	1.48°
1.5°	1.37°	1.46°	1.50°	2.0°	1.72°	1.71°	1.96°
2.5°	2.49°	2.58°	2.66°	5.0°	5.47°	5.45°	5.30°
5.0°	5.47°	5.45°	5.45°				

* Not measured in the case of the laser polarimeter or data not reduced in the case of the Exicor system.

Table 2 Measured tilt angles for quartz and sapphire.

Figure 3. Retardance plots for quartz (2.0°, left) and sapphire plates (2.5°, right).

Figure 4 Retardance plots for quartz plates (tilt angles at 0.125°, left; 0.5°, right).

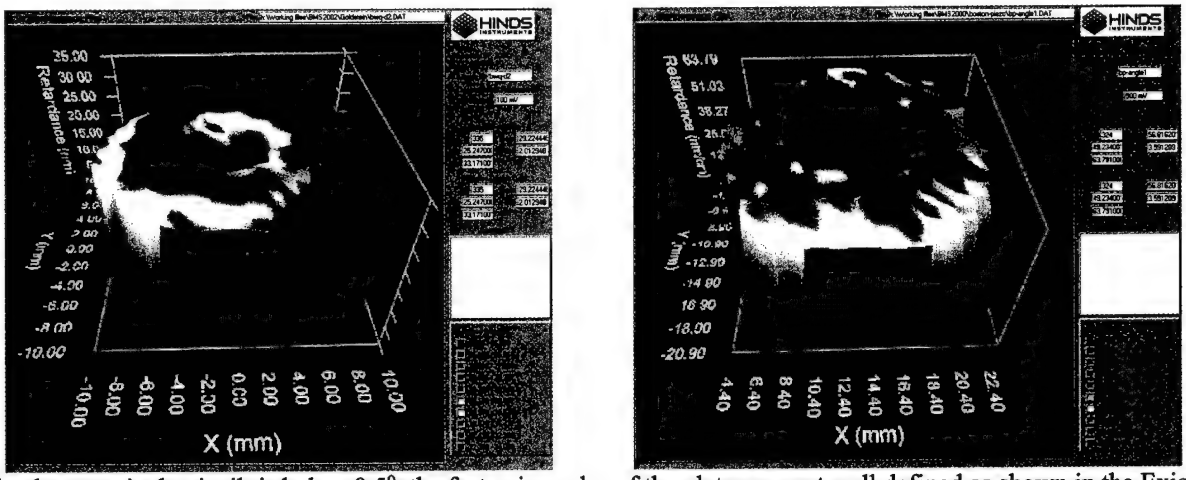

Third, when nominal axis tilt is below 0.5°, the fast axis angles of the plates are not well defined as shown in the Exicor birefringence map (left) of the 0.25° quartz plate in Figure 4. This is perhaps due to the fact that the residual birefringence in

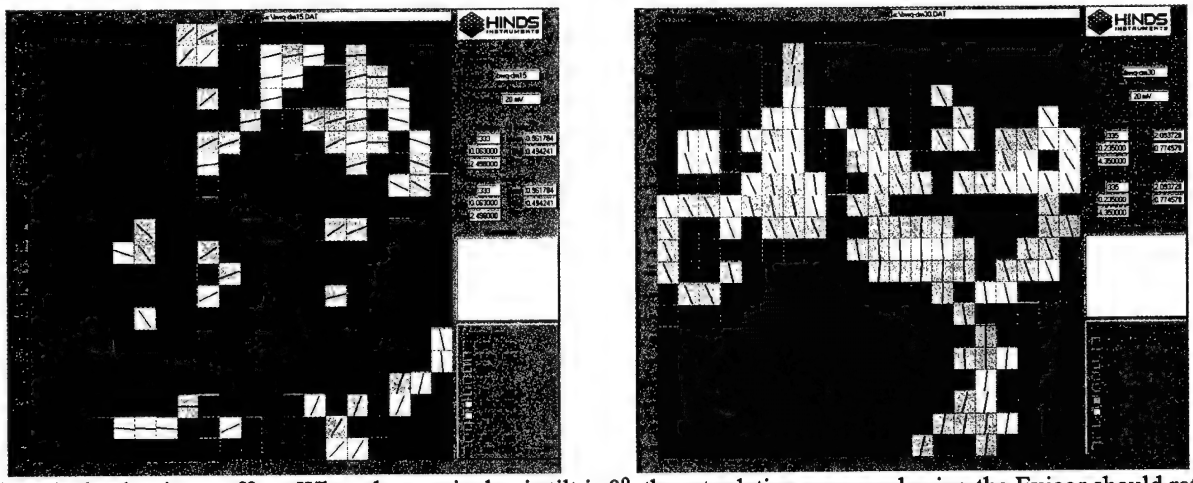

the plates is the dominant effect. When the nominal axis tilt is 0°, the retardation measured using the Exicor should reflect the residual birefringence level of the plates. The Exicor measurements of over 300 data points for the quartz plate with 0° nominal axis tilt give a retardation average of 0.511 nm, a standard deviation of 0.201 nm, and a maximum retardation of 1.3 nm. A retardation of 0.511 nm at a fixed fast axis angle would correspond to 0.23° optical axis tilt in a quartz sample of 0.0036 m thick. However, the birefringence map of the 0.25° quartz plate clearly shows that the fast axis angles at different

sampling spots are nearly random. Therefore, it is not meaningful to calculate tilt angles below 0.5° for those plates. When the nominal tilt angle is 0.5°, the fast axes at different spot of the plate still change, but there is, at least, a clear angular pattern for the fast axis of the quartz plate.

Once the Exicor measurements had been made and the anomalous pattern observed, laser polarimeter measurements were made at 1 mm intervals for ±10 mm on either side of the estimated center of the quartz plate with nominal 2° tilt. The results of this scan are plotted in Figure 5. While there was no absolute orientation maintained from laser polarimeter measurements to the Exicor measurements, a plot of the retardance along a diameter of the plate is also shown in Figure 5. The plots in Figures 5, while not necessarily for the same physical points on the plate, have similar profiles, and the laser polarimeter finds the same anomalous pattern.

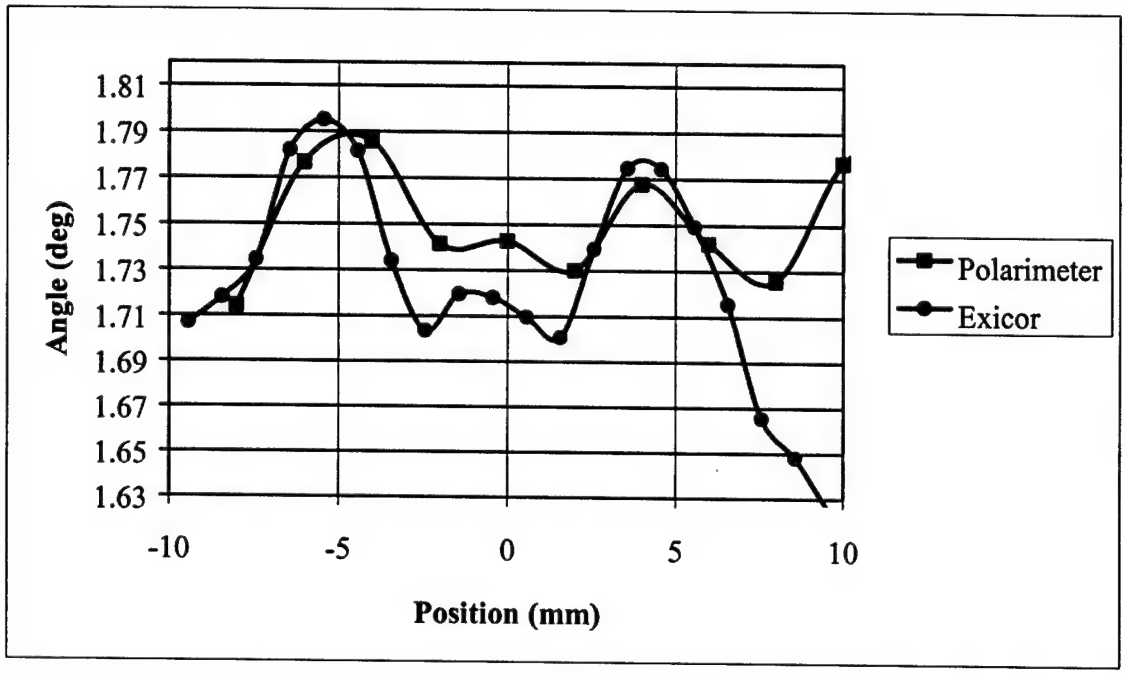

Figure 5. Comparison of the variation in measured tilt angle across the 2 degree quartz sample as measured with the Exicor system and the laser polarimeter.

5. DISCUSSION

Both the differences between the nominal values and the optical measurements, and the anomalous birefringence pattern are unexpected. The nominal tilt angles are established for these samples using x-ray diffraction where the error is said to be on the order of 1 arc minute (0.0167°). The optical measurements for the sample center are occasionally within this error bar, but the variation across the sample is usually well outside this error.
The anomalous birefringence pattern is observed by two totally different optical instruments, and we believe it is not an artifact of either measurement process. When one of the sapphire samples was scanned using the Exicor system under different orientations and with slightly different incident angles, the retardation pattern remained. As mentioned earlier in the paper, similar retardation patterns were also observed for certain quarter- and half-wave plates.[13] The samples are cut and polished using techniques to minimize subsurface damage, yet the small birefringence variation appears to have a regularity that may be due to the manufacturing process.

The objectives of this study have been attained. The nominal values of the axis tilt were measured with two optical techniques. The laser polarimeter measurements have been compared to the Exicor measurements, and the lower limits of birefringence measurement capability have been explored. The usefulness of these samples as low birefringence standards

has been assessed; the determination here is, unfortunately, that they are not useful because of nonuniformity and because of sensitivity to sample-source geometry.

REFERENCES

1. D.H. Goldstein, "Mueller matrix dual-rotating retarder polarimeter," Appl. Opt. 31, pp. 6676-6683, 1992.
2. R.M.A. Azzam, "Photopolarimetric measurement of the Mueller matrix by Fourier analysis of a single detected signal," Opt. Lett. 2, 6 pp. 148-150, 1978.
3. D.H. Goldstein and R.A. Chipman, "An Error Analysis of a Mueller Matrix Polarimeter," J. Opt. Soc. Am. A 7, pp. 693-700, 1990.
4. David B. Chenault and J. Larry Pezzaniti, "Mueller matrix polarimeter algorithms," Proc. SPIE 1746, Polarization Analysis and Measurement, July 1992.
5. B. Wang and T.C. Oakberg, "A New Instrument for Measuring Both the Magnitude and Angle of Low Level Linear Birefringence," Rev. Sci. Instrum., 70, 3847 (1999).
6. B. Wang and W. Hellman, "Accuracy Assessment of a Linear Birefringence Measurement System Using a Soleil-Babinet Compensator," Rev. Sci. Instrum., 72, 4066 (2001).
7. B. Wang, "Residual birefringence in photomask substrates," J. Microlith. Microfab. Microsys., 1, 43-48 (2002).
8. J. L. Ladison, J. F. Ellison, D. C. Allan, D. R. Fladd, A. W. Fanning and R. Priestley, "Achieving Low Wavefront Specifications for DUV Lithography; Impact of Residual Stress in HPFS Fused Silica," SPIE Proceedings 4346, 1416-1423 (2001).
9. A. J. Marker III, B. Wang and R. A. Klimek, "Effect of residual stress in optical glass on the transmitted wavefront" SPIE Proceedings 4102, 211 (2000).
10. B. B. Wang, "Linear birefringence measurement instrument using two photoelastic modulators," Opt. Eng. 41, 981-987 (2002).
11. G. E. Jellison, Jr. and F. A. Modine, "Two-Modulator Generalized Ellipsometry: Experiment and Calibration," Appl. Opt. 36, 8184 (1997); "Two-Modulator Generalized Ellipsometry: Theory," 36, 8190 (1997).
12. G. E. Jellison, Jr. and F. A. Modine, "Two Modulator Generalized Ellipsometer for Complete Mueller Matrix Measurement" US patent No. 5,956,147 (1999).
13. B. Wang, "A near infrared linear birefringence measurement system using a photoelastic modulator," SPIE Proceedings 4399, 89-97 (2001).

APPENDIX F

Spectropolarimetric Reflectometer

Dennis H. Goldstein and David B. Chenault

Optical Engineering Volume 41 Number 5 pp. 1013-1020, May 2002

Spectropolarimetric reflectometer

Dennis H. Goldstein
Air Force Research Laboratory

David B. Chenault
SY Technology, Inc.

ABSTRACT

An instrument is presented that combines the functions of a reflectometer, a spectrometer, and a polarimeter. A Fourier transform spectrometer serves as a light source for a dual rotating retarder polarimeter. Operation of the instrument results in measurement of the complete Mueller matrix of a sample in reflection over a wide spectral band. Calibration and error compensation is described. Polarization characteristics of materials in reflection are determined.

Subject terms: polarimetry, Mueller matrix, reflectometer, spectropolarimetry

1. INTRODUCTION AND BACKGROUND

Many sensors rely on reflected light from natural or manmade sources to obtain the energy for their detector elements. The light that is reflected may be polarized. The ability of the sensor to detect and process the reflected energy may depend upon knowledge of the reflection characteristics of the materials. We describe here an instrument that measures the polarization of reflected light over broad regions of the visible and infrared in order to evaluate polarized reflection properties of materials.

An instrument that measures spectral infrared polarization properties of materials in transmission has been designed and patented previously[1]. The infrared spectropolarimeter (Patent #5,045,701) is based on a Fourier transform infrared (FTIR) spectrometer containing a dual rotating retarder Mueller matrix polarimeter in the sample compartment[2]. Measurement of polarization properties of transmissive samples is possible with this instrument over large wavelength regions in the infrared (wavelengths of 2.5 μm and greater). A scatterometer which measures Mueller matrices of samples in transmission or reflection has been constructed by Schiff et al., but does not give spectral information[3].

The current work extends the concept of using a polarimeter in conjunction with a Fourier transform spectrometer by incorporating a modern Fourier transform spectrometer which is capable of measurements from the ultraviolet to the far infrared, and adds the capability to measure samples in reflection.

2. INTRUMENTATION

The spectropolarimetric reflectometer is based around a commercial Fourier transform spectrometer. The spectrometer must be one which generates radiation from the ultraviolet to the far infrared, it must be computer-controlled, and it must have a software system which allows insertion of control over the instrument, control over additional hardware, and data processing. We are using a Bio-Rad FTS-6000 with the Win-IR Pro software system. The spectrometer is configured with three sources, three beamsplitters, and four detectors which make the useful wavelength range of the instrument from the ultraviolet to approximately 25 μm in the infrared. Additional components could easily extend the operating range to longer wavelengths.

The Bio-Rad spectrometer serves as a radiation source for the polarimetric portion of the instrument and is operated in the conventional absorption spectroscopy mode. The radiation generated by the spectrometer is brought out through the spectrometer's external port. Figure 1a shows the basic optical schematics of the instrument for bidirectional reflectance distribution function (BRDF) measurements.

For bistatic measurements, the detector sits on a large circular platter. The platter is able to rotate about a central vertical axis, and is rotated by a computer-controlled motor on the platter. The platter is annular; there is a circular opening where the sample resides. The sample is mounted on a computer-controlled motorized rotational stage, and has a common central rotation axis with the detector platter. The sample can be rotated so that any in-plane incidence angle is obtained. The optical system that collects light for the detector consists of an off-axis parabolic mirror. This mirror is fixed to look toward the central axis of the detector platter and focus light onto the detector which is mounted perpendicularly to the light coming from the central axis. The parabolic mirror, detector, and mounting devices will be referred to as the detector assembly. The detector assembly may be rotated to any position around the sample, except that the detector assembly may block light from the spectrometer if it is within a few degrees of the source beam direction. The sample is mounted vertically so that its surface comprises a vertical plane, and it may be rotated to any position around a vertical axis. Data collection proceeds by rotating both sample and detector platter such that sample and detector assembly are in the desired geometric relationship; spectropolarimetric data is then collected. The instrument may be used for transmissive measurements as well by placing the transmissive sample on the central rotation stage and lining up the detector assembly with the source beam on the far side of the sample. This is illustrated in Figure 1b. A photograph of the system is shown in Figure 2.

The reflectometer may be used without any modification of the polarization of the source radiation, and in this mode, it is a spectral reflectometer. In order to obtain spectropolarimetric measurements, a dual rotating retarder Mueller matrix polarimeter, described by Azzam[4], is included in the system. This polarimeter consists of a polarization state generator before the sample and a polarization state analyzer after the sample, and is shown in Figure 3. The polarization state generator consists of a linear polarizer followed by a quarter wave retarder and is located in the source beam prior to the platter region. The polarization state analyzer consists of a quarter wave retarder followed by a linear polarizer and is located on the platter in front of the detector assembly. Although we use retarders that are nominally quarter wave in the spectral region being measured, the exact retardance is not critical as will be discussed later. When the retarders are rotated in a five to one ratio, all sixteen elements of the sample Mueller matrix are encoded onto twelve harmonics of the detected signal, which can then be Fourier analyzed to recover the Mueller matrix elements. Other previous implementations of this Mueller matrix polarimeter have been described elsewhere[1,2,5].

The data reduction algorithm for this polarimeter as originally presented by Azzam assumes ideal polarization elements and no orientation errors. The data reduction algorithms may be generalized to compensate for systematic errors which result when orientation misalignment and non-ideal retarders are used. If the polarization elements are rotationally misaligned, or the retarders do not have exactly one-quarter wave of retardance, the changes in Fourier amplitudes and phases result in errors in the sample Mueller matrix. Even small orientation and retardance errors (<1°) can lead to large errors in the measured Mueller matrix (> 10% in some matrix elements). These errors become especially important when the retardance and alignment vary significantly from their nominal values such as in multi-wavelength or spectral instruments. We have incorporated correction terms for orientation and retardance errors into the dual rotating retarder data reduction algorithm. Small angle approximation error correction equations are given in Goldstein and Chipman[6], and this is generalized to larger angles in Chenault et al[7]. These equations are quite lengthy and will not be presented here.

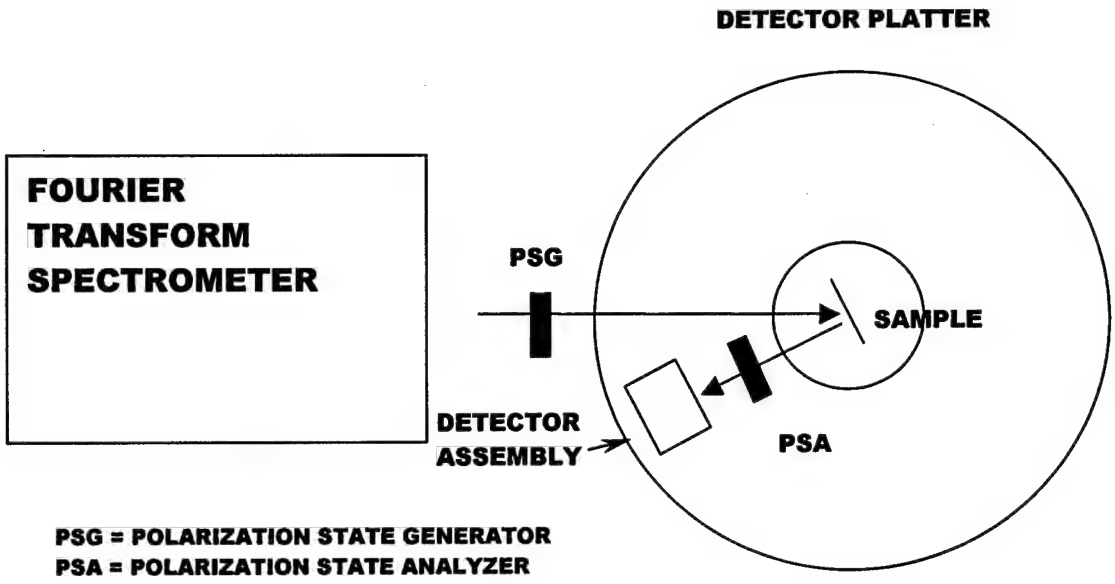

Figure 1a. Bistatic configuration.

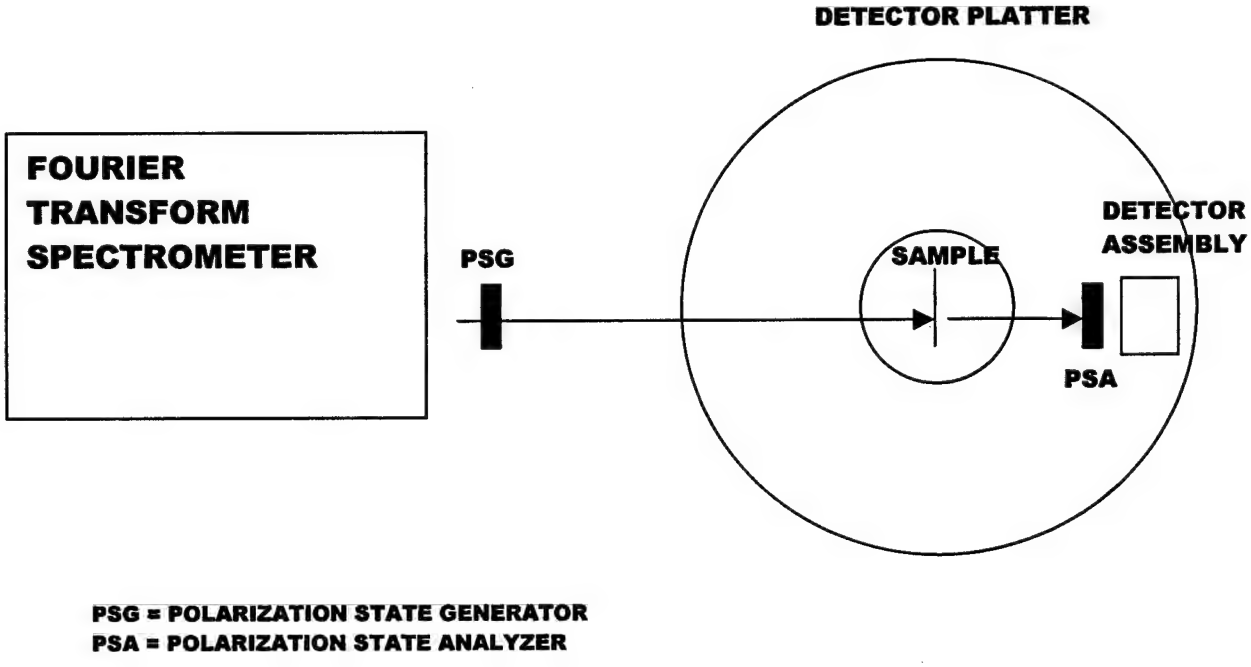

Figure 1b. Transmission-mode configuration.

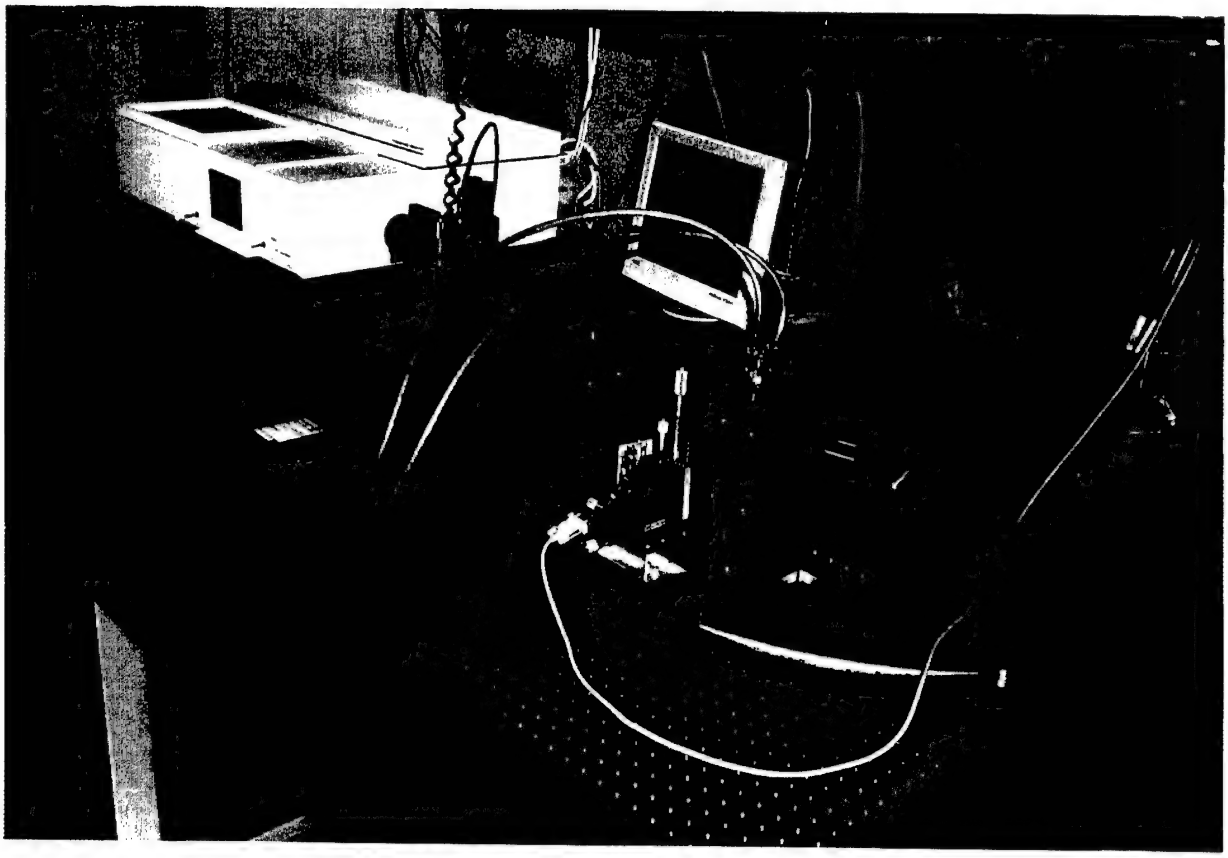

Figure 2. Photograph of spectropolarimetric reflectometer.

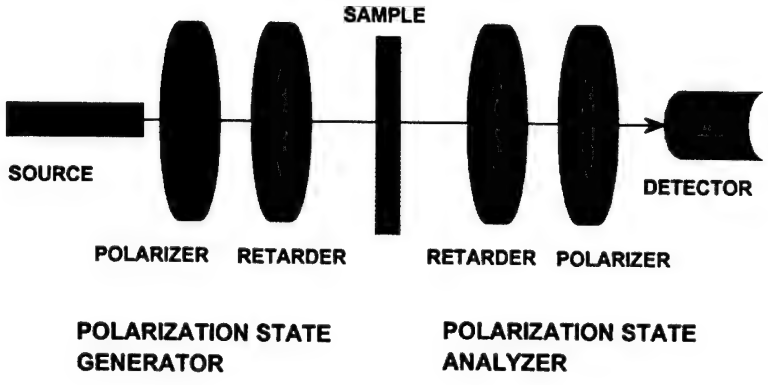

Figure 3. Dual rotating retarder configuration.

The dual rotating retarder configuration has a number of advantages. First, the effect of any constant instrumental polarization preceding the polarizing optics or following the polarimeter is negated by the fixed position of the polarizers. Second, the Fourier transform on the data automatically performs a least squares fit to the overdetermined data set. Third, this configuration is largely immune to beam wander if measurements are made over a 2π cycle. In this case, modulation from beam wander produced by wedges in the rotating retarders is encoded principally on the first and fifth Fourier amplitudes. Since the polarimeter does not modulate these frequencies, the beam wander signal does not affect the accuracy of the measured Mueller matrix.

Since spectral measurements are made with this instrument, polarizers and retarders should be as achromatic as possible. Polarizers are generally achromatic in terms of polarization performance over their region of useful transmission. Retarders are not generally achromatic, although some retarders that are achromatic over specific spectral regions are available commercially. In the present instrument, some commercial retarders are used and some specially designed retarders, particularly for the infrared, are used (see Goldstein et al[2], and Chipman and Chenault[8]).

3. ALIGNMENT, CALIBRATION, AND ERROR COMPENSATION

To set the instrument up for use, the first procedure is to align the optical and polarization elements. The detector is rotated on the detector platter to a point opposite the polarization state generator position. The optical beam is aligned to the detector without the polarization elements. The polarization elements are then placed into the beam in a specific order and rotationally positioned such that the polarization axes of the polarizers and the fast axes of the retarders are all aligned, typically vertically. The first polarizer is set at the desired orientation, and the final polarizer is oriented with the first polarizer. The retarders are placed in the beam individually and the fast axis of each is aligned to the orientation axis of the polarizers.

A calibration run must then be performed. This consists of a Mueller matrix data collection without a sample. The detector is rotated into a position opposite the polarization state generator as explained in the alignment procedure (as mentioned earlier, this configuration can be used for transmission mode measurements). This calibration run establishes the remaining errors in orientation and allows determination of the retardation of the retarders. These errors are then compensated out during the sample data reduction.

4. DATA COLLECTION

The instrument is completely under computer control. Software controls the operation of the hardware and subsequent collection and reduction of data. Spectropolarimeter data collection proceeds according to the procedure presented next. With all polarization element axes aligned, a spectrum is acquired in the normal fashion for a Fourier transform spectrometer (involving the Fourier transform of the interferogram). The retarder elements are rotated to the first azimuthal position followed by acquisition of the next spectrum. This process of moving retarders followed by spectrum acquisition is continued until spectra at all retarder positions have been collected. The sample and detector are then moved to their new positions and the next spectropolarimetric data set is acquired. After all spectral data are collected, the Mueller matrix for each sample and detector position is recovered by performing a Fourier analysis on the polarization modulation at each spectral point. The output includes the Mueller matrices for each wavelength over a specified spectral range.

A normal data collection consists of the calibration run, which also serves as the spectrometer background acquisition, and one or more sample runs. Each sample run is initiated by setting in software a number of spectrometer parameters and the geometrical relationships of the sample and detector. Once these are set, the instrument automatically collects and processes the data. The output includes the Mueller matrix of the sample as well as derived quantities such as retardance and diattenuation. A polarization BRDF can be constructed from the results.

5. RESULTS

Many measurements have been made with the spectropolarimetric reflectometer. Studies of Spectralon and Federal Standard paint have been done[9,10]. Several other materials have been examined including cloth, paving materials, and vegetation. Mueller matrices are always computed, but in the Spectralon and Federal Standard paint studies, only the derived quantity of polarizance was quoted in the published papers. We present examples of complete Mueller matrix results here.

The coordinate system for the measurements is shown in Figure 4.

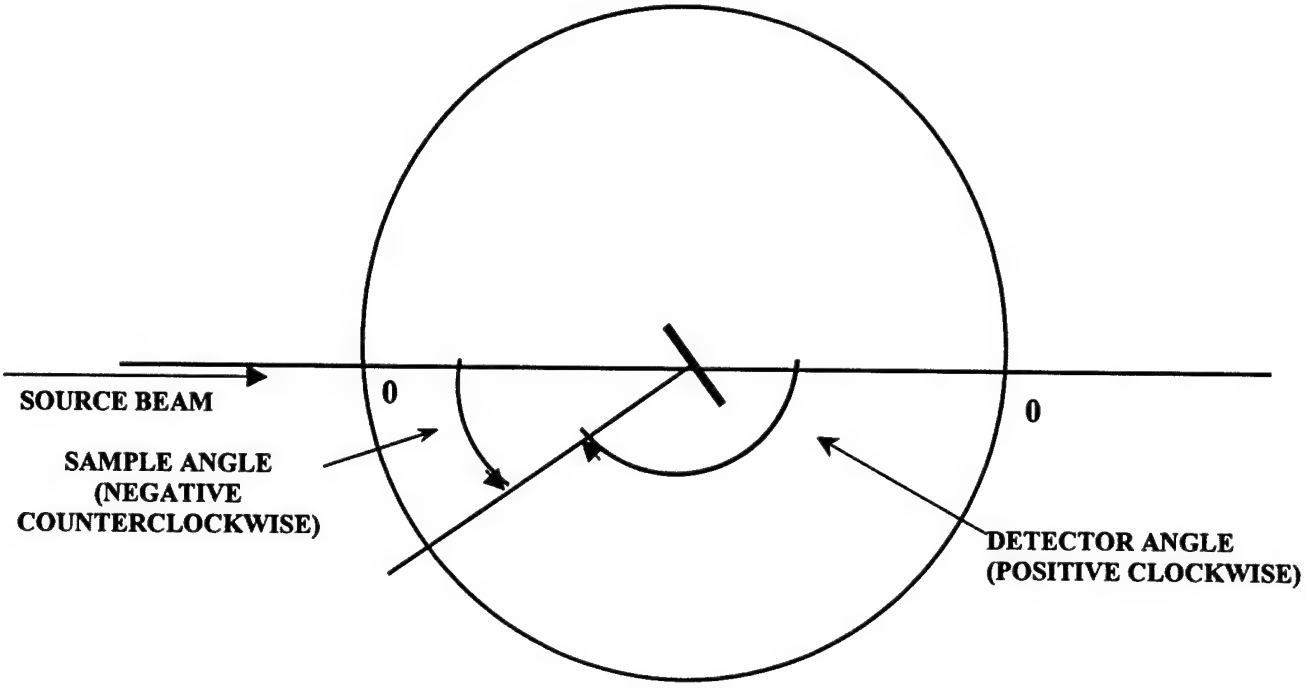

Figure 4. Reflectometer coordinate system.

When the detector is furthest from and in line with the source beam, this is its zero position. Clockwise rotation of the platter gives a positive detector angle. When the sample is normal to the source beam, this is its zero position and counterclockwise rotation of the sample results in a negative sample angle. The first Mueller matrix, shown in Figure 5, is that for a sample of 99% reflective Spectralon where the sample angle is –45° and the detector angle is 135° (the sample is being viewed along its surface normal). Note that the Mueller matrix exhibits essentially no polarization, and this is true across the 0.5 to 1.0 μm wavelength region. This is to be expected for Spectralon, a well-known near-Lambertian diffuse reflectance material. Figure 6 shows maps of degree of polarization, degree of linear polarization, and degree of circular polarization and are plotted as a function of incident polarization state. These two-dimensional plots correspond to a cylindrical projection of the surface of the Poincaré sphere where theta is a latitude (theta of 0° and 180° correspond to the poles of the sphere, and 90° to the equator) and phi is a longitude on the sphere. Thus, theta of 0° corresponds to right circularly polarized light and theta of 180° corresponds to left circularly polarized light. Theta of 90° corresponds to linearly polarized light, and any other value of theta is elliptically polarized light. Note that the scales on the degree of polarization plots are quite small. These plots are based on the spectrally averaged (0.5 to 1.0 μm) Mueller matrix given in this figure.

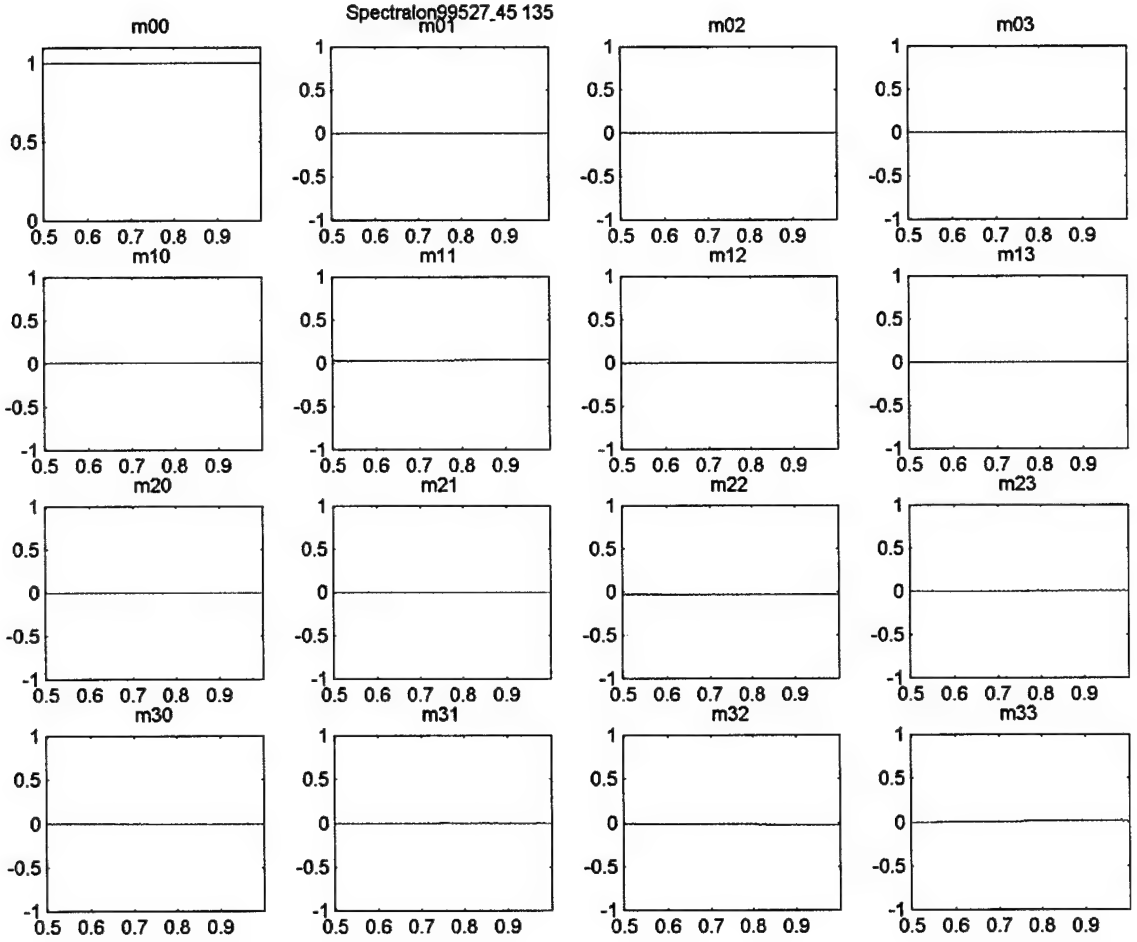

Figure 5. Spectral Mueller matrix for 99% Spectralon at -45° viewed at 135°, 16 cm^{-1} resolution.

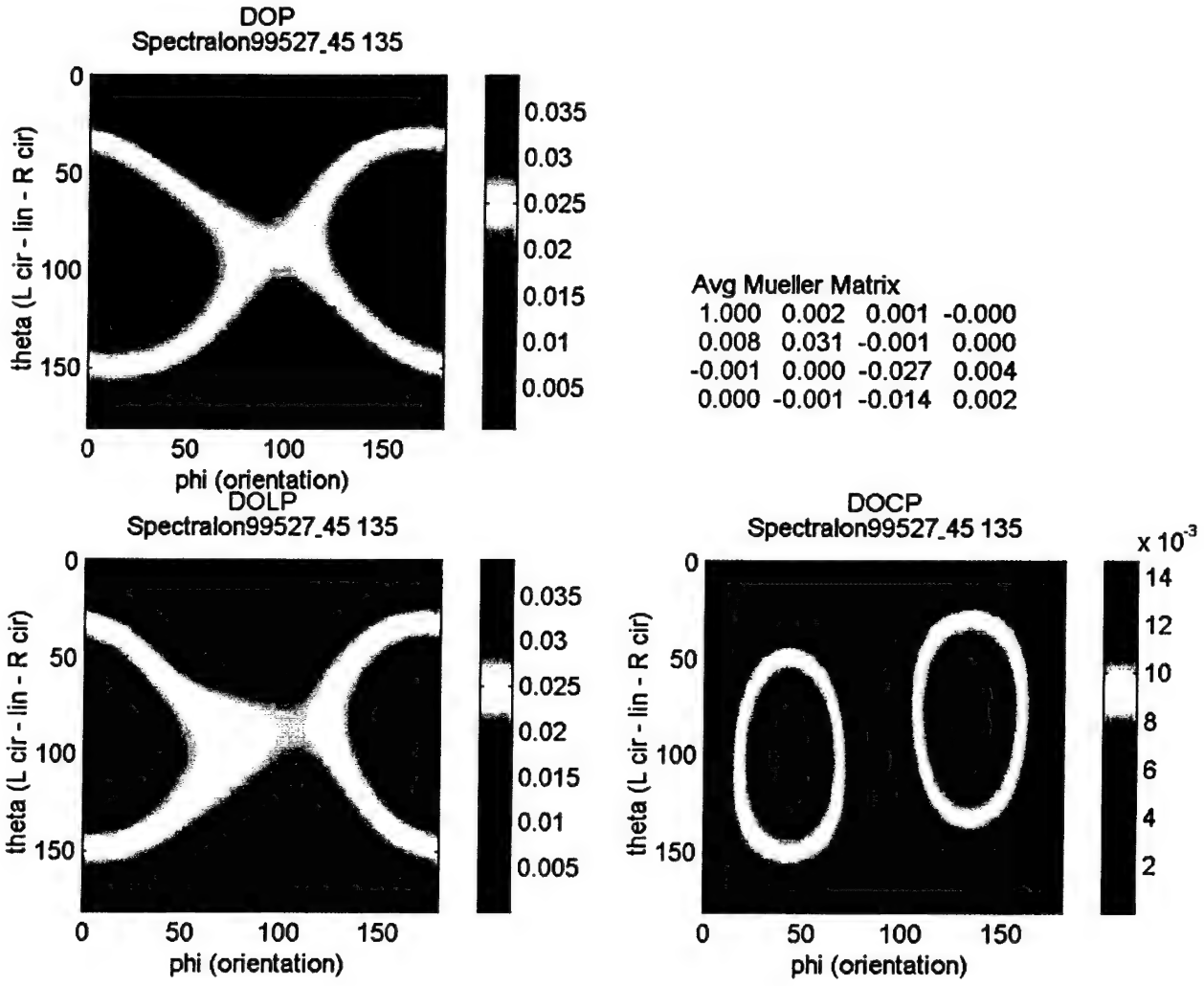

Figure 6. Degree of polarization plots for 99% Spectralon.

Figure 7 is the Mueller matrix for 50% reflective Spectralon where the sample angle is –60° and the detector angle is 60°. This geometry corresponds to specular reflection and will be used for the remainder of the examples. The Mueller matrix now departs significantly from the non-polarizing example in Figure 5, and the maps of the degree of polarization and spectrally averaged Mueller matrix are shown in Figure 8. The scales on the degree of polarization maps are now significantly larger.

A Mueller matrix for 2% Spectralon is shown in Figure 9 and the corresponding degree of polarization maps are shown in Figure 10. This Mueller matrix looks very much like one for a horizontal polarizer, i.e.

$$\begin{bmatrix} 1 & 1 & 0 & 0 \\ 1 & 1 & 0 & 0 \\ 0 & 0 & 0 & 0 \\ 0 & 0 & 0 & 0 \end{bmatrix},$$

and has slightly more spectral structure than the previous Spectralon measurements. It has been reported that low reflectance materials exhibit increased polarization. The incidence angle is also larger in this case, which also tends to increase polarization.

Two final examples are for painted metal and brick. Figure 11 shows the spectral Mueller matrix for olive drab paint on a metal plate. At the specular reflection angle of 60°, this sample appears to have much of the characteristics of a vertical polarizer and the Mueller matrix spectrum is virtually flat from 0.5 to 1.0 μm. The degree of polarization maps are shown in Figure 12. Results for red brick are shown in Figure 13. This sample also shows much of the characteristics of a vertical polarizer, although it has more spectral structure. The degree of polarization maps and the spectrally-averaged Mueller matrix are shown in Figure 14. Diattenuation, polarizance, and retardance were calculated from the spectrally averaged Mueller matrices and are given in Table 1.

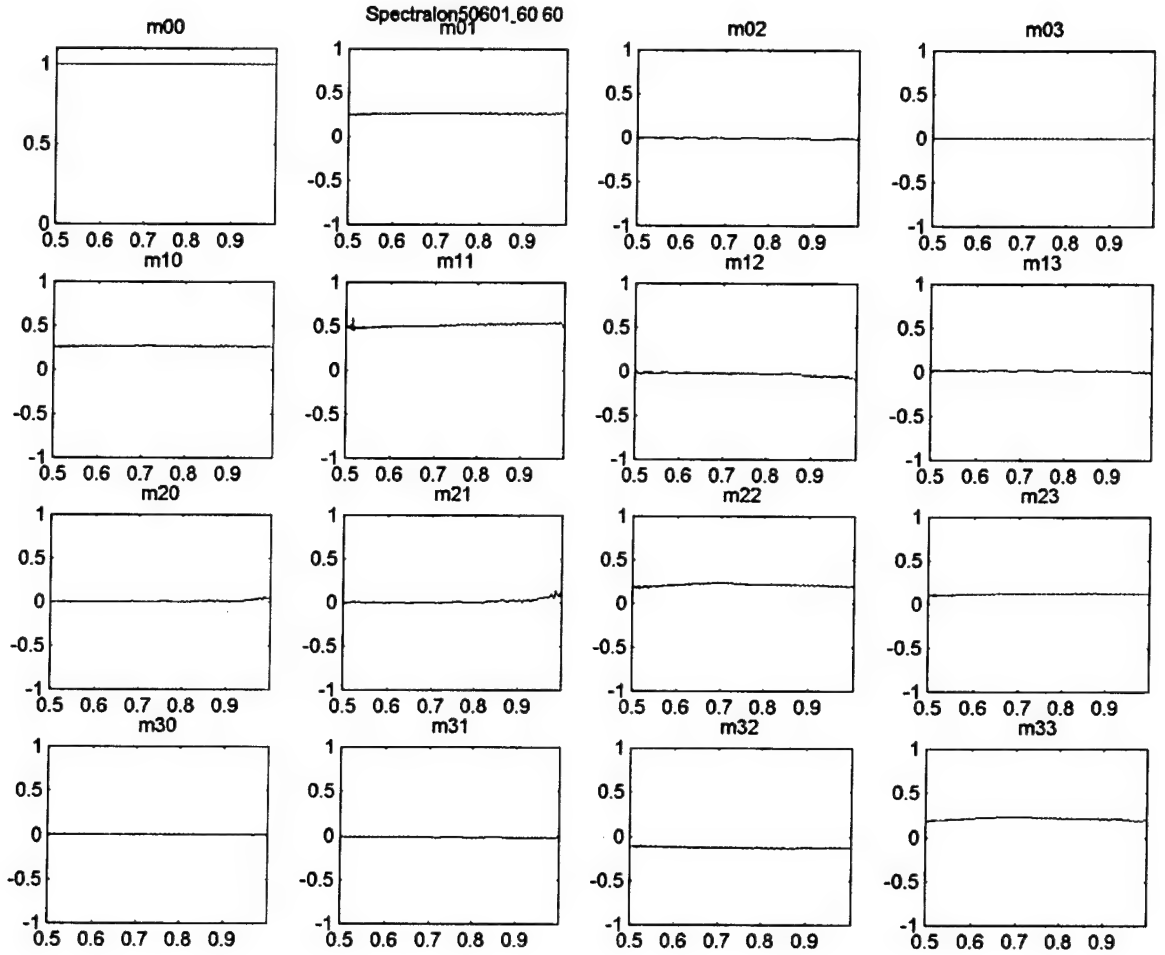

Figure 7. Spectral Mueller matrix for 50% Spectralon at –60° viewed at 60°, 16 cm^{-1} resolution.

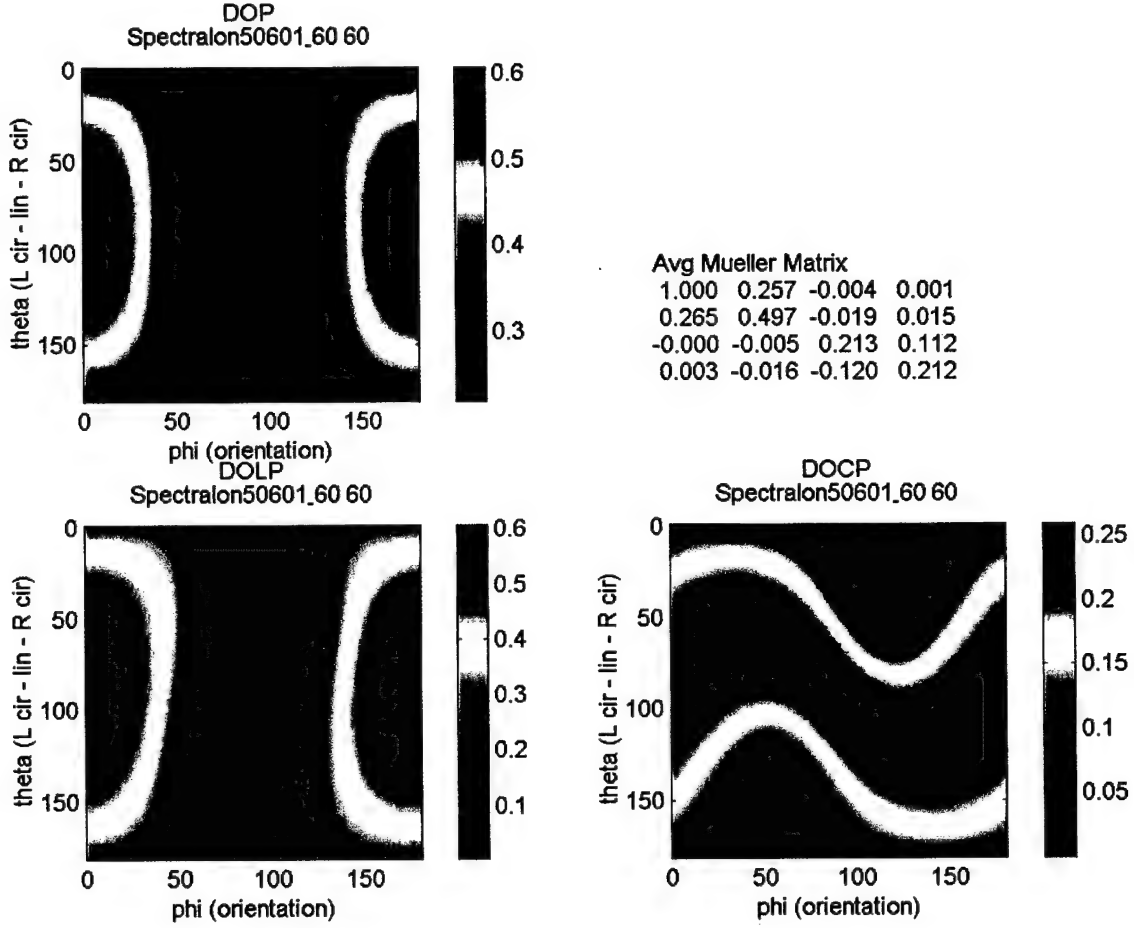

Figure 8. Degree of polarization plots for 50% Spectralon.

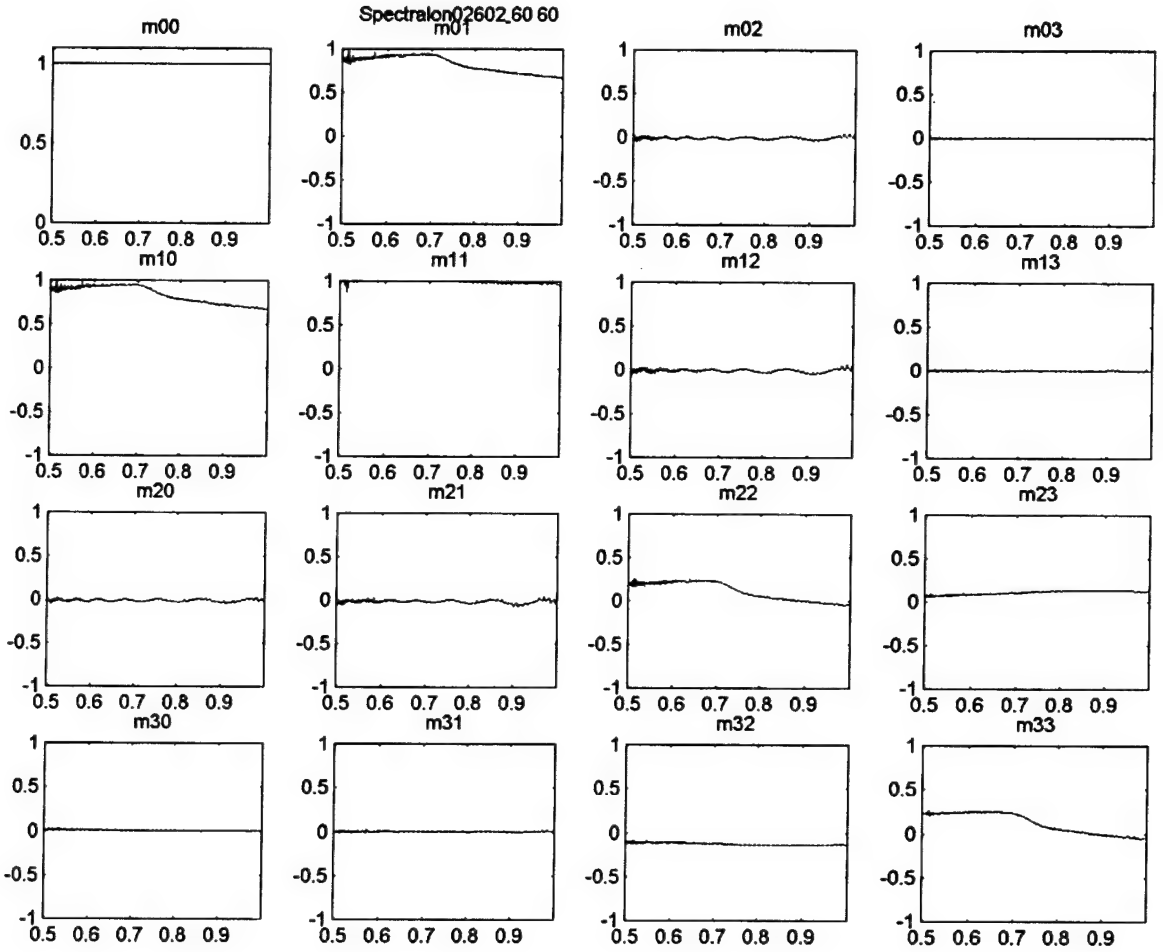

Figure 9. Spectral Mueller matrix for 2% Spectralon at –60° viewed at 60°, 16 cm^{-1} resolution.

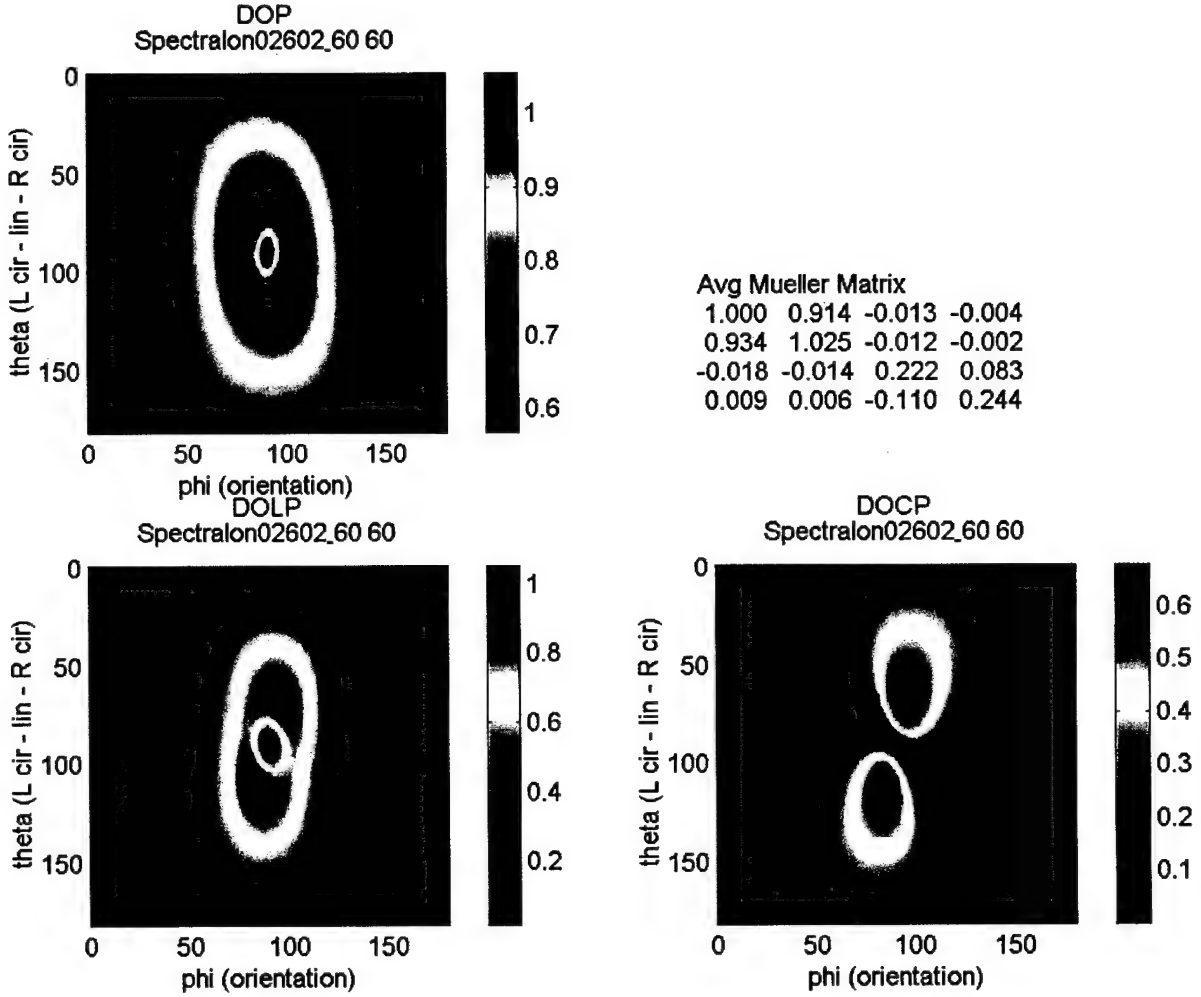

Figure 10. Degree of polarization plots for 2% Spectralon.

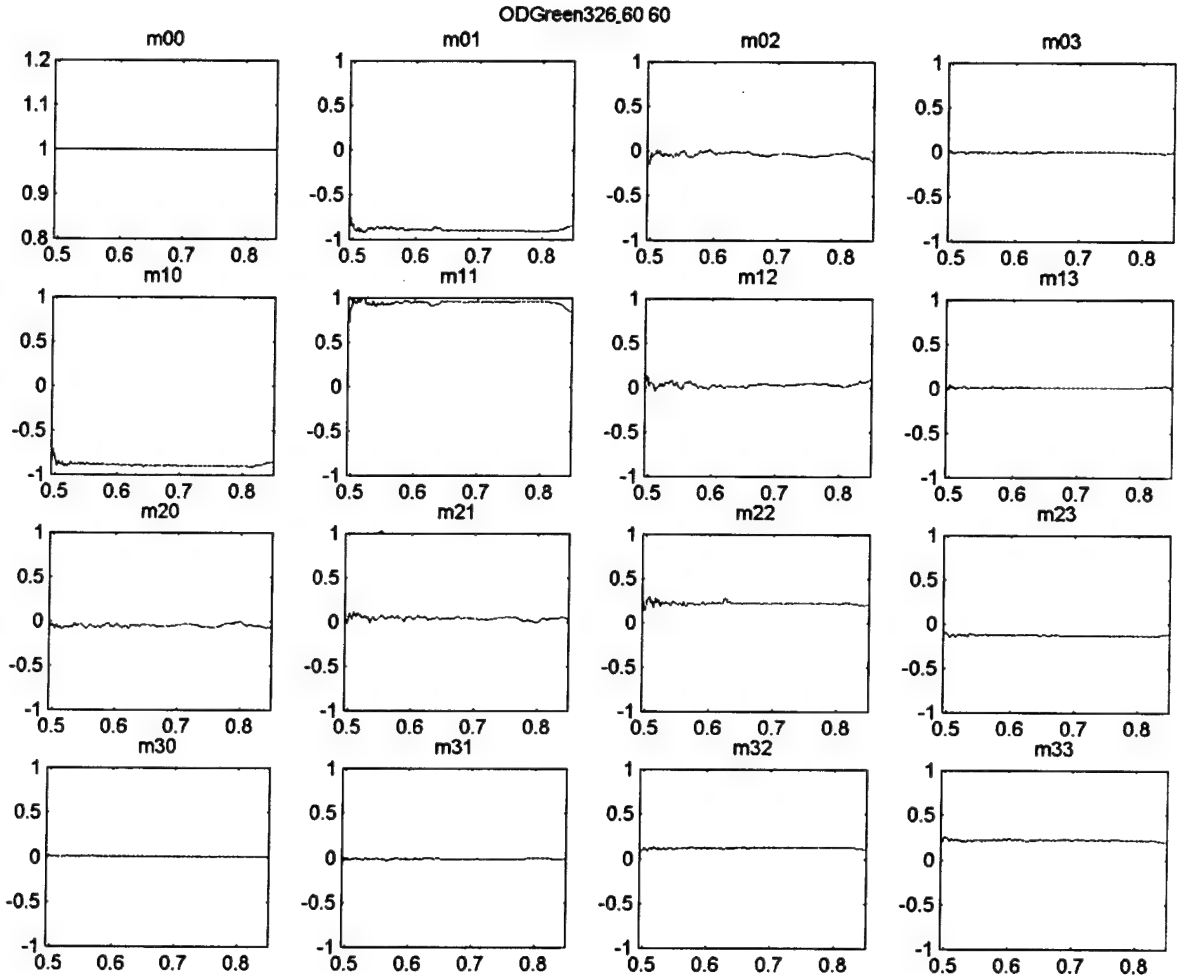

Figure 11. Spectral Mueller matrix for olive drab painted metal at –60° viewed at 60°, 16 cm^{-1} resolution.

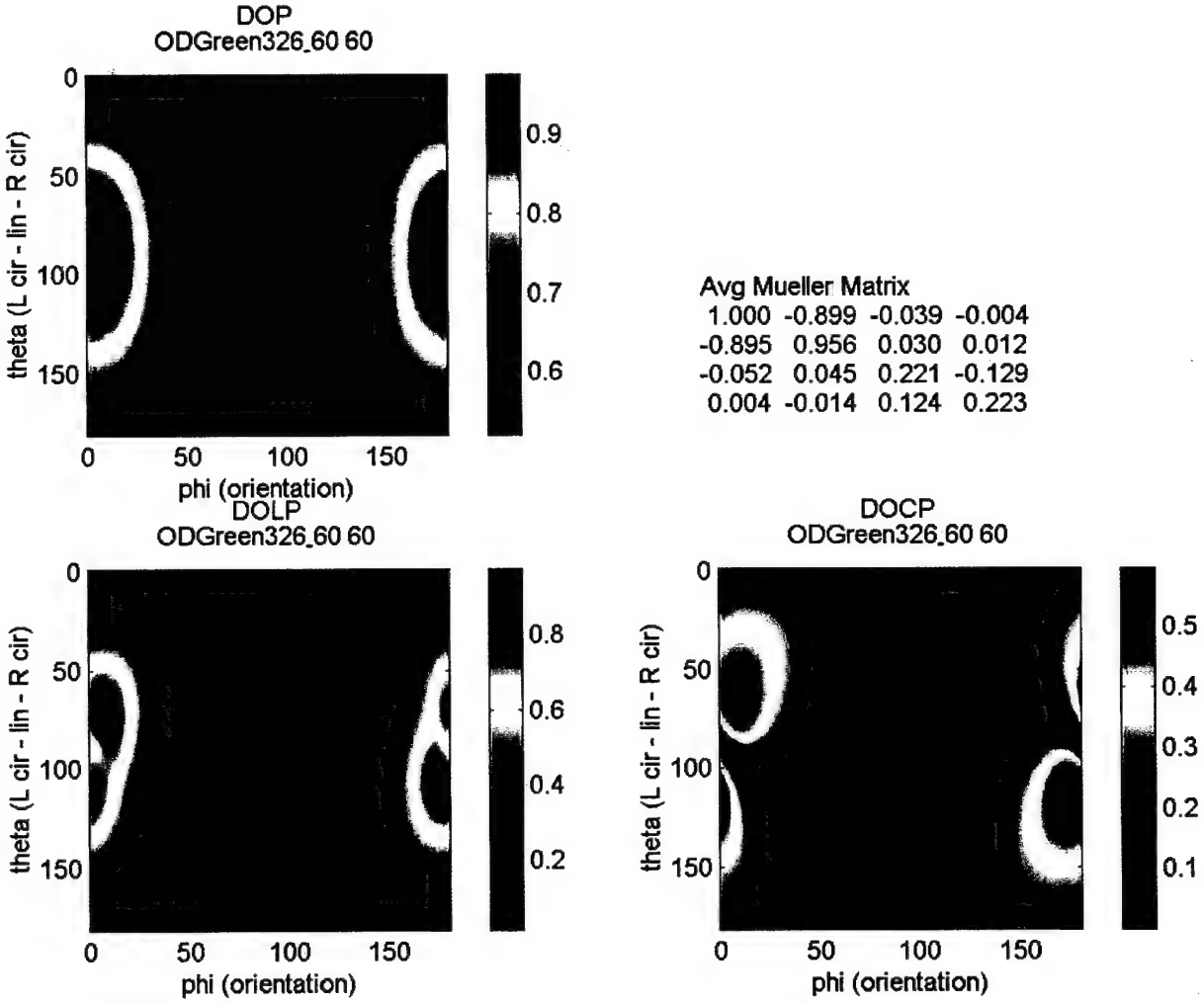

Figure 12. Degree of polarization plots for olive drab painted metal.

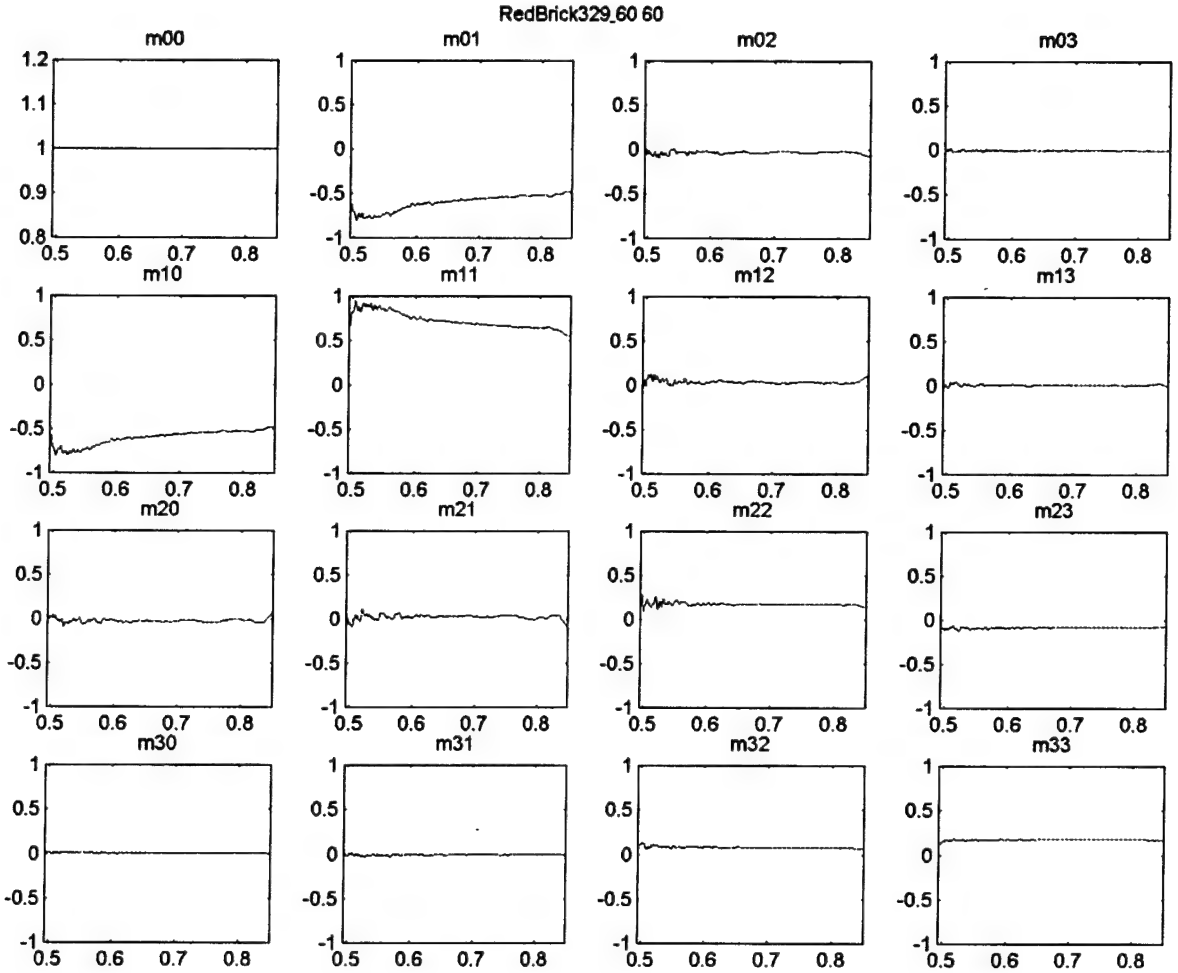

Figure 13. Spectral Mueller matrix for red brick at –60° viewed at 60°, 16 cm^{-1} resolution.

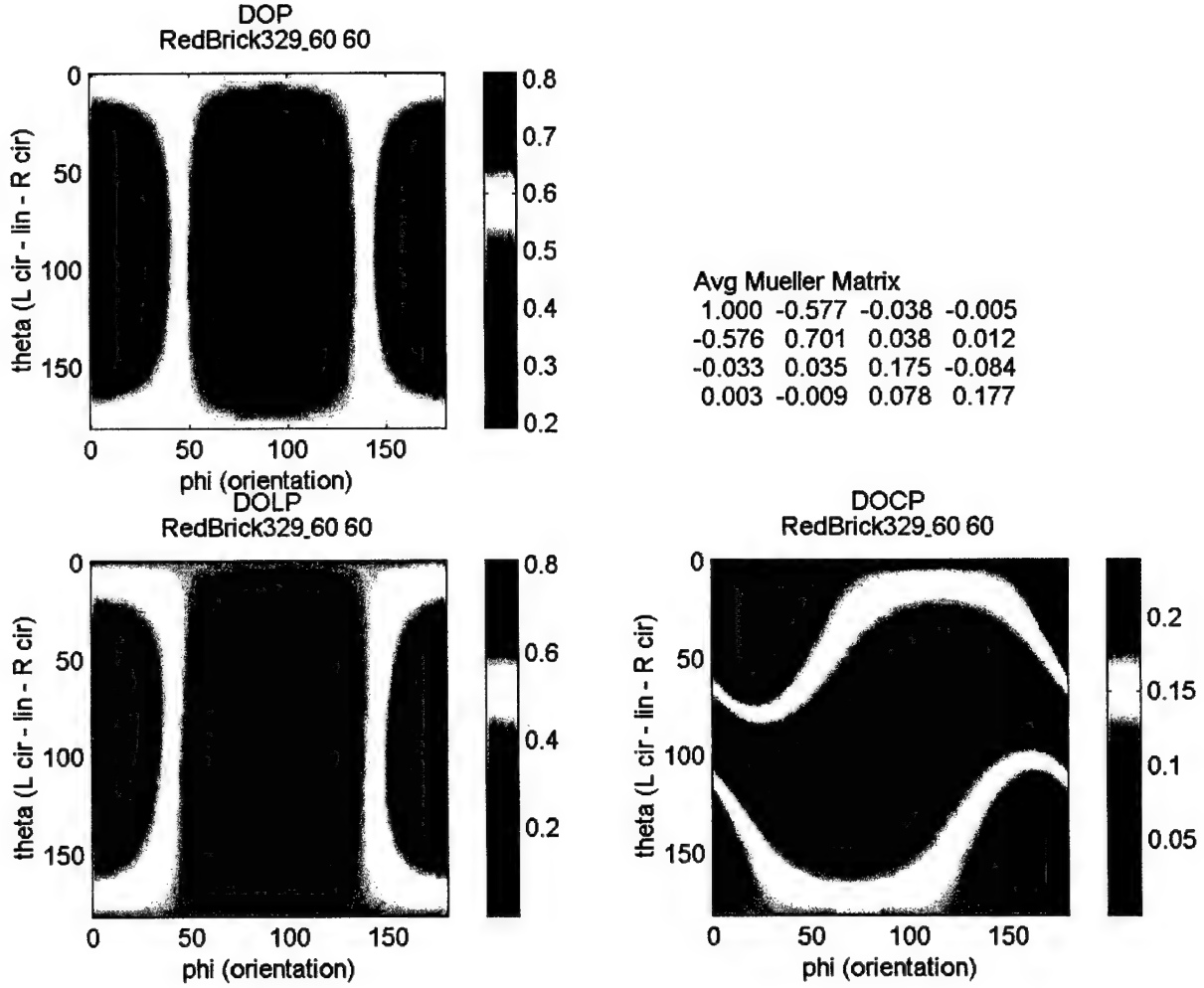

Figure 14. Degree of polarization plots for red brick.

	Diattenuation	Polarizance	Retardance
99% Spectralon Sample: -45° Detector: 135°	.002	.008	2.52
50% Spectralon Sample: -60° Detector: 60°	.257	.265	.504
2% Spectralon Sample: -60° Detector: 60°	.914	.934	.393
Olive Drab Paint Sample: -60° Detector: 60°	.900	-.895	.522
Red Brick Sample: -60° Detector: 60°	.578	-.576	.437

Table 1. Diattenuation, polarizance, and retardance for spectrally averaged Mueller matrices in Figures 6, 8, 10, 12, and 14.

6. DISCUSSION

This instrument collects massive amounts of data describing the polarization properties of the reflectance of materials over broad wavelength regions of the spectrum from the ultraviolet to the far infrared. The two great advantages of this instrument are (1) the use of the Fourier transform spectrometer as the source, giving quick but complete spectral information over broad spectral regions, and (2) the use of the dual rotating retarder configuration for the polarimeter, giving complete information about the polarization properties of the sample. The combination of these two features results in an instrument that provides data that no other instrument can provide.

The spectropolarimetric reflectometer has the potential to impact remote sensing applications in several ways. A large volume of data on natural and manmade surfaces can provide insight into phenomenology and empirical understanding of those materials of most interest to polarimetric sensing and discrimination. In addition, this same information can be used to populate databases for existing models such as Irma and Polar SPIRITS and extend their capability for modeling polarization in a variety of scenes. These databases can also be used for assessing the validity of current models and those under development.

The spectropolarimetric reflectometer can also be used for calibration of polarimetric systems. Polarization elements can be characterized in the transmission configuration of the instrument, as has been described previously[11]. Calibration of imaging polarimeter systems with partially polarized light can also be performed with the spectropolarimetric reflectometer. Since most scenes of interest for remote sensing applications are estimated to have degrees of polarization only at the 5 - 10% level, it is desirable to assess the performance of the imaging system with known partially polarized input. A well-characterized and controllable source is constructed by placing a uniform surface such as spectralon or gold in the sample position. By controlling the sample angle and the incident polarization state, the degree of polarization of the light incident on the sensor can be varied from zero to nearly 100%. Once the reflected beam is characterized by the spectropolarimeter polarization state analyzer, the system under test replaces the polarization state analyzer. The resulting spectral Stokes vector measured by the spectropolarimeter is integrated over the waveband of the imaging polarimeter to give the incident calibration state.

These applications of the spectropolarimetric reflectometer can be advanced by several potential configurations for the instrument. For example, the instrument can be configured to measure samples which are to remain flat, i.e. samples like liquids or soils that must remain nominally horizontal. A platter mounted on a vertical table is placed next to the spectrometer table and the spectrometer beam directed to the sample. The beam can be incident on the sample from a range of angles, and the detector assembly can be rotated throughout a range of angles.

Out-of-plane measurements are possible by placing the detector assembly on a semicircular rail above the detector platter. Alternatively, the sample could be mounted on a goniometer so that the detector is effectively placed out of the incident plane. Neither of these alternatives has been implemented.

The instrument could be configured for monostatic measurements as well, although this has not been implemented. For monostatic measurements, the source beam would pass through a beamsplitter before reaching the sample. The beamsplitter would be positioned such that the return beam is directed toward the detector assembly which remains fixed throughout the measurements. The sample would be rotated to the desired angle and data collected.

ACKNOWLEDGEMENTS

The authors gratefully acknowledge the assistance of Dr. Lynn Deibler of the Air Force Research Laboratory.

REFERENCES

1. D.H. Goldstein and R.A. Chipman, "Infrared Spectropolarimeter," US Patent No. 5,045,701, September 3, 1991.
2. D.H. Goldstein, R.A. Chipman, and D.B. Chenault, "Infrared Spectropolarimetry," *Opt. Eng.* **28**, 120-125 (1989).
3. T.C. Schiff, J.C. Stover, D.R. Bjork, B.D. Swimley, D.J. Wilson, and M.E. Southwood, "Mueller matrix measurements with an out-of-plane polarimetric scatterometer," *Proc. SPIE* **1746**, 295-306, (1992).
4. R.M.A. Azzam, "Photopolarimetric measurement of the Mueller matrix by Fourier analysis of a single detected signal," *Opt. Lett.* **2**, 148-150 (1978).
5. D.H. Goldstein, "Mueller matrix dual-rotating retarder polarimeter," *Appl. Opt.* **31**, 6676-6683 (1992).
6. D.H. Goldstein and R.A. Chipman, "Error Analysis of Mueller Matrix Polarimeters," *J. Opt. Soc. Am.* **7** (4), 693-700 (1990).
7. D.B. Chenault, J.L. Pezzaniti, and R.A. Chipman, "Mueller matrix algorithms," *Proc. SPIE* **1746**, 231-246, (1992).
8. R.A. Chipman, and D.B. Chenault, U.S. Patent #4,961,634, "Infrared achromatic retarder," October, 1990.
9. D.H. Goldstein, D.B. Chenault, and L. Pezzaniti, "Polarimetric characterization of Spectralon," *Proc. SPIE* **3754**, 126-136, (1999).
10. D.H. Goldstein, "Polarimetric characterization of Federal Standard paints," *Proc. SPIE* **4133**, 112-123, (2000).
11. D.H. Goldstein, D.B. Chenault, and M. Owens, "Evaluation of a selection of commercial polarizers and retarders at visible and near-infrared wavelengths," *Proc of SPIE* **3121** 203-212 (1997).

DISTRIBUTION
(AFRL-MN-EG-TR-2003-7013)

Defense Technical Information Center 8725 John J. Kingman Road, Suite 0944 Ft. Belvoir VA 22060-6218	1
Naval Air Weapons Center Attn: Dr. Dave Burdick Code C2901A China Lake CA 93555-6001	1
Comdr, U.S. Army Missile Command Attn: AMSMI-RD-GC-N (Mr. Monte Helton) Redstone Arsenal AL 35898-5241	1
IIT RESEARCH INSTITUTE/GACIAC 10 WEST 35TH STREET CHICAGO IL 60616-3799	1
AFRL/MN/CA-N 101 W Eglin Blvd, Suite 105 Eglin AFB FL 32542-5434	1
AFRL/MNOC-1 (STINFO Office) 203 W Eglin Blvd, Suite 300 Eglin AFB FL 32542-6843	1
AFRL/MNG 101 W Eglin Blvd, Suite 268 Eglin AFB FL 32542	2
AFRL/MNGG 101 W Eglin Blvd, Eglin AFB FL 32542	1
AFRL/MNGI Dr. D. Goldstein 101 W Eglin Blvd, Suite 280 Eglin AFB FL 32542-6810	7
AFRL/MNGN 101 W Eglin Blvd, Suite 268 Eglin AFB FL 32542	1

AFRL/MNGS 1
101 W Eglin Blvd, Suite 268
Eglin AFB FL 32542

AFRL/MNA 1
101 W Eglin Blvd,
Eglin AFB FL 32542

AFRL/MNM 1
101 W Eglin Blvd,
Eglin AFB FL 32542